

Copyright
by
Sri Harsha Tharkabhushanam
2008

The Dissertation Committee for Sri Harsha Tharkabhushanam
certifies that this is the approved version of the following dissertation:

**A Conservative Deterministic Spectral Method for Rarefied Gas
Flows**

Committee:

Irene M. Gamba, Supervisor

Philip Varghese

Bjorn Engquist

Omar Ghattas

Todd Arbogast

**A Conservative Deterministic Spectral Method for Rarefied Gas
Flows**

by

Sri Harsha Tharkabhushanam, B.Tech.; M.S.E.C.E; M.S.

DISSERTATION

Presented to the Faculty of the Graduate School of

The University of Texas at Austin

in Partial Fulfillment

of the Requirements

for the Degree of

DOCTOR OF PHILOSOPHY

THE UNIVERSITY OF TEXAS AT AUSTIN

December 2008

Dedicated to my wife Krishna for her unconditional support and patience.

Acknowledgments

I thank the multitudes of people who helped me. I thank my advisor Professor Gamba for her constant words of encouragement and support. I thank Professor Varghese for the discussions we had during his class which gave me a better picture of the application aspect of my research. I thank Professor Rjasanow of Universitat Des Saarlandes for discussions on conservation schemes for spectral Boltzmann equation. I also thank Mauricio Santillana, Ricardo Alonso, Ross Heath, Chris Mirabito and Fred Qiu for the time we spent discussing research, politics and sports. My parents (Nanna and Amma) and brother (Ravi) and sister (Mridula) back home have always been a great inspiration and support for me. Finally, I thank my wife Krishna for supporting me through my emotional ups and downs and for understanding my long hours at school. I would not have been able to pursue my dream without her inspiration.

A Conservative Deterministic Spectral Method for Rarefied Gas Flows

Publication No. _____

Sri Harsha Tharkabhushanam, Ph.D.
The University of Texas at Austin, 2008

Supervisor: Irene M. Gamba

The mathematical analysis of the Boltzmann equation for a wide range of important models is well developed. It describes physical phenomena which are often of great engineering importance (in aerospace industry, semiconductor design, etc.). For that reason, analytical and computational methods of solving the Boltzmann equation are studied extensively. The idea of describing processes on a scale of the order of the relaxation scales of time and space has been realized. The non-linear Boltzmann equation possesses the important essence of a physically realistic equation, so it is possible not only to consider the flows of simple media but to formulate new problems due to the ability of this equation to describe nonequilibrium states. In this dissertation, a new spectral Lagrangian based deterministic solver for the non-linear Boltzmann transport equation for variable hard potential (VHP) collision kernels with conservative or non-conservative binary interactions is proposed. The method is based on symmetries of the Fourier transform of the collision integral, where the complexity in the collision integral computation is reduced to a separate integral over the unit sphere S^2 . In addition, the conservation of moments is enforced by Lagrangian constraints. The resulting scheme, implemented in free

space, is very versatile and adjusts in a very simple manner to several cases that involve energy dissipation due to local micro-reversibility (inelastic interactions) or to elastic model of slowing down processes.

We prove the accuracy, consistency and conservation properties of the proposed conservative spectral method. Existing spectral methods have consistency proofs which are only for elastic collisions, and also such methods do not conserve all the necessary moments of the collision integral. In this dissertation, error estimates for the conservation routine are provided. Such conservation correction is implemented as an extended isoperimetric problem with the moment conservation properties as the constraints. We use and extend an existing bound estimate of Gamba, Panferov and Villani for the inelastic/elastic space homogeneous Boltzmann collision operator. The result is an original extension to the work of Gustaffson. Using these estimates along with projection error estimates and conservation correction estimates, we prove that the conservation correction is bounded by the spectral accuracy.

Simulations are benchmarked with available exact self-similar solutions, exact moment equations and analytical estimates for the homogeneous Boltzmann equation for both elastic and inelastic VHP interactions. Benchmarking of the self-similar simulations involves the selection of a time rescaling of the numerical distribution function which is performed using the continuous spectrum of the equation for Maxwell molecules. The method also produces accurate results in the case of inelastic diffusive Boltzmann equations for hard-spheres (inelastic collisions under thermal bath), where overpopulated non-Gaussian exponential tails have been conjectured in computations by stochastic methods. Recognizing the importance of the Boltzmann equation in the analysis of shock structures and nonequilibrium states,

such a study is done for $1D(\mathbf{x}) \times 3D(\mathbf{v})$. The classic Riemann problem is numerically analyzed for Knudsen numbers close to continuum. The shock tube problem of Sone and Aoki, where the wall temperature is suddenly changed, is also studied. We consider the problem of heat transfer between two parallel plates with diffusive boundary conditions for a range of Knudsen numbers from close to continuum to a highly rarefied state. Finally, the classical infinite shock tube problem that generates a non-moving shock wave is studied. The point worth noting is that the flow in the final case turns from a supersonic flow to a subsonic flow across the shock.

Table of Contents

Acknowledgments	v
Abstract	vi
List of Figures	xii
Chapter 1. Preliminaries	1
1.1 Introduction	1
1.2 Literature Review	6
1.3 Brief Description and Organization of the Dissertation	10
Chapter 2. Description and Properties of the Boltzmann Transport Equation	14
2.1 The Space Inhomogeneous Boltzmann Transport Equation	14
2.2 The Space Homogeneous Boltzmann Equation	19
2.2.1 Boltzmann Collisional Models with Homogeneous Heating Sources	21
2.3 Properties of the Boltzmann Equation and the Collision Integral . .	25
2.3.1 Well-posedness of the Boltzmann Transport Equation	25
2.3.1.1 The Space Homogeneous Boltzmann Equation	25
2.3.1.2 The Space Inhomogeneous Boltzmann Equation	28
2.3.2 Weak Form of the Collision Integral	30
2.3.3 H - Theorem for the Space Homogeneous Boltzmann Equation	30
2.3.4 Conservation Equations	31
2.3.4.1 The Maxwell Boltzmann Distribution (Equilibrium Dis- tribution)	32
2.3.4.2 Kinetic Boundary Conditions: Simple boundary	33
2.4 Non-dimensional Expressions	34

Chapter 3. The Conservative Deterministic Spectral Method	38
3.1 Spectral Collision Integral Representation	38
3.2 Conservation Method - An Isomoment problem	42
3.2.1 Conservation Method - An Extended Isoperimetric problem .	43
3.2.2 Discrete in Time Conservation Method: Lagrange Multiplier Method	52
3.3 Accuracy and Consistency	55
 Chapter 4. Self-Similar Asymptotics for the Space Homogeneous Problem with Maxwell Type Interactions	 67
4.1 Self-Similar Solution for a Non-negative Thermostat Temperature . .	67
4.2 Self Similar Asymptotics for Cold Thermostat	73
4.3 Self-Similar Asymptotics for a General Problem	75
 Chapter 5. Numerical Results	 81
5.1 Velocity and Fourier Space Discretization	82
5.2 Collision Integral Algorithm	83
5.3 Temporal and Advection Approximation	84
5.3.1 Time Splitting	85
5.3.2 Space Discretization	86
5.3.3 Time Discretization	87
5.4 The Space Homogenous Boltzmann Equation	88
5.4.1 Maxwell Type Elastic Collisions	89
5.4.2 Maxwell Type Elastic Collisions: Bobylev-Krook-Wu (BKW) Solution	90
5.4.3 Hard-Sphere Elastic Collisions	93
5.4.4 Inelastic Collisions	93
5.4.5 Inelastic Collisions with Diffusion Term	99
5.4.6 Maxwell Type Elastic Collisions: Slow Down Process Problem	100
5.5 The Space Inhomogeneous Boltzmann Equation	106
5.5.1 The Riemann Problem	109
5.5.2 Shock Due to a Sudden Change in Wall Temperature	110
5.5.3 Heat transfer Between Two Parallel Plates	115
5.5.4 Classic Shock in an Infinite Tube: Supersonic \rightarrow Subsonic Flow	118

Chapter 6. Conclusions and Future Work	123
Bibliography	126
Index	135
Vita	136

List of Figures

4.1	Spectral Function $\mu(p)$ for a general homogeneous Boltzmann collisional problem of Maxwell type interactions.	79
5.1	Maxwell type elastic collisions: Momentum flow $M_{11}, M_{12}, M_{22}, M_{33}$ and energy flow r_1, r_2	91
5.2	Maxwell type elastic collisions: Evolution of the distribution function	92
5.3	BKW, $\rho, E(t)$ conserved.	93
5.4	Hard sphere, elastic: Momentum flow $M_{11}, M_{12}, M_{22}, M_{33}$, energy flow r_1, r_2	94
5.5	Hard sphere, elastic: Evolution of the distribution function, $N = 32$.	95
5.6	Inelastic: Kinetic energy (left) and $f(\mathbf{v}, t)$ (right).	98
5.7	Maxwell type inelastic collisions, diffusion term for $N = 16$	100
5.8	Hard sphere, inelastic collisions, diffusion term, $T_\infty^{HS} < T_0$ for $N = 16$.	101
5.9	Maxwell type collisions, slow down process with $\Theta = 4/3, \mu = 2/3, N = 24$	102
5.10	Slow down process: $N = 32, \mathcal{T} = \frac{1}{4}e^{-2t/3}$	104
5.11	Computed distribution Vs. Maxwellian with temperature of the computed distribution.	105
5.12	$m_q(t)$ for $\mathcal{T} = \frac{1}{4}e^{-2t/3}$	107
5.13	$m_q(t)$ for $\mathcal{T} = \frac{1}{4}e^{-2t/3}$	108
5.14	Riemann problem: Stationary profiles for $Kn = 0.01$ at $t = 0.15$. . .	111
5.15	Formation of an expansion wave by an initial sudden change of wall temperature from T_0 to $T_0/2$	114
5.16	Formation of a shock wave by an initial sudden change of wall temperature from T_0 to $2T_0$	116
5.17	Marginal Distribution at $t = 0.5t_r$ for $N = 16$	117
5.18	Stationary Temperature Profile for increasing Knudsen number values.	118
5.19	Stationary Density Profile for increasing Knudsen number values. . .	119
5.20	Stationary Shock: Mach number 1.5, and $Kn = 1$, Maxwell interactions.	122

Chapter 1

Preliminaries

1.1 Introduction

A gas flow may be modeled on either a microscopic or a macroscopic level. The macroscopic model regards the gas as a continuum and the description is in terms of variations of the macroscopic velocity, density, pressure and temperature with space and time. On the other hand, the microscopic or molecular model recognizes the particulate structure of a gas as a myriad of discrete molecules and ideally provides information on the position and velocity of every molecule at all times. However, a description in such detail is rarely, if ever, practical and a gas flow is almost invariably described in terms of macroscopic quantities. The two models must therefore be distinguished by the approach through which the description is obtained, rather than by the nature of the description itself. This dissertation is concerned with the microscopic approach and the first question which must be answered is whether this approach can solve problems that could not be solved through the conventional continuum approach.

A gas at standard conditions (1 bar, 25°C) contains ca. 2.43×10^{16} particles per cubic millimeter. Despite this huge number of individual particles, a wide variety of flow and heat transfer problems can be described by a rather low number of partial differential equations, namely the well known equations of Navier-Stokes. Due to the many collisions between particles which effectively distribute disturbances between particles, the particles behave not as individuals, but as a continuum. Under stan-

dard conditions, a particle collides with the others very often, about 10^9 times per second, and travels only very short distances between collisions, about $5 \times 10^{-8}\text{m}$. Both numbers, known as collision frequency ν and mean free path l_0 , depend on the number density of the gas.

The macroscopic quantities at any point in a flow may be identified with average values of appropriate molecular quantities; the averages being taken over the molecules in the vicinity of the point. The continuum description is valid as long as the smallest significant volume in the flow contains a sufficient number of molecules to establish meaningful averages. The existence of a formal link between the macroscopic and microscopic quantities means that the equations which express the conservation of mass, momentum and energy in the flow may be derived from either approach. While this might suggest that neither of the approaches can provide information that is not also accessible to the other, it must be remembered that the conservation equations do not form a determinate set unless the shear stresses and heat flux can be expressed in terms of the other macroscopic quantities. It is the failure to meet this requirement, rather than the breakdown of the continuum description, that places a limit on the range of validity of the continuum equations. More specifically, the Navier-Stokes equations of continuum gas dynamics fail when gradients of the macroscopic variables become so steep that their scale length is of the same order as the average distance traveled by the molecules between collisions, or *mean free path*, l_0 . A less precise but more convenient parameter is obtained if the scale length of the gradients is replaced by the characteristic dimension of the flow, L_{flow} . Flow problems in which typical length scales L_{flow} are much larger than the mean free path l_0 , or in which the typical frequencies ω are much smaller than ν , are well described through the laws of Navier-Stokes. The *Knudsen number* $Kn = \frac{l_0}{L_{flow}}$ is the relevant dimensionless measure to describe these conditions, and

the Navier-Stokes equations are valid as long as $Kn \ll 1$.

This condition fails to hold when the relevant length scale L_{flow} becomes comparable to the mean free path l_0 . This can happen either when the mean free path becomes large, or when the length L_{flow} becomes small. A typical example of a gas with large mean free path is high altitude flight in the outer atmosphere, where the mean free path must be measured in meters, not nanometers, and the Knudsen number becomes large for, e.g., a spacecraft. Miniaturization, on the other hand, produces smaller and smaller devices, e.g., micro-electro-mechanical systems (MEMS), where the length L_{flow} approaches the mean free path.

Moreover, the Navier-Stokes equations will fail in the description of rapidly changing processes, when the process frequency ω approaches, or exceeds, the collision frequency ν . The Knudsen number ($Kn = \frac{\omega}{\nu}$) is used to classify flow regimes as follows:

- $Kn \ll 1$, i.e., $Kn \lesssim 0.01$: The hydrodynamic regime, which is very well described by the Navier-Stokes equations.
- $0.01 \lesssim Kn \lesssim 0.1$: The slip flow regime, where the Navier-Stokes equations can describe the flow well, but must be supplied with boundary conditions that describe velocity slip and temperature jumps at gas-wall interfaces (rarefaction effects).
- $0.1 \lesssim Kn \lesssim 10$: The transition regime, where the Navier-Stokes equations fail, and the gas must be described in greater detail, e.g., by the Boltzmann equation, or by extended macroscopic models.

- $Kn \gtrsim 10$: Free molecular flow, where collisions between particles do not play an important role and the flow is dominated by particle-wall interactions.

Rarefied gases are gases which are outside the hydrodynamic regime, i.e., $Kn \gtrsim 0.01$. For Knudsen numbers $0.01 \lesssim Kn \lesssim 1$, the gas still behaves as a continuum but Navier-Stokes equations fail to describe the underlying physical processes and thus lose their validity and must be replaced by more refined sets of continuum equations that describe the behavior of the gas. There are certain *approximation methods* to derive equations that allow one to describe these physical processes in rarefied gases and the evaluation of the resulting equations. Most of these methods rely on expansions in the Knudsen number, Kn , and thus yield equations that cannot cover the full transition regime, but are restricted to $0.01 \lesssim Kn \lesssim 1$.

A rarefied gas is well described by the Boltzmann equation which describes the gas on the *microscopic* level accounting for the translation and collisions of the particles. The solution of the Boltzmann equation is the phase density f which is a measure for the likelihood to find molecules at a location \mathbf{x} with molecular velocities \mathbf{v} . The Boltzmann equation is the central equation in the *kinetic theory of gases*.

Macroscopic quantities such as mass density ρ , mean velocity (bulk velocity) \mathbf{V} , temperature T , pressure tensor \mathbf{p} , and heat flux vector \mathbf{q} are the weighted averages of the phase density, obtained by integration over the molecular velocity. One way to compute the macroscopic quantities is to use *rational methods* to deduce *macroscopic transport equations* from the Boltzmann equation, that is to get transport equations for the macroscopic quantities ρ, \mathbf{V}, T , etc. This is suitable for processes at small and moderate Knudsen numbers, which as it turns out, can be described by a small number of equations. Alternatively, the Boltzmann equation can be

solved and its solution f integrated over the molecular velocity, \mathbf{v} , domain. Such an approach is not restricted by the range of the Knudsen number values and can be used in analysis of systems where $Kn \gtrsim 0.01$ (rarefied gases). The work in this dissertation concentrates on solving the Boltzmann equation for rarefied gases and subsequent analysis of $3D$ in \mathbf{v} (space homogenous) and $1D$ in \mathbf{x} and $3D$ in \mathbf{v} (space inhomogeneous) systems.

In addition to the description based on the Boltzmann equation, the study of rarefied flows requires an additional piece of information concerning the interaction of gas molecules with the solid (or, possibly liquid) surfaces that bound the gas expanse. It is to this interaction that one can trace the origin of the drag and lift exerted by the gas on the body and the heat transfer between the gas and the solid boundary.

The study of gas-surface interaction may be regarded as a bridge between the kinetic theory of gases and solid state physics. The difficulties of a theoretical investigation are due mainly to our lack of knowledge of the structure of surface layers of solid bodies and hence of the effective interaction potential of the gas molecules with the wall. When a molecule impinges upon a surface, it is absorbed and may form chemical bonds, dissociate, become ionized, or displace surface molecules. Its interaction with the solid surface depends on the surface finish, the cleanliness of the surface, its temperature, etc. It may also vary with time because of outgassing from the surface. Preliminary heating of a surface also promotes purification of the surface through emission of adsorbed molecules. In general, adsorbed layers may be present; in this case, the interaction of a given molecule with the surface may also depend on the distribution of molecules impinging on a surface element. This physical aspect has a mathematical counterpart: The Boltzmann equation must be accompanied by boundary conditions, which describe the aforementioned interaction of the gas

molecules with the solid walls.

Rarefied gas analysis using the Boltzmann equation has a vast number of applicable areas. In the area of environmental problems, understanding and controlling the formation, motion, reactions, and evolution of particles of varying composition and shapes, as well as their space-time distribution under gradients of concentration, pressure, temperature, and the action of radiation, has grown in importance. This is because of the increasing awareness of the local and global problems related to the emission of particles from electric power plants, chemical plants, and vehicles as well as of the role of small particles in fog and cloud formation, radioactive releases, etc. Another area of application of rarefied gas dynamics is in the design of micromachines whose sizes range from a few microns to a few millimeters. Rarefied flows can form the basis of design of important micromechanical systems. In this dissertation, the areas of formation, propagation and analysis of shocks and some some classical hydrodynamic examples have been studied.

1.2 Literature Review

From the computational point of view, one of the well-known and well-studied methods developed in order to solve the Boltzmann equation is a stochastic based method called “Direct Simulation Monte-Carlo” (DSMC) developed initially by Bird[3] and Nanbu[76] and more recently by [82; 83]. This method is usually employed as an alternative to hydrodynamic solvers to model the evolution of moments or hydrodynamic quantities. In particular, this method have been shown to converge to the solution of the classical Boltzmann equation in the case of monatomic rarefied gases [88]. One of the main drawbacks of such methods is the inherent statistical fluctuations in the numerical results, which becomes very expensive or unreliable in the

presence of non-stationary flows or non equilibrium statistical states, where more information is desired about the evolving probability distribution. Currently, there is extensive work from Rjasanow and Wagner [83] and references therein, to determine accurately the high-velocity tail behavior of the distribution functions from DSMC data. Implementations for micro irreversible interactions such as inelastic collisions have been carefully studied in [49].

In contrast, a deterministic method computes approximations of the probability distribution function using the Boltzmann equation, as well as approximations to the observables like density, momentum, energy, etc. There are currently two deterministic approaches to the computations of non-linear Boltzmann, one is the well known discrete velocity models and the second a spectral based method, both implemented for simulations of elastic interactions, i.e., energy conservative evolution. Discrete velocity models were developed by Broadwell [27] and mathematically studied by Illner, Cabannes, Kawashima among many authors [61; 62; 28]. More recently these models have been studied for many other applications on kinetic elastic theory in [10; 33; 68; 91; 58]. These models have not adapted to inelastic collisional problems up to this point according to our best knowledge.

Spectral based models, which are the ones of our choice in this work, have been developed by Pareschi, Gabetta and Toscani [45], and later by Bobylev and Rjasanow[21] and Pareschi and Russo[81]. These methods are supported by the ground breaking work of Bobylev[5] using the Fourier Transformed Boltzmann Equation to analyze its solutions in the case of Maxwell type of interactions. After the introduction of the inelastic Boltzmann equation for Maxwell type interactions and the use of the Fourier transform for its analysis by Bobylev, Carrillo and Gamba [8], the spectral based approach is becoming the most suitable tool to deal with deterministic compu-

tations of kinetic models associated with the Boltzmann non-linear binary collisional integral, both for elastic or inelastic interactions. More recent implementations of spectral methods for the non-linear Boltzmann equation are due to Bobylev and Rjasanow[25], who developed a method using the Fast Fourier Transform (FFT) for Maxwell type interactions, and then for Hard-Sphere interactions[22] using generalized Radon and X-ray transforms via FFT. Simultaneously, L. Pareschi and B. Perthame[80] developed a similar scheme using FFT for Maxwell type interactions. Later, I. Ibragimov and S. Rjasanow[60] developed a numerical method to solve the space homogeneous Boltzmann Equation on a uniform grid for variable hard potential (VHP) interactions with elastic collisions. This particular work has been a great inspiration for the current work and was one of the first initiating steps in the direction of a new numerical method.

We mention that, most recently, Filbet and Russo[40],[41] implemented a method to solve the space inhomogeneous Boltzmann equation using the previously developed spectral methods in [81; 80]. The afore mentioned work in developing deterministic solvers for the non-linear BTE have been restricted to elastic, conservative interactions. Finally, Mouhot and Pareschi[74] are currently studying the approximation properties of the schemes. Part of the difficulties in their strategy arises from the constraint that the numerical solution has to satisfy conservation of the initial mass. To this end, the authors propose the use of a periodic representation of the distribution function to avoid aliasing. There is no conservation of momentum and energy in [41], [40] and [74]. Both methods ([41], [40], [74]), which are developed in 2 and 3 dimensions, do not guarantee the positivity of the solution due to the fact that the truncation of the velocity domain combined with the Fourier method makes the distribution function negative at times. This last shortcoming of the spectral approach remains in our proposed technique; however we are able to handle conservation in

a very natural way by means of Lagrange multipliers. We also want to credit an unpublished calculation of V. Panferov and S. Rjasanow [79] who wrote a method to calculate the particle distribution function for inelastic collisions in the case of hard spheres, but there were no numerical results to corroborate the efficiency of the method. Our proposed approach is slightly different and it takes a smaller number of operations to compute the collision integral.

The interest in shock tube problems is the analysis of *shock waves* or *shock layers*. In the Euler set of equations in classical fluid dynamics, the shock layer is treated as a discontinuity. Its internal structure is discussed using the Navier-Stokes equations. However, the thickness of such a shock layer is of the order of mean free path and thus the Navier-Stokes equations are invalid for such an analysis. For this purpose, the Boltzmann equation is used.

Consider a time-independent unidirectional flow in an infinite expanse of a gas, where the states at infinities are both uniform. The states at infinities being uniform, the velocity distribution functions are Maxwellian with corresponding densities, flow velocities and pressures. Such a choice of averages cannot be made arbitrarily and are derived from the *Rankine-Hugoniot relations*. Obviously, when the two states at infinities are equal, the uniform state is a solution. The mathematical theory of the existence of a nontrivial solution is studied by Caflisch and Nicolaenko [30] and Liu and Yu [66], and the existence and uniqueness of a weak shock wave solution, where the two uniform states at infinities are very close, is proved. Such a profile has been described by Grad [53] and is given by a slowly varying local Maxwellian with the parametric averages given from the fluid dynamic equations. Liu and Yu [66] also prove that the distribution function is positive in the shock layer and that the solution is stable.

Other numerical analysis of shock structures include the pioneering work of Mott and Smith in [73], Liepmann, Narasimha and Chahine [64], Salwen, Grosch and Ziering [84], Ohwada [78], Cercignani, Frezzotti and Grosfils [34], Takata, Aoki and Cercignani [86]. Many of the above are discussions of numerical approximations of the shock wave rather than their physical nature. Takata, Aoki and Cercignani [86] carried out the analysis on the basis of Grad [53] and Caflisch [29] for a hard-sphere gas, according to which the trace of the singular character at upstream infinity remains at downstream infinity. Yu [90] used Hilbert expansions to study the behavior of a gas when the length and time scales of variations are much larger than the mean free path and mean free time respectively. Yu [90] extended the expansion to include a discontinuity caused by the shock wave in the solution. The above analysis was done for a one space dimensional case. It was also proven by Yu that the solution thus obtained approximates the Boltzmann solution for weak shocks. Ha, Liu and Yu in a private communication, studied a one dimensional problem where the two equilibrium states are in contact with each other initially. The Euler equations dictate the propagation of the initial shock discontinuity, where no expansion wave appears. The time evolution of the Boltzmann equation reveals the formation of a shock layer through the initial layer and its propagation. This supplements the work of Yu [90].

1.3 Brief Description and Organization of the Dissertation

Our current approach, based on a modified version of the work in [21] and [60], works for elastic or inelastic collisions and energy dissipative non-linear Boltzmann type models for variable hard potentials. We do not use periodic representations for the distribution function. The only restriction of the current method is that it re-

quires that the distribution function at any time step be Fourier transformable. The required conservation properties of the distribution function are enforced through a Lagrange multiplier constrained optimization problem with the desired conservation quantities set as the constraints. Such corrections to the distribution function to make it conservative are very small but crucial for the evolution of the probability distribution function according to the Boltzmann equation.

This Lagrange optimization problem gives the freedom of not conserving the energy, independent of the collision mechanism, as long as momentum is conserved. Such a technique plays a major role as it gives the option of computing energy dissipative solutions by just eliminating one constraint in the corresponding optimization problem. The current method can be easily implemented in any dimension. A novel aspect of the presented approach here relies on a new method that uses the Fourier Transform as a tool to simplify the computation of the collision operator that works both for elastic and inelastic collisions. It is based on an integral representation of the Fourier Transform of the collision kernel as used in [21]. If N is the number of discretizations in one direction of the velocity domain in d -dimensions, the total number of operations required to solve for the collision integral are of the order of N^{2d} . This number of operations remains the same for elastic/ inelastic, isotropic/anisotropic VHP type of interactions. However, when the differential cross section is independent of the scattering angle, the integral representation kernel is further reduced by an exact closed integrated form that is used to reduce the number of computational operations to $O(N^d \log(N))$. This reduction is possible when computing hard spheres in $d+2$ dimensions or Maxwell type models in 2-dimensions. Nevertheless, the method can be employed without much change for the other case. In particular the method becomes $O(P^{d-1} N^d \log(N))$, where P , the number of each angular discretizations is expected to be much smaller than N used for energy dis-

cretizations. Such reduction in number of operations was also reported in [41] with $O(N\log(N))$ number of operations, where the authors are assuming N to be the total number of discretizations in the d -dimensional space (i.e., our N^d and P of order of unity).

Our numerical study is performed for several examples of well establish behavior associated with solutions of energy dissipative space homogeneous collisional models under heating sources that secure existence of stationary states with positive and finite energy. We shall consider heating sources corresponding to randomly heated inelastic particles in a heat bath, with and without friction; elastic or inelastic collisional forms with anti-divergence terms due to dynamically (self-similar) energy scaled solutions [47; 18] and a particularly interesting example of inelastic collisions added to a slow down linear process that can be derived as a weakly coupled heavy/light binary mixture. On this particular case, when Maxwell type interactions are considered, it is shown that [16; 17; 15], on one hand, dynamically energy scaled solutions exist; they have a close, explicit formula in Fourier space for a particular choice of parameters; and their corresponding inverse Fourier transform in probability space exhibits a singularity at the origin and power law high energy tails, while remaining integrable and with finite energy. On the other hand they are stable within a large class of initial states. We used this particular example to benchmark our computations by spectral methods by comparing the dynamically scaled computed solutions to the explicit self similar one.

It is expected that the proposed spectral approximation of the free space problem will have optimal algorithmic complexity using the non-equispaced FFT as obtained by Greengard and Lin [55] for spectral approximation of the free space heat kernel. The spectral-Lagrangian scheme methodology proposed here can be extended to

cases of Pareto tails, opinion dynamics and N player games, where the evolution and asymptotic behavior of probabilities are studied in Fourier space as well [45; 15].

The dissertation is organized as follows. In Chapter 2, some preliminaries and description of the various approximated models associated with the elastic or inelastic Boltzmann equation are presented. In Chapter 3, the actual numerical method is discussed along with the moment conservation method. In Chapter 4, the special case of a spatially homogeneous collisional model for a slow down process derived from a weakly coupled binary problem with isotropic elastic Maxwell type interactions is considered wherein an explicit solution is derived and shown to have power-like tails in some particular cases corresponding to a cold thermostat problem. Chapter 5 describes the various discretizations used, the proposed algorithm and numerical results for both space homogenous and inhomogeneous (*shock structure analysis*) examples. Finally in Chapter 6, direction of future work is proposed along with a summary of the current work.

Chapter 2

Description and Properties of the Boltzmann Transport Equation

2.1 The Space Inhomogeneous Boltzmann Transport Equation

The Boltzmann Transport Equation describes the statistical (kinetic) evolution of a single point probability distribution function $f(\mathbf{x}, \mathbf{v}, t)$ for $\mathbf{x} \in \Omega_x \subset \mathbb{R}^3$, $\mathbf{v} \in \mathbb{R}^d$ (where d is the velocity space dimension). The probability distribution function $f(\mathbf{x}, \mathbf{v}, t)$ describes the probability of finding a particle at \mathbf{x} with velocity \mathbf{v} at time t . For variable hard potential interactions, the corresponding initial value-boundary value problem in the presence of a force field \mathbf{F} with a post-collisional specular reflection direction σ , is given by

$$\frac{\partial}{\partial t} f(\mathbf{x}, \mathbf{v}, t) + \mathbf{v} \cdot \nabla_{\mathbf{x}} f(\mathbf{x}, \mathbf{v}, t) + \nabla_{\mathbf{v}} \cdot (\mathbf{F} f(\mathbf{x}, \mathbf{v}, t)) = Q(f, f), \quad (2.1.1)$$

with

$$\begin{aligned} f(\mathbf{x}, \mathbf{v}, 0) &= f_0(\mathbf{x}, \mathbf{v}), \\ f(\mathbf{x}, \mathbf{v}, t) &= f_B(\mathbf{x}, \mathbf{v}, t) \quad \forall \quad \mathbf{x} \in \partial\Omega_x, \end{aligned}$$

where the initial probability distribution $f_0(\mathbf{x}, \mathbf{v})$ is assumed to be integrable and the boundary condition $f_B(\mathbf{x}, \mathbf{v}, t) \quad \forall \quad \mathbf{x} \in \partial\Omega_x$ is given in Section 2.3.4.2.

The collision or interaction operator $Q(f, f)$ is a bi-linear integral form that can be defined in weak or strong form. The classical Boltzmann formulation is given in

strong form is classically given in three space dimensions for hard spheres by

$$Q(f, f) = \int_{\mathbf{w} \in \mathbb{R}^d, \eta \in S^{d-1}} \left[\frac{1}{e'J} f(\mathbf{x}, \mathbf{v}, t) f(\mathbf{x}, \mathbf{w}, t) - f(\mathbf{x}, \mathbf{v}, t) f(\mathbf{x}, \mathbf{w}, t) \right] |\mathbf{u} \cdot \eta| d\eta d\mathbf{w} \quad (2.1.2)$$

where the integration over the sphere is done with respect to η , the direction that contains the two centers at the time of the interaction, also referred as the impact direction. We denote by \mathbf{v} and \mathbf{w} the pre-collisional velocities corresponding to \mathbf{v} and \mathbf{w} . In the case of micro-reversible (elastic) collisions one can replace \mathbf{v} and \mathbf{w} with \mathbf{v}' and \mathbf{w}' respectively in the integral part of (2.1.2). The exchange of velocities law is given by

$$\begin{aligned} \mathbf{u} &= \mathbf{v} - \mathbf{w} && \text{relative velocity} \\ \mathbf{v}' &= \mathbf{v} - \frac{1+e}{2}(\mathbf{u} \cdot \eta)\eta, && \mathbf{w}' = \mathbf{w} + \frac{1+e}{2}(\mathbf{u} \cdot \eta)\eta. \end{aligned} \quad (2.1.3)$$

This collisional law is equivalent to $\mathbf{u}' \cdot \eta = -e\mathbf{u} \cdot \eta$ and $\mathbf{u}' \wedge \eta = \mathbf{u} \wedge \eta$.

The parameter $e = e(|\mathbf{u} \cdot \eta|) \in [0, 1]$ is the restitution coefficient covering the range from sticky to elastic interactions, so $e' = e(|\mathbf{u}' \cdot \eta|)$, with \mathbf{u}' the pre-collisional relative velocity. The Jacobian $J = \left| \frac{\partial(\mathbf{v}', \mathbf{w}')}{\partial(\mathbf{v}, \mathbf{w})} \right|$ of post-collisional velocities with respect to pre-collisional velocities depends also on the local energy dissipation [31]. In particular, $J = \left| \frac{\partial(\mathbf{v}, \mathbf{w})}{\partial(\mathbf{v}', \mathbf{w}')} \right|$. In addition, it can be seen in general that it is a function of the quotient of relative velocities and the restitution coefficient as well. For example and in the particular case of hard spheres interactions

$$J(e(z)) = e(z) + z e(z) = (z e(z))_z \quad \text{with } z = |\mathbf{u} \cdot \eta|.$$

When $e = 1$ then the collision law is equivalent to specular reflection with respect to the plane containing η , orthogonal to the corresponding tangent plane to the sphere of influence. The direction η is also called the impact direction. We note that $J = 1$ when $e = 1$, that is, for elastic hard sphere interactions.

The corresponding weak formulation of the collisional form becomes more transparent and crucial in order to write the inelastic equation in higher dimensions or for more general collision kernels. Such formulation, originally due to Maxwell for the space homogeneous form is often called the Maxwell form of the Boltzmann equation. The integration is parametrized in terms of the center of mass and relative velocity. And on the $d - 1$ dimensional sphere, integration is done with respect to the unit direction σ given by the elastic post collisional relative velocity, that is

$$\int_{\mathbf{v} \in \mathbb{R}^d} Q(f, f) \phi(\mathbf{v}) d\mathbf{v} = \int_{\mathbf{v}, \mathbf{w} \in \mathbb{R}^{2d}, \sigma \in S^{d-1}} f(\mathbf{x}, \mathbf{v}, t) f(\mathbf{x}, \mathbf{w}, t) [\phi(\mathbf{v}') - \phi(\mathbf{v})] B(|\mathbf{u}|, \mu) d\sigma d\mathbf{w} d\mathbf{v}, \quad (2.1.4)$$

where the corresponding velocity interaction law is now given by

$$\begin{aligned} \mathbf{v}' &= \mathbf{v} + \frac{\beta}{2}(|\mathbf{u}|\sigma - \mathbf{u}), & \mathbf{w}' &= \mathbf{w} - \frac{\beta}{2}(|\mathbf{u}|\sigma - \mathbf{u}), \\ \mathbf{u}' &= (1 - \beta)\mathbf{u} + \beta|\mathbf{u}|\sigma & & \text{(inelastic relative velocity)}, \\ \mu = \cos(\theta) &= \frac{\mathbf{u} \cdot \sigma}{|\mathbf{u}|} & & \text{(cosine of the elastic scattering angle)}, \\ B(|\mathbf{u}|, \mu) &= |\mathbf{u}|^\lambda b(\cos \theta) & & \text{with } 0 \leq \lambda \leq 1, \\ \omega_{d-2} \int_0^\pi b(\cos \theta) \sin^{d-2} \theta d\theta &< K & & \text{(Grad cut-off assumption)}, \\ \beta &= \frac{1+e}{2} & & \text{(energy dissipation parameter)}. \end{aligned} \quad (2.1.5)$$

We denote by \mathbf{v} and \mathbf{w} the pre-collision velocities corresponding to \mathbf{v} and \mathbf{w} . In the case of micro-reversible (elastic) collisions one can replace \mathbf{v} and \mathbf{w} with \mathbf{v}' and \mathbf{w}' respectively in the integral part of (2.1.1). We assume the differential cross section function $b(\frac{\mathbf{u} \cdot \sigma}{|\mathbf{u}|})$ is integrable with respect to the post-collisional specular reflection direction σ in the $d - 1$ dimensional sphere, referred as the *Grad cut-off assumption*,

and that $b(\cos \theta)$ is renormalized such that

$$\begin{aligned} \int_{S^{d-1}} b\left(\frac{\mathbf{u} \cdot \boldsymbol{\sigma}}{|\mathbf{u}|}\right) d\boldsymbol{\sigma} &= \omega_{d-2} \int_0^\pi b(\cos \theta) \sin^{d-2} \theta d\theta \\ &= \omega_{d-2} \int_{-1}^1 b(\mu) (1 - \mu^2)^{(d-3)/2} d\mu = 1, \end{aligned} \quad (2.1.6)$$

where the constant ω_{d-2} is the measure of the $d - 2$ dimensional sphere and the corresponding scattering angle θ is defined by $\cos \theta = \frac{\boldsymbol{\sigma} \cdot \mathbf{u}}{|\mathbf{u}|}$. The above equation 2.1.6 is written for a general d .

The parameter λ regulates the collision frequency as a function of the relative speed $|\mathbf{u}|$. It accounts for inter particle potentials defining the collisional kernel and they are referred to as Variable Hard Potentials (VHP) whenever $0 < \lambda < 1$, Maxwell Molecules type interactions (MM) for $\lambda = 0$ and Hard Spheres (HS) for $\lambda = 1$. The Variable Hard Potential collision kernel then takes the following general form:

$$B(|\mathbf{u}|, \mu) = C_\lambda(\sigma) |\mathbf{u}|^\lambda, \quad (2.1.7)$$

with $C_\lambda(\sigma) = \frac{1}{4\pi} b(\theta)$, $\lambda = 0$ for Maxwell type of interactions; $C_\lambda(\sigma) = \frac{a^2}{4}$, $\lambda = 1$ for Hard Spheres (with a = particle diameter). For $3 - D$ in \mathbf{v} , $C_\lambda(\sigma) = 1/4\pi$. In addition, if $C_\lambda(\sigma)$ is independent of the scattering angle we call the interactions isotropic. Otherwise we refer to them as anisotropic Variable Hard Potential interactions.

Depending on their nature, collisions either conserve density, momentum and energy (elastic) or density and momentum (inelastic) or density (elastic - linear Boltzmann operator), depending on the number of collision invariants the operator $Q(f, f)$ has. In the case of the classical Boltzmann equation for rarefied (elastic) monatomic gases, the collision invariants are exactly $d + 2$, that is, according to the Boltzmann theorem, the number of polynomials in velocity space \mathbf{v} that generate $\phi(\mathbf{v}) = A + \mathbf{B} \cdot$

$\mathbf{v} + \mathbf{C}|\mathbf{v}|^2$, with $C \leq 0$. In particular, one obtains the following *conserved quantities*:

$$\begin{aligned}
\text{Density} \quad \rho(\mathbf{x}, t) &= \int_{\mathbf{v} \in \mathbb{R}^d} f(\mathbf{x}, \mathbf{v}, t) d\mathbf{v}, \\
\text{Flow velocity vector} \quad \mathbf{V}(\mathbf{x}, t) &= \frac{1}{\rho(\mathbf{x}, t)} \int_{\mathbf{v} \in \mathbb{R}^d} \mathbf{v} f(\mathbf{x}, \mathbf{v}, t) d\mathbf{v}, \\
\text{Temperature} \quad 3\mathbf{R}T(\mathbf{x}, t) &= \frac{1}{\rho(\mathbf{x}, t)} \int_{\mathbf{v} \in \mathbb{R}^d} |\mathbf{v} - \mathbf{V}|^2 f(\mathbf{x}, \mathbf{v}, t) d\mathbf{v}, \\
\text{Pressure} \quad p(\mathbf{x}, t) &= \frac{1}{3} \int_{\mathbf{v} \in \mathbb{R}^d} |\mathbf{v} - \mathbf{V}|^2 f(\mathbf{x}, \mathbf{v}, t) d\mathbf{v} = \mathbf{R}\rho(\mathbf{x}, t)T \quad (2.1.8) \\
\text{Specific internal energy} \quad e(\mathbf{x}, t) &= \frac{1}{2\rho(\mathbf{x}, t)} \int_{\mathbf{v} \in \mathbb{R}^d} |\mathbf{v} - \mathbf{V}|^2 f(\mathbf{x}, \mathbf{v}, t) d\mathbf{v} = \frac{3}{2}\mathbf{R}T, \\
\text{Stress tensor, } \mathbf{p}(\mathbf{x}, t) = \{p_{ij}\}(\mathbf{x}, t) \quad p_{ij} &= \int_{\mathbf{v} \in \mathbb{R}^d} (v_i - V_i)(v_j - V_j) f(\mathbf{x}, \mathbf{v}, t) d\mathbf{v}, \\
\text{Heat-flow vector} \quad \mathbf{q}(\mathbf{x}, t) &= \frac{1}{2} \int_{\mathbf{v} \in \mathbb{R}^d} (\mathbf{v} - \mathbf{V}) |\mathbf{v} - \mathbf{V}|^2 f(\mathbf{x}, \mathbf{v}, t) d\mathbf{v},
\end{aligned}$$

where \mathbf{R} is the specific gas constant. Of significant interest from the statistical view point are the evolution of moments or observables, at all orders. They are defined by the dynamics of the corresponding time evolution equation for the velocity averages, given by

$$\frac{\partial}{\partial t} M_j(\mathbf{x}, t) = \int_{\mathbf{v} \in \mathbb{R}^d} f(\mathbf{x}, \mathbf{v}, t) \mathbf{v}^{\odot j} d\mathbf{v} = \int_{\mathbf{v} \in \mathbb{R}^d} Q(f, f) \mathbf{v}^{\odot j} d\mathbf{v}, \quad (2.1.9)$$

where, $\mathbf{v}^{\odot j}$ = the standard symmetric tensor product of \mathbf{v} with itself, j times. Thus, according to (2.1.8), for the classical elastic Boltzmann equation, the first $d + 2$ moments are conserved, meaning, $M_j(\mathbf{x}, t) = M_{0,j} = \int_{\mathbf{v} \in \mathbb{R}^d} f_0(\mathbf{x}, \mathbf{v}) \mathbf{v}^{\odot j} d\mathbf{v}$ for $j = 0, 1$; and $\mathcal{E}(\mathbf{x}, t) = \text{tr}(M_2)(\mathbf{x}, t) = \mathcal{E}_0 = \int_{\mathbf{v} \in \mathbb{R}^d} f_0(\mathbf{x}, \mathbf{v}) |\mathbf{v}|^2 d\mathbf{v}$. Other higher order moments of interest and alternate moment forms are

$$\begin{aligned}
\text{Momentum Flow} \quad M_2(\mathbf{x}, t) &= \int_{\mathbb{R}^d} \mathbf{v} \mathbf{v}^T f(\mathbf{x}, \mathbf{v}, t) d\mathbf{v} \\
\text{Specific internal Energy} \quad \mathcal{E}(\mathbf{x}, t) &= \frac{1}{2\rho(t)} (\text{tr}(M_2(\mathbf{x}, t)) - \rho(\mathbf{x}, t) |\mathbf{V}(\mathbf{x}, t)|^2),
\end{aligned} \quad (2.1.10)$$

with \mathbf{k} — Boltzmann constant.

2.2 The Space Homogeneous Boltzmann Equation

Similar to the space inhomogeneous case, the initial value problem associated to space homogeneous Boltzmann Equation modeling the statistical (kinetic) evolution of a single point probability distribution function $f(\mathbf{v}, t)$ for $\mathbf{v} \in \mathbb{R}^d$ (where d is the velocity space dimension and could take a value of 2 or 3 depending on the underlying physics), for Variable Hard Potential (VHP) interactions in the absence of a force field is given by

$$\begin{aligned} \frac{\partial}{\partial t} f(\mathbf{v}, t) &= Q(f, f)(\mathbf{v}, t) \\ &= \int_{\mathbf{w} \in \mathbb{R}^d, \sigma \in S^{d-1}} [J_\beta f(\mathbf{v}', t) f(\mathbf{w}', t) - f(\mathbf{v}, t) f(\mathbf{w}, t)] B(|\mathbf{u}|, \mu) d\sigma d\mathbf{w} \\ f(\mathbf{v}, 0) &= f_0(\mathbf{v}), \end{aligned} \tag{2.2.1}$$

where the initial probability distribution $f_0(\mathbf{v})$ is assumed to be integrable and $J_\beta = \frac{\partial(\mathbf{v}', \mathbf{w}')}{\partial(\mathbf{v}, \mathbf{w})}$ is the Jacobian of post with respect to pre collisional velocities which depend the local energy dissipation [31]. The problem may or may not have finite initial energy $\mathcal{E}_0 = \int_{\mathbb{R}^d} f_0(\mathbf{v}) |\mathbf{v}|^2 d\mathbf{v}$ and the velocity interaction law, written in center of mass and relative velocity coordinates is given in (2.1.5).

Just like in the space inhomogeneous case, \mathbf{v}' and \mathbf{w}' are the pre-collision velocities corresponding to \mathbf{v} and \mathbf{w} . In the case of micro-reversible (elastic) collisions one can replace \mathbf{v}' and \mathbf{w}' with \mathbf{v}' and \mathbf{w}' respectively in the integral part of (2.1.1). The differential cross section function $b(\frac{\mathbf{u} \cdot \sigma}{|\mathbf{u}|})$ is assumed to be integrable with respect to the post-collisional specular reflection direction σ in the $d - 1$ dimensional sphere (*Grad cut-off assumption* eqrefgrad-cut-off). (2.1.7) gives the variable hard potential interparticle interaction potentials.

For classical case of elastic collisions, it has been established that the Cauchy prob-

lem for the space homogeneous Boltzmann equation has a unique solution in the class of integrable functions with finite energy (i.e., $C^1(L_2^1(\mathbb{R}^d))$), it is regular if initially so, and $f(., t)$ converges in $L_2^1(\mathbb{R}^d)$ to the Maxwellian distribution $M_{\rho, \mathbf{v}, \varepsilon}(\mathbf{v})$ associated to the $d + 2$ -moments of the initial state $f(\mathbf{v}, 0) = f_0(\mathbf{v}) \in L_2^1(\mathbb{R}^d)$. In addition, if the initial state has Maxwellian decay, this property will remain with a Maxwellian decay globally bounded in time ([46]), as well as all derivatives if initial so (see [1]).

Just as in the space inhomogeneous case, depending on the number of collision invariants of $Q(f, f)$ the conservation properties of the Boltzmann equation change accordingly. In particular, one obtains *conserved quantities* just as in (2.1.8) but without the space, \mathbf{x} dependence. Other higher order moments can also be derived for the space homogeneous case to give expressions identical to (2.1.9) and (2.1.10) but again without the space, \mathbf{x} dependence.

We finally point out that, in the case of Maxwell molecules ($\lambda = 0$), it is possible to write recursion formulas for higher order moments of all orders ([6] for the elastic case, and [8] in the inelastic case) which, in the particular case of isotropic solutions depending only on $|\mathbf{v}|^2/2$, take the form

$$m_n(t) = \int_{\mathbb{R}^d} |\mathbf{v}|^{2n} f(\mathbf{v}, t) d\mathbf{v} = e^{-\lambda_n t} m_n(0) + \sum_{k=1}^{n-1} \frac{1}{2(n+1)} \binom{2n+2}{2k+1} B_\beta(k, n-k) \int_0^t m_k(\tau) m_{n-k}(\tau) e^{-\lambda_n(t-\tau)} d\tau, \quad (2.2.2)$$

with

$$\lambda_n = 1 - \frac{1}{n+1} [\beta^{2n} + \sum_{k=0}^n (1-\beta)^{2k}],$$

$$B_\beta(k, n-k) = \beta^{2k} \int_0^1 s^k (1 - \beta(2-\beta)s)^{n-k} ds,$$

for $n \geq 1$, $0 \leq \beta \leq 1$, where $\lambda_0 = 0$, $m_0(t) = 1$, and $m_n(0) = \int_{\mathbb{R}^d} |\mathbf{v}|^{2n} f_0(\mathbf{v}) d\mathbf{v}$.

2.2.1 Boltzmann Collisional Models with Homogeneous Heating Sources

A collisional model associated to the space homogeneous Boltzmann transport equation (2.1.1) with grad cutoff assumption (2.1.5), can be modified in order to accommodate an energy or ‘heat source’ like term $\mathcal{G}(f(\mathbf{v}, t))$, where \mathcal{G} is a differential or integral operator. In these cases, it is possible to obtain stationary states with finite energy as it is for the case of inelastic interactions. In such general framework, the corresponding initial value problem model is

$$\begin{aligned} \frac{\partial}{\partial t} f(\mathbf{v}, t) &= \zeta(t) Q(f, f) + \mathcal{G}(f(\mathbf{v}, t)), \\ f(\mathbf{v}, 0) &= f_0(\mathbf{v}), \end{aligned} \tag{2.2.3}$$

where the collision operator $Q(f, f)$ is as in (2.1.1) and $\mathcal{G}(f(\mathbf{v}, t))$ models a ‘heating source’ due to different phenomena. The term $\zeta(t)$ may represent a mean field approximation that follows from proper time rescaling and is usually taken to be equal to 1. See [8] and [18] for several examples for these type of models and additional references.

Following the work initiated in [18] and [17] on Non-Equilibrium Stationary States (NESS), based on the proposed computational approach we shall present several computational simulations of non-conservative models for either elastic or inelastic collisions associated to (2.2.3) of the Boltzmann equation with ‘heating’ sources. In all the cases we have addressed, one can see that stationary states with finite energy are admissible, but they may not be Maxwellian distributions. Of this type of model we show computational output for three cases. First one is the pure diffusion thermal bath due to a randomly heated background [89; 77; 47], in which case

$$\mathcal{G}_1(f) = \mu \Delta_{\mathbf{v}} f, \tag{2.2.4}$$

where $\mu > 0$ is a constant. The second example relates to self-similar solutions of equation (2.2.3) for $\mathcal{G}(f) = 0$ [71; 38], but dynamically rescaled by

$$f(\mathbf{v}, t) = \frac{1}{v_0^d(t)} \tilde{f}(\tilde{\mathbf{v}}(\mathbf{v}, t), \tilde{t}(t)), \quad \tilde{v} = \frac{\mathbf{v}}{v_0(t)}, \quad (2.2.5)$$

where

$$v_0(t) = (a + \eta t)^{-1}, \quad \tilde{t}(t) = \frac{1}{\eta} \ln(1 + \frac{\eta}{a} t), \quad a, \eta > 0. \quad (2.2.6)$$

Then the equation for $\tilde{f}(\tilde{\mathbf{v}}, \tilde{t})$ coincides (after omitting the tildes) with equation (2.2.3) for

$$\mathcal{G}_2(f) = -\eta \operatorname{div}(\mathbf{v} f), \quad \eta > 0. \quad (2.2.7)$$

Of particular interest of dynamical time-thermal speed rescaling is the case of collisional kernels corresponding to Maxwell type interactions. Since the second moment of the collisional integral is a linear function of the energy, the energy evolves exponentially with a rate proportional to the energy production rate, that is

$$\frac{d}{dt} \mathcal{E}(t) = \lambda_0 \mathcal{E}(t), \quad \text{or equivalently } \mathcal{E}(t) = \mathcal{E}(0) e^{\lambda_0 t}, \quad (2.2.8)$$

with λ_0 the energy production rate. Therefore the corresponding rescaled variables and equations (2.2.5) and (2.2.3) for (2.2.7) to study the long time behavior of rescaled solutions are

$$f(\mathbf{v}, t) = \mathcal{E}^{-\frac{d}{2}(t)} \tilde{f}\left(\frac{\mathbf{v}}{\mathcal{E}^{\frac{1}{2}}(t)}\right) = (\mathcal{E}(0) e^{\lambda_0 t})^{-\frac{d}{2}} \tilde{f}(\mathbf{v} (\mathcal{E}(0) e^{\lambda_0 t})^{-\frac{1}{2}}), \quad (2.2.9)$$

and \tilde{f} satisfies the self-similar equation (2.2.3)

$$\mathcal{G}_{2'}(f) = -\lambda_0 x f_x, \quad \text{where } x = \mathbf{v} \mathcal{E}^{-\frac{1}{2}}(t) \text{ is the self-similar variable.} \quad (2.2.10)$$

We note that it has been shown that these dynamically self-similar states are stable under very specific scaling for a large class of initial states [15].

The last source type we consider is given by a model, related to a weakly coupled mixture modeling slowdown (cooling) process [17] given by an elastic model in the presence of a thermostat given by Maxwell type interactions of particles of mass \mathbf{m} having the Maxwellian distribution

$$M_{\mathcal{T}}(\mathbf{v}) = \frac{\mathbf{m}}{(2\pi\mathcal{T})^{d/2}} e^{-\frac{\mathbf{m}|\mathbf{v}|^2}{2\mathcal{T}}},$$

with a constant reference background or thermostat temperature \mathcal{T} (i.e., the average of $\int M_{\mathcal{T}} d\mathbf{v} = 1$ and $\int |\mathbf{v}|^2 M_{\mathcal{T}} d\mathbf{v} = \mathcal{T}$). Define

$$Q_L(f) \doteq \int_{\mathbf{w} \in \mathbb{R}^d, \sigma \in S^{d-1}} B_L(|\mathbf{u}|, \mu) f(\mathbf{v}, t) M_{\mathcal{T}}(\mathbf{w}) - f(\mathbf{v}, t) M_{\mathcal{T}}(\mathbf{w})] d\sigma d\mathbf{w}. \quad (2.2.11)$$

Then the corresponding evolution equation for $f(\mathbf{v}, t)$ is given by

$$\begin{aligned} \frac{\partial}{\partial t} f(\mathbf{v}, t) &= Q(f, f) + \Theta Q_L(f) \\ f(\mathbf{v}, 0) &= f_0(\mathbf{v}). \end{aligned} \quad (2.2.12)$$

where $Q(f, f)$, defined as in (2.1.1), is the classical collision integral for elastic interactions (i.e., $\beta = 1$), so it conserves density, momentum and energy. The second integral term in (2.2.12) is a linear collision integral which conserves just the density (but not momentum or energy). The collision rule for this particular case of a mixture can be rewritten as follows:

$$\begin{aligned} \mathbf{u} &= \mathbf{v} - \mathbf{w} \quad \text{the relative velocity} \\ \mathbf{v}' &= \mathbf{v} + \frac{\mathbf{m}}{\mathbf{m} + \mathbf{1}}(|\mathbf{u}|\sigma - \mathbf{u}), \quad \mathbf{w}' = \mathbf{w} - \frac{1}{\mathbf{m} + \mathbf{1}}(|\mathbf{u}|\sigma - \mathbf{u}). \end{aligned} \quad (2.2.13)$$

The coupling constant Θ depends on the initial density, the coupling constants and on \mathbf{m} . The collision kernel B_L of the linear part may not be the same as the one for the non-linear part of the collision integral, however we assume that the *Grad cut-off assumption* (2.1.6) is satisfied and that, in order to secure mass preservation,

the corresponding differential cross section functions b_N and b_L , the non-linear and linear collision kernels respectively, satisfy the renormalized condition

$$\int_{S^{d-1}} b_N\left(\frac{\mathbf{u} \cdot \boldsymbol{\sigma}}{|\mathbf{u}|}\right) + \Theta b_L\left(\frac{\mathbf{u} \cdot \boldsymbol{\sigma}}{|\mathbf{u}|}\right) d\boldsymbol{\sigma} = 1 + \Theta. \quad (2.2.14)$$

This last model describes the evolution of binary interactions of two sets of particles, heavy and light, in a weakly coupled limit, where the heavy particles have reached equilibrium. The heavy particle set constitutes the background or thermostat for the second set of particles. It is the light particle distribution that is modeled by (2.2.12). Indeed, $Q(f, f)$ corresponds to all the collisions which the light particles have with each other and the second linear integral term corresponds to collisions between light and heavy particles at equilibrium given by a classical distribution $M_{\mathcal{T}}(\mathbf{v})$. In this binary 3-dimensional, mixture scenario, collisions are assumed to be isotropic, elastic and the interactions kernels of Maxwell type.

In the particular case of equal mass (i.e., $\mathbf{m} = \mathbf{1}$), the model is of particular interest for the development of numerical schemes and simulations benchmarks. Even though the local interactions are reversible (elastic), it does not conserve the total energy. In such a case, there exists a special set of explicit, in spectral space, self-similar solutions which are attractors for a large class of initial states. When considering the case of Maxwell type interactions in three dimensions, i.e., $B(|\mathbf{u}|, \mu) = b(\mu)$ with a cooling background process corresponding to a time temperature transformation, $\mathcal{T} = \mathcal{T}(t)$ such that $\mathcal{T}(t) \rightarrow 0$ as $t \rightarrow 0$, the models have self similar asymptotics [17; 15] for a large class of initial states. Such long time asymptotics corresponding to dynamically scaled solutions of (2.2.12), in the form of (2.2.10), yields interesting behavior in $f(\mathbf{v}, t)$ for large time, converging to states with power like decay tails in \mathbf{v} . In particular, such a solution $f(\mathbf{v}, t)$ of (2.2.12) will lose moments as time grows, even if the initial state has all moments bounded.

2.3 Properties of the Boltzmann Equation and the Collision Integral

In this section, important properties of the collision integral and the Boltzmann equation are explored in detail.

2.3.1 Well-posedness of the Boltzmann Transport Equation

Existence of bounded global solutions and bounded derivatives is of great importance in the area of Boltzmann equations. *Renormalized solutions* were first developed by Diperna and Lions in the 90's to find existence results for Cauchy problem and boundary value problem for the Boltzmann equation. Most of the theory has been developed for elastic collisions. For inelastic collisions, there is some work done for space homogeneous Boltzmann but for the inhomogeneous case, there is very little work that has been done. For the purpose of completion of presentation, some important results will be presented in this section.

2.3.1.1 The Space Homogeneous Boltzmann Equation

Elastic collisions:

It is a convenient starting point to consider the symmetrized collision operator with cutoff

$$Q^M(f, g) = \frac{1}{2} \int d\mathbf{w} \int_{\mathbf{n} \cdot (\mathbf{v} - \mathbf{w}) \geq 0} d\mathbf{n} \cdot (\mathbf{v} - \mathbf{w}) \chi_M(|\mathbf{v} - \mathbf{w}|) (f' g'_* + g' f'_* - f g_* - g f_*) \quad (2.3.1)$$

where $\chi_M : \mathbb{R}^+ \rightarrow \mathbb{R}$ is defined by $\chi_M(r) = 1$ $r \leq M$ and zero otherwise i.e., ignoring the collisions between particles with a relative velocity bigger than M . Consider a modified initial value problem for the space homogeneous Boltzmann

equation:

$$\begin{aligned}\partial_t f^M &= Q^M(f^M, f^M) \\ f^M(., 0) &= f_0.\end{aligned}\tag{2.3.2}$$

For the modified problem (2.3.2) with (2.3.1) the following theorem exists:

Theorem 2.3.1. [35] Arkeryd '71-'73: *There exists a unique positive solution $f^M \in C^1([0, T]; L^1(\mathbb{R}^3))$ to the modified initial value problem (2.3.2) with (2.3.1) for arbitrary times $T \geq 0$, provided that $f_0 \geq 0$ and $\int f_0 = 1$. Suppose in addition that $E(f_0) = \frac{1}{2} \int |\mathbf{v}|^2 f_0(v) d\mathbf{v}$ and $H(f_0) = \int f_0 \log(f_0) d\mathbf{v}$ (energy and entropy) are initially finite. Then*

$$\begin{aligned}E(f_0) &= E(f^M(\mathbf{v}, t)) \\ H(f^M(\mathbf{v}, t)) &\leq H(f_0).\end{aligned}$$

Define $\|f\|_{1,s} = \int (1 + |\mathbf{v}|^2)^{s/2} |f(\mathbf{v})| d\mathbf{v}$ and the associated family of Banach spaces $L_s^1 = \{f : \|f\|_{1,s} < \infty\}$. Then for the original initial value problem:

Theorem 2.3.2. [35] Arkeryd '71-'73: *Let $f_0 \geq 0$ be an initial datum with finite entropy such that $f_0 \in L_4^1$. Then there exists a unique $f \in C^1([0, T]; L^1)$ satisfying the space homogeneous Boltzmann equation. Moreover $f(v, t) \in L_4^1$ and $H(f(\mathbf{v}, t)) \leq H(f_0(\mathbf{v}))$.*

An L^∞ -estimate was developed as follows:

Theorem 2.3.3. [35]: *Suppose that $f(\mathbf{v}) \leq \frac{C}{(1+|\mathbf{v}|^2)^{s/2}}$ with $s > 6$. Then the solutions of the Boltzmann equation $f(\mathbf{v}, t)$, (2.1.1) - (2.1.5) satisfies:*

$$\sup_{t \in \mathbb{R}^+} \|f(\mathbf{v}, t)\|_\infty < C$$

where C depends only on f_0 . In addition, for almost all $\mathbf{v} \in \mathbb{R}^3$ and all $t \in \mathbb{R}^+$, $f(\mathbf{v}, t)$ is differentiable in time and

$$\partial_t f = Q(f, f)$$

pointwise.

In the past decade, better estimates for the bound on the solutions to space homogeneous Boltzmann equation were developed. Some of the results are presented here for a general $d \geq 2$.

Theorem 2.3.4.

(1) If

$$0 < f_0 \in (L_2^1 \cap L^\infty)(\mathbb{R}^d),$$

then

$$f(t, \mathbf{v}) \in C^\infty((0, \infty), (L_k^1 \cap L^\infty)(\mathbb{R}^d)) \quad \forall k > 0.$$

(2) Propagation of L_{exp}^1 estimates [7; 50; 19]: In addition, if

$$f_0 \in L_{exp, r}^1 = \left\{ f : \int_{\mathbf{v}} f(\mathbf{v}, t) e^{r|\mathbf{v}|^2} d\mathbf{v} < \infty \right\},$$

then, $\exists r_* < r$ such that

$$f(\mathbf{v}, t) \in L_{exp, r_*}^1.$$

This estimate is valid for both elastic variable hard potentials and inelastic hard spheres.

(3) Propagation of L_{exp}^∞ estimates [50; 69; 2]: If

$$0 < C_1 e^{-r_1|\mathbf{v}|^2} < f_0(\mathbf{v}) < C_2 e^{-r_2|\mathbf{v}|^2},$$

then

$$0 < \bar{C}_1 e^{-r_{1*}|\mathbf{v}|^2} < f_0(\mathbf{v}) < \bar{C}_2 e^{-r_{2*}|\mathbf{v}|^2},$$

where $r_{1*} > r_1 > r_2 > r_{2*} \quad \forall t$.

(4) *Weighted bound estimates for derivatives [2; 75] for elastic variable hard potentials:*

(i) *If $f_0 \in (L_2^1 \cap H_1^s)(\mathbb{R}^d)$ then \exists a unique solution $f(\mathbf{v}, t) \in (C^\infty(0, \infty), C^\infty(\mathbb{R}^d))$.*

(ii) *If*

$$0 \leq C_1 e^{-r_1|\mathbf{v}|^2} \leq |D^\alpha f_0(\mathbf{v})| \leq C_2 e^{-r_2|\mathbf{v}|^2},$$

then $\exists r_{1}, r_{2*}$ such that*

$$0 \leq \bar{C}_1 e^{-r_{1*}|\mathbf{v}|^2} \leq |D^\alpha f(\mathbf{v}, t)| \leq \bar{C}_2 e^{-r_{2*}|\mathbf{v}|^2}.$$

Inelastic collisions:

For a detailed investigation of various aspects of the inelastic Maxwell potential space homogeneous Boltzmann equation like existence and uniqueness of solutions, self-similar solutions and moment equations, the work of Bobylev, Carrillo and Gamba [9] serves as a good reference. In the hard sphere case, a complete study for inelastic interactions has been done by Gamba, Panferov and Villani [48], where a diffusively granular media is considered.

2.3.1.2 The Space Inhomogeneous Boltzmann Equation

Considering the Space inhomogeneous Boltzmann equation have:

Theorem 2.3.5. *Local existence and uniqueness [35] Kaniel-Shinbrot, Babovsky: Suppose that $f_0 \in L_+^1(\Omega \times \mathbb{R}^3)$ and a.e. $0 \leq f_0(\mathbf{x}, \mathbf{v}) \leq C e^{-\beta_0|\mathbf{v}|^2}$ for some $C, \beta_0 > 0$, and impose the specular reflection boundary condition for $\mathbf{x} \in \partial\Omega$. Then there is a*

$t_0 > 0$ (depending on C, β_0) such that the Cauchy problem for the Boltzmann equation with initial value f_0 has an a.e. non-negative mild solution $f(\mathbf{x}, \mathbf{v}, t)$, defined for $t \in [0, t_0)$. In particular, $t \rightarrow f(T^t(\mathbf{x}, \mathbf{v}), t)$ is absolutely continuous for almost all (\mathbf{x}, \mathbf{v}) .

Theorem 2.3.6. *Global existence and uniqueness for a rare gas cloud in all space [35] Kaniel-Shinbrot iteration scheme: Suppose that $f_0 \in L^1_+(\mathbb{R}^3_x \times \mathbb{R}^3_v)$ and that a.e.*

$$0 \leq f_0(\mathbf{x}, \mathbf{v}) \leq b e^{-\beta_0(|\mathbf{x}|^2 + |\mathbf{v}|^2)}$$

for some $b > 0, \beta_0 > 0$. Then, if $b.C$ is sufficiently small, the Cauchy problem for the Boltzmann equation has a unique mild solution, which satisfies

$$0 \leq f(\mathbf{x}, \mathbf{v}, t) \leq C.b e^{-\beta_0(|\mathbf{x} - t\mathbf{v}|^2)} \text{ a.e.}$$

For the initial-boundary value problem, the global existence of a *renormalized solution* for the Cauchy problem for the Boltzmann equation was first obtained by DiPerna and Lions. Their proof applies to non-negative data with finite energy and entropy. When considering the time evolution of a rarefied gas in a vessel Ω whose boundaries ($\partial\Omega$ piecewise C^1) are kept at a constant temperature, one needs to extend the DiPerna-Lions proof. In this aspect, Hamdache proved the global existence of weak solution by assuming the boundary condition to be a linear combination of Diffusive reflection term and Specular reflection term. Arkeryd and Cercignani treated the case with non-isothermal boundaries. The space inhomogeneous theory is more advanced for the linear Boltzmann equation than for the fully nonlinear case.

2.3.2 Weak Form of the Collision Integral

The Boltzmann collision operator can be re-written in the following form with $(\mathbf{v}_* = \mathbf{w}; f = f(\mathbf{v}), f'_* = f(\mathbf{v}_*), f_* = f(\mathbf{v}_*), f = f(\mathbf{v})$, ignoring the dependence in \mathbf{x}, t):

$$Q(f, f) \doteq \int_{\mathbf{v}_* \in \mathbb{R}^d} \int_{\sigma \in S^{d-1}} B(|\mathbf{u}|, \mu) [J_\beta f'_* f_* - f f_*] d\sigma d\mathbf{v}_*. \quad (2.3.3)$$

Multiplying equation (2.3.3) with a suitably regular test function $\phi(\mathbf{v})$ and exploring the symmetric properties of the collision integral, one of the weak forms of the collision integral is given as:

$$\int_{\mathbb{R}^d} Q(f, f) \phi(\mathbf{v}) d\mathbf{v} = \int_{\mathbb{R}^d} \int_{\mathbb{R}^d} \int_{S^{d-1}} f f_* B(\mathbf{u}, \sigma) (\phi' - \phi) d\mathbf{v}_* d\sigma d\mathbf{v}. \quad (2.3.4)$$

Another weak form is

$$\begin{aligned} \int_{\mathbb{R}^d} Q(f, g) \phi(\mathbf{v}) d\mathbf{v} = \\ \frac{1}{8} \int_{\mathbb{R}^d} \int_{\mathbb{R}^d} \int_{S^{d-1}} (f'g_* + g'f_* - fg_* - gf_*) B(\mathbf{u}, \sigma) (\phi + \phi_* - \phi' - \phi'_*) d\mathbf{v}_* d\sigma d\mathbf{v}. \end{aligned}$$

Equation (2.3.4) is an important property of the collision integral that is instrumental in deriving the deterministic scheme proposed in this dissertation. In the rest of the dissertation, we use $d = 3$.

2.3.3 H - Theorem for the Space Homogeneous Boltzmann Equation

Boltzmann Inequality or H-Theorem: If f is a non-negative function such that $\log(f)Q(f, f)$ is integrable and the manipulations involved in collision invariants hold for $\phi = \log(f)$ then:

$$\int_{\mathbb{R}^3} \log(f) Q(f, f) d\mathbf{v} \leq 0$$

Further, the equality sign applies if and only if $\log(f)$ is a collision invariant with $c < 0$:

$$f = \exp(a + \mathbf{b} \cdot \mathbf{v} + c|\mathbf{v}|^2)$$

i.e., a Maxwellian distribution. Above inequality is true only for **elastic** interactions. Nothing can be said for inelastic collisions. Starting from the space inhomogeneous **Elastic** Boltzmann equation multiplying both sides with $\log(f)$ and integrating with respect to \mathbf{v} , obtain:

$$\frac{\partial \mathcal{H}}{\partial t} + \frac{\partial}{\partial x} \mathcal{J} = \mathcal{S}$$

where

$$\begin{aligned}\mathcal{H} &= \int_{\mathbb{R}^3} f \log(f) d\mathbf{v} \\ \mathcal{J} &= \int_{\mathbb{R}^3} \mathbf{v} f \log(f) d\mathbf{v} \\ \mathcal{S} &= \int_{\mathbb{R}^3} \log(f) Q(f, f) d\mathbf{v}\end{aligned}$$

With $\mathcal{H} = \int_{\mathbb{R}^3} f \log(f) d\mathbf{v}$; $\mathcal{S} = \int_{\mathbb{R}^3} \log(f) Q(f, f) d\mathbf{v}$ from the Boltzmann inequality have $\mathcal{S} \leq 0$ and $\mathcal{S} = 0$ if and only if f is a Maxwellian. This then implies for space homogeneous case:

$$\frac{\partial \mathcal{H}}{\partial t} = \mathcal{S} \leq 0$$

This results in a simplified form, the **H-Theorem** (space homogeneous case):

\mathcal{H} is a decreasing quantity, unless f is a Maxwellian (in which case the time derivative of \mathcal{H} is zero). Again such a theorem exists only for **elastic** collisions. There is no H-Theorem for inelastic interactions.

2.3.4 Conservation Equations

In the elastic collision case, multiplying the Boltzmann equation (2.1.1) by $1, \mathbf{v}, |\mathbf{v}|^2$ and integrating the result over the whole space of \mathbf{v} , we obtain the following con-

servation equations:

$$\begin{aligned} \frac{\partial \rho}{\partial t} + \nabla_{\mathbf{x}} \cdot (\rho \mathbf{V}) &= 0 \\ \frac{\partial}{\partial t}(\rho V_i) + \sum_{j=1}^d \frac{\partial}{\partial x_j}(\rho V_i V_j + p_{ij}) &= \rho F_i \quad \forall i = 1, 2, 3, \\ \frac{\partial}{\partial t} \left[\rho \left(e + \frac{1}{2} |\mathbf{V}|^2 \right) \right] + \sum_{j=1}^d \frac{\partial}{\partial x_j} \left[\rho V_j \left(e + \frac{1}{2} |\mathbf{V}|^2 \right) + \mathbf{V} \cdot \mathbf{p}_j + q_j \right] &= \rho \mathbf{V} \cdot \mathbf{F}, \end{aligned} \quad (2.3.5)$$

where \mathbf{F} is assumed to be independent of molecular velocities \mathbf{v} . The collision term vanishes on integration in the velocity domain. Equations (2.3.5) are referred to as the *conservation equations of mass, momentum and energy* respectively. In classical fluid dynamics in statistical equilibrium, p_{ij} and q_i are assumed to be in appropriate forms to close the system (2.3.5). For example,

$$p_{ij} = p \delta_{ij}, \quad q_i = 0, \quad (2.3.6)$$

or

$$p_{ij} = p \delta_{ij} - \mu \left(\frac{\partial V_i}{\partial x_j} + \frac{\partial V_j}{\partial x_i} - \frac{2}{3} \sum_{k=1}^d \frac{\partial V_k}{\partial x_k} \delta_{ij} \right) - \mu_B \sum_{k=1}^d \frac{\partial V_k}{\partial x_k} \delta_{ij}, \quad q_i = -\lambda \frac{\partial T}{\partial x_i}, \quad (2.3.7)$$

where δ_{ij} is Kronecker's delta and μ, μ_B and λ , called the *viscosity*, *bulk viscosity*, and *thermal conductivity* of the gas respectively, are functions of temperature. The set of equations with the former stress and heat flow is called the *Euler equations*, and the set with the latter the *Navier-Stokes equations*. The relations for p_{ij} and q_i given in (2.3.7) are called the Newton's law and Fourier's law, respectively.

2.3.4.1 The Maxwell Boltzmann Distribution (Equilibrium Distribution)

For the space homogeneous Boltzmann equation (so $\nabla_{\mathbf{x}} \cdot f = 0$), when the force field $\mathbf{F} = \mathbf{0}$ there exists a stationary ($\frac{\partial f}{\partial t} = 0$) solution $M_{\rho, \mathbf{V}, T}$ called the *Maxwell*

Boltzmann (or Maxwellian) distribution with constant parameters ρ , \mathbf{V} and T given by

$$M_{\rho, \mathbf{V}, T} = \frac{\rho}{(2\pi \mathbf{R}T)^{3/2}} \exp\left(-\frac{|\mathbf{v} - \mathbf{V}|^2}{2\mathbf{R}T}\right). \quad (2.3.8)$$

2.3.4.2 Kinetic Boundary Conditions: Simple boundary

On a boundary or a wall where there is no mass flux across it, which will be called a *simple boundary*, the following condition called the *Maxwell-type condition* is widely used (for $d = 3$):

$$\begin{aligned} f(\mathbf{x}, \mathbf{v}, t) &= (1 - \alpha)f(\mathbf{x}, \mathbf{v} - 2[(\mathbf{v} - \mathbf{V}_w) \cdot \mathbf{n}]\mathbf{n}, t) \\ &\quad + \frac{\alpha\sigma_w}{(2\pi \mathbf{R}T_w)^{3/2}} \exp\left(-\frac{|\mathbf{v} - \mathbf{V}_w|^2}{2\mathbf{R}T_w}\right) \quad [(\mathbf{v} - \mathbf{V}_w) \cdot \mathbf{n} > 0], \\ \sigma_w &= -\left(\frac{2\pi}{\mathbf{R}T_w}\right)^{1/2} \int_{[(\mathbf{v} - \mathbf{V}_w) \cdot \mathbf{n} < 0]} [(\mathbf{v} - \mathbf{V}_w) \cdot \mathbf{n}] f(\mathbf{x}, \mathbf{v}, t) d\mathbf{v}, \end{aligned} \quad (2.3.9)$$

where T_w and \mathbf{V}_w are, respectively, the temperature and velocity of the boundary; \mathbf{n} is the unit normal vector to the boundary, pointed to the gas, and α ($0 \leq \alpha \leq 1$) is the *accommodation coefficient*. These quantities depend on the position of the boundary. In (2.3.9), the case $\alpha = 1$ is called the *diffuse-reflection condition*, and $\alpha = 0$ the *specular-reflection condition*.

More generally, the boundary condition is expressed in terms of a *scattering kernel* $K_B(\mathbf{v}, \mathbf{v}_*, \mathbf{x}, t)$ as

$$f(\mathbf{x}, \mathbf{v}, t) = \int_{(\mathbf{v}_* - \mathbf{V}_w) \cdot \mathbf{n} < 0} K_B(\mathbf{v}, \mathbf{v}_*, \mathbf{x}, t) f(\mathbf{x}, \mathbf{v}_*, t) d\mathbf{v}_* \quad [(\mathbf{v} - \mathbf{V}_w) \cdot \mathbf{n} > 0]. \quad (2.3.10)$$

The kernel $K_B(\mathbf{v}, \mathbf{v}_*, \mathbf{x}, t)$ is required to satisfy the following conditions:

- $K_B(\mathbf{v}, \mathbf{v}_*) \geq 0 \quad [(\mathbf{v} - \mathbf{V}_w) \cdot \mathbf{n} > 0, (\mathbf{v}_* - \mathbf{V}_w) \cdot \mathbf{n} < 0].$

- $-\int_{[(\mathbf{v}-\mathbf{V}_w)\cdot\mathbf{n}>0]} \frac{(\mathbf{v}-\mathbf{V}_w)\cdot\mathbf{n}}{(\mathbf{v}_*-\mathbf{V}_w)\cdot\mathbf{n}} K_B(\mathbf{v}, \mathbf{v}_*) d\mathbf{v} = 1 \quad [(\mathbf{v}-\mathbf{V}_w)\cdot\mathbf{n} > 0, (\mathbf{v}_*-\mathbf{V}_w)\cdot\mathbf{n} < 0],$
which corresponds to the condition of a simple boundary.
- When the kernel K_B is determined by the local condition of the boundary,

$$f_B(\mathbf{v}) = \int_{[(\mathbf{v}_*-\mathbf{V}_w)\cdot\mathbf{n}<0]} K_B(\mathbf{v}, \mathbf{v}_*) f_B(\mathbf{v}_*) d\mathbf{v}_* \quad [(\mathbf{v}-\mathbf{V}_w)\cdot\mathbf{n} > 0], \quad (2.3.11)$$

where

$$f_B(\mathbf{v}) = \frac{\rho}{2\pi\mathbf{R}T_w} \exp\left(-\frac{|\mathbf{v}-\mathbf{V}_w|^2}{2\mathbf{R}T_w}\right),$$

with ρ being arbitrary, and the other Maxwellians do not satisfy the relation (2.3.11). This uniqueness condition excludes the specular reflection. The condition (2.3.11) is the result of the local property of the kernel K_B and the natural requirement that the equilibrium state at temperature \bar{T}_w and the velocity \bar{V}_w is established in a box with a uniform temperature \bar{T}_w and moving with a uniform velocity \bar{v}_w .

For the Maxwell-type condition (2.3.9), the scattering kernel K_B is given by

$$\begin{aligned} K_B(\mathbf{v}, \mathbf{v}_*) &= K_{BM}(\mathbf{v}, \mathbf{v}_*) \\ &= \frac{-\alpha}{2\pi(\mathbf{R}T_w)^2} [(\mathbf{v}_* - \mathbf{V}_w) \cdot \mathbf{n}] \exp\left(-\frac{|\mathbf{v}-\mathbf{V}_w|^2}{2\mathbf{R}T_w}\right) \\ &\quad + (1-\alpha)\delta(\mathbf{v}_* - [\mathbf{v} - 2[(\mathbf{v}-\mathbf{V}_w) \cdot \mathbf{n}]\mathbf{n}]), \end{aligned}$$

where $\delta(\mathbf{v})$ is the Dirac delta function.

When dealing with special boundary conditions like an interface of a gas with its condensed phase, a mixed-type condition is often used [85].

2.4 Non-dimensional Expressions

Throughout the rest of the dissertation, nondimensional variables and equations will be used. Such a representation is essential as it captures the flow scales of the

physical system. In order to nondimensionalize the Boltzmann equation and related variables, we introduce reference quantities. Let x_r, p_r, T_r and t_r be reference length, pressure, temperature and time, respectively, and let $\rho_r = \frac{p_r}{\mathbf{R}T_r}, v_r = \sqrt{2\mathbf{R}T_r} =$ reference velocity. Then the nondimensional variables are defined as follows:

$$\begin{aligned}
\hat{\mathbf{x}} &= \frac{\mathbf{x}}{x_r}, & \hat{t} &= \frac{t}{t_r}, & \hat{\mathbf{v}} &= \frac{\mathbf{v}}{v_r}, \\
\hat{f} &= \frac{f}{\rho_r v_r^{-3}}, & \hat{\mathbf{F}} &= \frac{\mathbf{F}}{v_r^2/x_r}, & \hat{\rho} &= \frac{\rho}{\rho_r}, \\
\hat{\mathbf{V}} &= \frac{\mathbf{V}}{v_r}, & \hat{T} &= \frac{T}{T_r}, & \hat{p} &= \frac{p}{p_r}, \\
\hat{\mathbf{p}} &= \frac{\mathbf{p}}{p_r}, & \hat{\mathbf{q}} &= \frac{\mathbf{q}}{p_r v_r}, & \hat{\mathbf{V}}_w &= \frac{\mathbf{V}_w}{v_r}, \\
& & & & \hat{T}_w &= \frac{T_w}{T_r}, \\
& & & & \hat{p}_w &= \frac{p_w}{p_r} = \hat{\rho}_w \hat{T}_w.
\end{aligned} \tag{2.4.1}$$

Then, the nondimensional form of the Boltzmann equation for \hat{f} is

$$\begin{aligned}
&\text{Sh} \frac{\partial \hat{f}}{\partial \hat{t}} + \hat{\mathbf{v}} \cdot \nabla_{\hat{\mathbf{x}}}(\hat{\mathbf{f}}) + \nabla_{\hat{\mathbf{v}}} \cdot (\hat{\mathbf{f}} \hat{\mathbf{F}}) = \frac{1}{\mathbf{k}} \hat{\mathbf{Q}}(\hat{\mathbf{f}}, \hat{\mathbf{f}}), \\
\hat{Q}(\hat{f}, \hat{g}) &= \frac{1}{2} \int_{\hat{\mathbf{v}}_* \times \alpha} (\hat{f}' \hat{g}'_* + \hat{f}'_* \hat{g}' - \hat{f} \hat{g}'_* - \hat{f}'_* \hat{g}') \hat{B} d\Omega(\alpha) d\hat{\mathbf{v}}_*,
\end{aligned} \tag{2.4.2}$$

where

$$\begin{aligned}
\text{Sh} &= \frac{x_r}{t_r \sqrt{2\mathbf{R}T_r}}, \\
k &= \frac{\sqrt{\pi}}{2} Kn, \\
\hat{B} &= B(|\alpha \cdot (\hat{\mathbf{v}}_* - \hat{\mathbf{v}})| / |\hat{\mathbf{v}}_* - \hat{\mathbf{v}}|, |\hat{\mathbf{v}}_* - \hat{\mathbf{v}}|), \\
d\hat{\mathbf{v}} &= d\hat{v}_1 d\hat{v}_2 d\hat{v}_3, & d\hat{\mathbf{v}} &= d\hat{v}_{*1} d\hat{v}_{*2} d\hat{v}_{*3}, \\
\hat{f} &= \hat{f}(\hat{\mathbf{v}}), & \hat{f}_* &= \hat{f}(\hat{\mathbf{v}}_*), & \hat{f}' &= \hat{f}(\hat{\mathbf{v}}'), & \hat{f}'_* &= \hat{f}(\hat{\mathbf{v}}'_*), \\
\hat{\mathbf{v}}' &= \hat{\mathbf{v}} + \alpha(\alpha \cdot (\hat{\mathbf{v}}_* - \hat{\mathbf{v}})), & \hat{\mathbf{v}}'_* &= \hat{\mathbf{v}}_* - \alpha(\alpha \cdot (\hat{\mathbf{v}}_* - \hat{\mathbf{v}})),
\end{aligned} \tag{2.4.3}$$

where Sh is called the *Strahal number* and Kn is the *Knudsen number*. The nondimensional generalized collision integral satisfies the following symmetry relation for

$$\phi(\hat{\mathbf{v}}), \hat{f}(\hat{\mathbf{v}}), \hat{g}(\hat{\mathbf{v}}),$$

$$\int \phi(\hat{\mathbf{v}}) \hat{Q}(\hat{f}, \hat{g}) d\hat{\mathbf{v}} = \frac{1}{8} \int (\phi + \phi_* - \phi' - \phi'_*) (\hat{f}' \hat{g}'_* + \hat{f}_* \hat{g}' - \hat{f} \hat{g}'_* - \hat{f}'_* \hat{g}) \hat{B} d\Omega d\hat{\mathbf{v}}_* d\hat{\mathbf{v}}. \quad (2.4.4)$$

From (2.4.4) and (2.4.2), the relations between the nondimensional macroscopic variables $\hat{\rho}, \hat{\mathbf{V}}, \hat{T}$, etc. and the nondimensional velocity distribution function \hat{f} can be derived to give

$$\begin{aligned} \hat{\rho} &= \int \hat{f} d\hat{\mathbf{v}}, \\ \hat{\rho} \hat{\mathbf{V}} &= \int \hat{\mathbf{v}} \hat{f} d\hat{\mathbf{v}}, \\ \frac{3}{2} \hat{\rho} \hat{T} &= \int |\hat{\mathbf{v}} - \hat{\mathbf{V}}|^2 \hat{f} d\hat{\mathbf{v}}, \\ \hat{p} &= \hat{\rho} \hat{T}, \\ \hat{\mathbf{p}} &= 2 \int (\hat{\mathbf{v}} - \hat{\mathbf{V}})(\hat{\mathbf{v}} - \hat{\mathbf{V}})^T \hat{f} d\hat{\mathbf{v}}, \\ \hat{\mathbf{q}} &= 2 \int (\hat{\mathbf{v}} - \hat{\mathbf{V}}) |\hat{\mathbf{v}} - \hat{\mathbf{V}}|^2 \hat{f} d\hat{\mathbf{v}}. \end{aligned} \quad (2.4.5)$$

The nondimensional Maxwellian distribution function is given by

$$\hat{M}_{\hat{\rho}, \hat{\mathbf{V}}, \hat{T}} = \frac{\hat{\rho}}{(\pi \hat{T})^{3/2}} \exp \left(-\frac{|\hat{\mathbf{v}} - \hat{\mathbf{V}}|^2}{\hat{T}} \right). \quad (2.4.6)$$

The nondimensional forms of the conservation equations are then

$$\begin{aligned} \text{Sh} \frac{\partial \hat{\rho}}{\partial \hat{t}} + \nabla_{\hat{\mathbf{x}}} \cdot (\hat{\rho} \hat{\mathbf{V}}) &= 0 \\ \text{Sh} \frac{\partial}{\partial \hat{t}} (\hat{\rho} \hat{V}_i) + \sum_{j=1}^3 \frac{\partial}{\partial \hat{x}_j} (\hat{\rho} \hat{V}_i \hat{V}_j) + \frac{1}{2} \hat{p}_{ij} &= \hat{\rho} \hat{F}_i \quad \forall i = 1, 2, 3 \\ \text{Sh} \frac{\partial}{\partial \hat{t}} \left[\hat{\rho} \left(\frac{1}{2} \hat{T} + |\hat{\mathbf{V}}|^2 \right) \right] + \sum_{j=1}^3 \frac{\partial}{\partial \hat{x}_j} \left[\hat{\rho} \hat{V}_j \left(\frac{1}{2} \hat{T} + |\hat{\mathbf{V}}|^2 \right) + \hat{\mathbf{V}} \cdot \hat{\mathbf{p}}_j + \hat{q}_j \right] \\ &= 2 \hat{\rho} \hat{\mathbf{V}} \cdot \hat{\mathbf{F}}, \end{aligned} \quad (2.4.7)$$

where $\hat{\mathbf{F}}$ is assumed to be independent of $\hat{\mathbf{v}}$.

The Maxwell-type nondimensional boundary conditions on a simple boundary can be expressed as:

$$\begin{aligned}
\hat{f}(\hat{\mathbf{x}}, \hat{\mathbf{v}}, \hat{\mathbf{t}}) &= (1 - \alpha)\hat{f}(\hat{\mathbf{x}}, \hat{\mathbf{v}} - 2[(\hat{\mathbf{v}} - \hat{\mathbf{V}}_{\mathbf{w}}) \cdot \mathbf{n}]\mathbf{n}, \hat{\mathbf{t}}) \\
&\quad + \frac{\alpha\hat{\sigma}_w}{(\pi\hat{T}_w)^{3/2}} \exp\left(-\frac{|\hat{\mathbf{v}} - \hat{\mathbf{V}}_{\mathbf{w}}|^2}{\hat{T}_w}\right) \quad [(\hat{\mathbf{v}} - \hat{\mathbf{V}}_{\mathbf{w}}) \cdot \mathbf{n} > 0], \\
\hat{\sigma}_w &= -2\left(\frac{\pi}{\hat{T}_w}\right)^{1/2} \int_{(\hat{\mathbf{v}} - \hat{\mathbf{V}}_{\mathbf{w}}) \cdot \mathbf{n} < 0} [(\hat{\mathbf{v}} - \hat{\mathbf{V}}_{\mathbf{w}}) \cdot \mathbf{n}] \hat{f}(\hat{\mathbf{x}}, \hat{\mathbf{v}}, \hat{\mathbf{t}}) d\hat{\mathbf{v}}. \quad (2.4.8)
\end{aligned}$$

Similarly, the nondimensional form of the boundary kernel can also be derived [85]. Depending on the underlying physics and the rarefied gas system being considered, other nondimensional forms of the Boltzmann equation can be derived using the corresponding flow scales as reference variables.

In the rest of the dissertation, nondimensional equations and variables are used, but to simplify notation, the “hats” in the nondimensional notation are dropped.

Chapter 3

The Conservative Deterministic Spectral Method

In the current chapter, the spectral approach to computing the collision integral, is described in detail along with accuracy and consistency results of the modified (conservative) spectral method. Extensions to a standard Fourier approximation estimate will be proven for a finite domain ($\mathbf{v} \in \Omega_v = [-L, L]^3$) of our interest in a weighted $L^2(\Omega_v)$ norm, i.e., $L_m^2(\Omega_v)$. A bound on the optimization correction is developed in terms of spectral accuracy. Based on the work of [48], we prove Sobolev bounds for the asymmetric collision integral. The chapter is organized as follows. In Section 3.1, some preliminaries and description of the spectral method is presented. In Section 3.2, the conservation correction method is described as an extension to an isoperimetric type of problem (isomoment problem). In Section 3.3, the accuracy and consistency estimates of the conservative spectral method are proved.

3.1 Spectral Collision Integral Representation

One of the pivotal points in the derivation of the spectral numerical method for the computation of the non-linear Boltzmann equation lies in the representation of the collision integral in Fourier space by means of its weak form. For ease of notation, the time and space dependence in f are ignored in the rest of this chapter. Then for a suitably regular test function $\psi(\mathbf{v})$, the weak form of the collision integral is

given by

$$\int_{\mathbf{v} \in \mathbb{R}^d} Q(f, f) \psi(\mathbf{v}) d\mathbf{v} = \int_{(\mathbf{w}, \mathbf{v}) \in \mathbb{R}^d \times \mathbb{R}^d, \sigma \in S^{d-1}} f(\mathbf{v}) f(\mathbf{w}) B(|\mathbf{u}|, \mu) [\psi(\mathbf{v}') - \psi(\mathbf{v})] d\sigma d\mathbf{w} d\mathbf{v}, \quad (3.1.1)$$

where $\mathbf{v}', \mathbf{w}', \mathbf{u}, B(|\mathbf{u}|, \mu)$ are given by (2.1.5). In particular, taking $d = 3$ and

$$\psi(\mathbf{v}) = e^{-i\zeta \cdot \mathbf{v}} / (\sqrt{2\pi})^3,$$

where ζ is the Fourier variable, we get the Fourier Transform of the collision integral through its weak form

$$\begin{aligned} \widehat{Q}(\zeta) &= \frac{1}{(\sqrt{2\pi})^3} \int_{\mathbf{v} \in \mathbb{R}^3} Q(f, f) e^{-i\zeta \cdot \mathbf{v}} d\mathbf{v} \\ &= \int_{(\mathbf{w}, \mathbf{v}) \in \mathbb{R}^3 \times \mathbb{R}^3, \sigma \in S^2} f(\mathbf{v}) f(\mathbf{w}) \frac{B(|\mathbf{u}|, \mu)}{(\sqrt{2\pi})^3} [e^{-i\zeta \cdot \mathbf{v}'} - e^{-i\zeta \cdot \mathbf{v}}] d\sigma d\mathbf{w} d\mathbf{v}. \end{aligned} \quad (3.1.2)$$

We will use $\widehat{[\cdot]} = \mathcal{F}(\cdot)$ to denote the Fourier transform and \mathcal{F}^{-1} for the classical inverse Fourier transform. Plugging in the definitions of collision kernel $B(|\mathbf{u}|, \mu) = C_\lambda(\sigma) |\mathbf{u}|^\lambda$ (which in the case of isotropic collisions would just be the Variable Hard Potential collision kernel) and the post collisional velocity, \mathbf{v}' from (2.1.5), we get

$$\widehat{Q}(\zeta) = \frac{1}{(\sqrt{2\pi})^3} \int_{(\mathbf{w}, \mathbf{v}) \in \mathbb{R}^3 \times \mathbb{R}^3, \sigma \in S^2} f(\mathbf{v}) f(\mathbf{w}) C_\lambda(\sigma) |\mathbf{u}|^\lambda e^{-i\zeta \cdot \mathbf{v}} [e^{-i\frac{\beta}{2}\zeta \cdot (|\mathbf{u}|\sigma - \mathbf{u})} - 1] d\sigma d\mathbf{w} d\mathbf{v}. \quad (3.1.3)$$

From $\mathbf{u} = \mathbf{v} - \mathbf{w}$, have $\mathbf{w} = \mathbf{v} - \mathbf{u} \Rightarrow d\mathbf{w} = d\mathbf{u}$ [Jacobian of this change of variable matrix is 1]. This gives

$$\widehat{Q}(\zeta) = \int_{\mathbf{v} \in \mathbb{R}^3} \int_{\mathbf{u} \in \mathbb{R}^3} \int_{\sigma \in S^2} f(\mathbf{v}) f(\mathbf{v} - \mathbf{u}) C_\lambda(\sigma) |\mathbf{u}|^\lambda e^{-i\zeta \cdot \mathbf{v}} [e^{-i\frac{\beta}{2}\zeta \cdot (|\mathbf{u}|\sigma - \mathbf{u})} - 1] d\sigma d\mathbf{u} d\mathbf{v} \quad (3.1.4)$$

Upon further simplification, (3.1.4) can be rewritten as

$$\begin{aligned} \widehat{Q}(\zeta) &= \frac{1}{(\sqrt{2\pi})^3} \int_{\mathbf{u} \in \mathbb{R}^3} G_{\lambda, \beta}(\mathbf{u}, \zeta) \int_{\mathbf{v} \in \mathbb{R}^3} f(\mathbf{v}) f(\mathbf{v} - \mathbf{u}) e^{-i\zeta \cdot \mathbf{v}} d\mathbf{v} d\mathbf{u} \\ &= \int_{\mathbf{u} \in \mathbb{R}^3} G_{\lambda, \beta}(\mathbf{u}, \zeta) \mathcal{F}[f(\mathbf{v}) f(\mathbf{v} - \mathbf{u})] d\mathbf{u}, \end{aligned} \quad (3.1.5)$$

where

$$\begin{aligned}
G_{\lambda,\beta}(\mathbf{u}, \zeta) &= \int_{\sigma \in S^2} C_\lambda(\sigma) |\mathbf{u}|^\lambda [e^{-i\frac{\beta}{2}\zeta \cdot (|\mathbf{u}|\sigma - \mathbf{u})} - 1] d\sigma \\
&= |\mathbf{u}|^\lambda \left[e^{i\frac{\beta}{2}\zeta \cdot \mathbf{u}} \int_{\sigma \in S^2} (C_\lambda(\sigma) e^{-i\frac{\beta}{2}|\mathbf{u}|\zeta \cdot \sigma} - 1) d\sigma \right]. \quad (3.1.6)
\end{aligned}$$

Note that (3.1.6) is valid for both isotropic and anisotropic interactions. For the former type, a simplification ensues due to the fact the $C_\lambda(\sigma)$ is independent of $\sigma \in S^2$:

$$G_{\lambda,\beta}(\mathbf{u}, \zeta) = C_\lambda \omega_2 |\mathbf{u}|^\lambda \left[e^{i\frac{\beta}{2}\zeta \cdot \mathbf{u}} \text{sinc}\left(\frac{\beta|\mathbf{u}||\zeta|}{2}\right) - 1 \right]. \quad (3.1.7)$$

Thus, it is seen that the integration over σ on the unit sphere S^2 is completely independent, and there is actually a closed form expression for this integration, given by (3.1.7) in the case of isotropic collisions. In the case of anisotropic collisions, the dependence of C_λ on σ is again isolated into a separate integral over the unit sphere S^2 as given in (3.1.6). The above expression can be transformed for elastic collisions $\beta = 1$ into a form suggested by Rjasanow and Ibragimov [60].

Further simplification of (3.1.5) is possible by observing that the Fourier transform inside the integral can be written in terms of the Fourier transform of $f(\mathbf{v})$ since it can also be written as a convolution of the Fourier transforms. Let $h(\mathbf{v}) = f(\mathbf{v} - \mathbf{u})$.

Then, (3.1.5) can be written as

$$\begin{aligned}
\widehat{Q}(\zeta) &= \int_{\mathbf{u} \in \mathbb{R}^3} G_{\lambda, \beta}(\mathbf{u}, \zeta) \mathcal{F}[f(\mathbf{v})h(\mathbf{v})] d\mathbf{u} = \int_{\mathbf{u} \in \mathbb{R}^3} G_{\lambda, \beta}(\mathbf{u}, \zeta) \frac{1}{(\sqrt{2\pi})^3} (\hat{f} * \hat{h})(\zeta) d\mathbf{u} \\
&= \int_{\mathbf{u} \in \mathbb{R}^3} G_{\lambda, \beta}(\mathbf{u}, \zeta) \frac{1}{(\sqrt{2\pi})^3} \int_{\xi \in \mathbb{R}^3} \hat{f}(\zeta - \xi) \hat{h}(\xi) d\xi d\mathbf{u} \\
&= \int_{\mathbf{u} \in \mathbb{R}^3} G_{\lambda, \beta}(\mathbf{u}, \zeta) \frac{1}{(\sqrt{2\pi})^3} \int_{\xi \in \mathbb{R}^3} \hat{f}(\zeta - \xi) \hat{f}(\xi) e^{-i\xi \cdot \mathbf{u}} d\xi d\mathbf{u} \\
&= \frac{1}{(\sqrt{2\pi})^3} \int_{\xi \in \mathbb{R}^3} \hat{f}(\zeta - \xi) \hat{f}(\xi) \left[\int_{\mathbf{u} \in \mathbb{R}^d} G_{\lambda, \beta}(\mathbf{u}, \zeta) e^{-i\xi \cdot \mathbf{u}} d\mathbf{u} \right] d\xi \\
&= \frac{1}{(\sqrt{2\pi})^3} \int_{\xi \in \mathbb{R}^3} \hat{f}(\zeta - \xi) \hat{f}(\xi) \bar{G}_{\lambda, \beta}(\xi, \zeta) d\xi, \tag{3.1.8}
\end{aligned}$$

where $\bar{G}_{\lambda, \beta}(\xi, \zeta) = \int_{\mathbf{u} \in \mathbb{R}^3} G_{\lambda, \beta}(\mathbf{u}, \zeta) e^{-i\xi \cdot \mathbf{u}} d\mathbf{u}$. Let $\mathbf{u} = r\mathbf{e}$, $\mathbf{e} \in S^2, r \in \mathbb{R}$. Using (3.1.7), this gives

$$\begin{aligned}
\bar{G}_{\lambda, \beta}(\xi, \zeta) &= \int_r \int_{\mathbf{e}} r^2 G(r\mathbf{e}, \zeta) e^{-ir\xi \cdot \mathbf{e}} d\mathbf{e} dr \\
&= 16\pi^2 C_\lambda \int_r r^{\lambda+2} [\text{sinc}(\frac{r\beta|\zeta|}{2}) \text{sinc}(r|\xi - \frac{\beta}{2}\zeta|) - \text{sinc}(r|\xi|)] dr.
\end{aligned}$$

Since the domain of the computation is restricted to $\Omega_v = [-L, L]^3$, $u \in [-2L, 2L]^3$, and so $r \in [0, 2\sqrt{3}L]$ and

$$\bar{G}_{\lambda, \beta}(\xi, \zeta) = 16\pi^2 C_\lambda \int_0^{2\sqrt{3}L} r^{\lambda+2} [\text{sinc}(\frac{r\beta|\zeta|}{2}) \text{sinc}(r|\xi - \frac{\beta}{2}\zeta|) - \text{sinc}(r|\xi|)] dr. \tag{3.1.9}$$

Note that (3.1.9) is evaluated over a sphere with radius $2L$. This sphere contains the domain of interest of u i.e., $[-2L, 2L]^3$. A point worth noting is that the above formulation (3.1.8) results in $O(N^6)$ number of operations, where N is the number of discretizations in each velocity direction. Also, exploiting the symmetric nature in particular cases of the collision kernel, one can reduce the number of operations to $O(N^3 \log N)$.

3.2 Conservation Method - An Isomoment problem

In the current section, we are following the path suggested by [81] for $d = 3$. Let $\Omega_v = [-L, L]^3$ and $\Omega_\zeta = [-L_\zeta, L_\zeta]^3$ be the domains of $\mathbf{v} = (v_1, v_2, v_3)$ and $\zeta = (\zeta_1, \zeta_2, \zeta_3)$ respectively. Define $h_\zeta = \frac{2L_\zeta}{N}$ and $\zeta_i^k = k_i h_\zeta$ for $i = 1, 2, 3$. Also, let

$$\mathbb{P}^N = \text{span}\{e^{i\zeta_k \cdot \mathbf{v}} \mid -L_\zeta \leq \zeta_l^k < L_\zeta, l = 1, 2, 3; -N/2 \leq k_l < N/2\},$$

be the set of trigonometric polynomials of degree N . For the sake of brevity, we denote $\mathbf{k} = (k_1, k_2, k_3)$ and let

$$\sum_{k_1, k_2, k_3 = -N/2}^{N/2+1} = \sum_{|\mathbf{k}| < N/2} = \sum_{\mathbf{k}}.$$

Also, let $\Pi : L^2(\Omega_v) \rightarrow \mathbb{P}^N$ to be the orthogonal projection operator upon \mathbb{P}^N in the $L^2(\Omega_v)$ inner product such that

$$\begin{aligned} \langle f - \Pi f, \psi \rangle &= 0 \quad \forall \quad \psi \in \mathbb{P}^N, \\ \langle f, f \rangle &= \|f\|_{L^2(\Omega_v)}^2. \end{aligned}$$

Then the probability distribution function $f(\mathbf{v})$ can be approximated by a truncated Fourier series defined (ignoring the integration weights and the Fourier normalization coefficient $(1/(2\pi)^{3/2})$) as

$$\Pi f(\mathbf{v}) = f^\Pi(\mathbf{v}) = \sum_{\mathbf{k}} \hat{f}_N(\zeta_k) e^{i\zeta_k \cdot \mathbf{v}}, \quad (3.2.1)$$

where

$$\hat{f}_N(\zeta_k) = \frac{1}{(\sqrt{2\pi})^3} \int_{\mathbf{v}} f(\mathbf{v}) e^{-i\zeta_k \cdot \mathbf{v}} d\mathbf{v}.$$

Also, it is easy to prove that

$$\langle \Pi\psi, \phi \rangle = \langle \psi, \Pi\phi \rangle = \langle \Pi\psi, \Pi\phi \rangle, \quad \psi, \phi \in L^2(\Omega_v). \quad (3.2.2)$$

Define

$Q(f, f)$: Classic non-linear Boltzmann collision integral

with $\text{supp}[Q(f, f)] \cap \text{supp}[f] \subset \Omega_v$

$Q(f^\Pi, f^\Pi)$: Classic collision integral

evaluated at the truncated Fourier series of $f(\mathbf{v})$

$Q^\Pi(f^\Pi, f^\Pi)$: Projection of $Q(f^\Pi, f^\Pi)$

$$= \Pi Q(f^\Pi, f^\Pi) = \sum_{\mathbf{k}} \hat{Q}(\zeta_k) e^{i\zeta_k \cdot \mathbf{v}},$$

$$\text{where } \hat{Q}(\zeta_k) = \left(\frac{1}{\sqrt{2\pi}} \right)^3 \int_{\mathbf{v}} \Pi Q(f^\Pi, f^\Pi) e^{-i\zeta_k \cdot \mathbf{v}} d\mathbf{v}$$

$Q_C^\Pi(f^\Pi, f^\Pi)$: Conserved version of $Q^\Pi(f^\Pi, f^\Pi)$

i.e., $Q^\Pi(f^\Pi, f^\Pi)$ after Lagrangian correction.

Using the above definitions, it is easy to see that the space homogeneous Boltzmann equation can be approximated in terms of the Fourier series expansions as

$$\frac{\partial}{\partial t} f(\mathbf{v}, t) = Q^\Pi(f^\Pi, f^\Pi). \quad (3.2.3)$$

The conserved version of $Q^\Pi(f^\Pi, f^\Pi)$ is obtained by defining a constrained Lagrange multiplier minimization problem with the moment conservation properties of $Q_C^\Pi(f^\Pi, f^\Pi)$ as the constraints and finding the critical points of the objective function.

3.2.1 Conservation Method - An Extended Isoperimetric problem

Due to the truncation of the velocity domain, $Q^\Pi(f^\Pi, f^\Pi)$ does not preserve all the moments that its unrestricted counterpart $Q(f, f)$ does. This issue of non-conservation of moments cannot be ignored as it is a very important property of

the space homogeneous Boltzmann equation. In order to achieve this, one needs to enforce these moment conservation properties artificially by imposing them as constraints in a optimization problem. For the sake of brevity, let

$$\begin{aligned} q_u(\mathbf{v}) &:= Q^\Pi(f^\Pi, f^\Pi)(\mathbf{v}), \\ q_c(\mathbf{v}) &:= Q_C^\Pi(f^\Pi, f^\Pi)(\mathbf{v}). \end{aligned} \tag{3.2.4}$$

The method explained in the previous Section is invariant under elasticity of collisions, i.e., it works for both elastic and inelastic collisions. The moment conservation properties for an elastic collision differ from those of an inelastic collision. So, we form two similar but different optimization problems, one for elastic collisions and one for inelastic collisions (described later). We form the following optimization problem for the elastic case.

Elastic Problem (E):

$$\begin{aligned} \text{Minimize - Objective Function} \quad & A^e(q_c) := \int_{\Omega_v} (q_u(\mathbf{v}) - q_c(\mathbf{v}))^2 d\mathbf{v} \\ \text{Subject to} \quad & \psi_1(q_c) := \int_{\Omega_v} q_c(\mathbf{v}) d\mathbf{v} = 0; \\ & \psi_{j+1}(q_c) := \int_{\Omega_v} v_j q_c(\mathbf{v}) d\mathbf{v} = 0, \quad \forall j = 1, 2, 3; \\ & \psi_5(q_c) := \int_{\Omega_v} |\mathbf{v}|^2 q_c(\mathbf{v}) d\mathbf{v} = 0; \end{aligned} \tag{3.2.5}$$

that is, minimize the quadratic cost functional of the correction to the projected collision integral subject to conservation constraints in (3.2.5).

Lemma 3.2.1. (Elastic Lagrange Estimate): *A solution to (3.2.5) exists and is given by*

$$q_c(\mathbf{v}) = q_u(\mathbf{v}) - \frac{1}{2}(\gamma_1 + \sum_{j=1}^3 \gamma_{j+1} v_j + \gamma_5 |\mathbf{v}|^2),$$

and the minimized objective function is given by

$$A^e(q_c) = \|q_u - q_c\|_{L^2(\Omega_v)}^2 = 2L^3 \gamma_1^2 + \frac{2L^5(\gamma_2^2 + \gamma_3^2 + \gamma_4^2)}{3} + \gamma_5^2 \frac{38}{15} L^7 + \gamma_1 \gamma_5 4L^5, \tag{3.2.6}$$

where γ_j , for $j = 1, \dots, 5$, are Lagrange multipliers associated with the elastic optimization problem given by

$$\begin{aligned}\gamma_1 &= O_3\rho_u + O_5e_u, \\ \gamma_{i+1} &= O_5\mu_u^i, \quad i = 1, 2, 3, \\ \gamma_5 &= O_5\rho_u + O_7e_u,\end{aligned}$$

where ρ_u, e_u, μ_u^i are defined below in (3.2.8) and $O_r = O(\frac{1}{L^r})$ for $r \in \mathbb{Z}$ and O_r depends on $\Omega_v = [-L, L]^3$ defining the integration domain and also on the integrals of moment weights over Ω_v .

Proof. From calculus of variations, when the objective function is an integral equation and the constraints are also integrals, the optimization problem can be solved by forming the Lagrangian functional and finding its critical points. Define

$$\begin{aligned}H(q_c, \gamma) &= A^e(q_c) + \sum_{i=1}^5 \gamma_i \psi_i(q_c) \\ &= \int_{\Omega_v} \left[(q_c(\mathbf{v}) - q_u(\mathbf{v}))^2 + \gamma_1 q_c(\mathbf{v}) + \sum_{j=1}^3 \gamma_{j+1} v_j q_c(\mathbf{v}) + \gamma_5 |\mathbf{v}|^2 q_c(\mathbf{v}) \right] d\mathbf{v}\end{aligned}$$

where $\gamma = (\gamma_1, \dots, \gamma_5)$. Let $h(\mathbf{v}, q_c, q'_c, \gamma) = (q_c(\mathbf{v}) - q_u(\mathbf{v}))^2 + \gamma_1 q_c(\mathbf{v}) + \sum_{j=1}^3 \gamma_{j+1} v_j q_c(\mathbf{v}) + \gamma_5 |\mathbf{v}|^2 q_c(\mathbf{v})$. Then

$$H(q_c, q'_c, \gamma) = \int_{\Omega_v} h(\mathbf{v}, q_c, q'_c, \gamma) d\mathbf{v}.$$

To find the critical point, one needs to compute $D_{q_c}H$ and $D_{\gamma_j}H, j = 1, \dots, 5$. In order to find $D_{q_c}H$ we can get the Euler-Lagrange equations and solve for the function $q_c(\mathbf{v})$ that satisfies them. $D_{\gamma_i}H, i = 1, \dots, 5$, just retrieves the constraint integrals. From the calculus of variations, for multiple independent variables v_1, v_2, v_3 and a

single dependent function $q_c(\mathbf{v})$, the Euler-Lagrange equations are given by

$$\begin{aligned} D_2 h(\mathbf{v}, q_c, q'_c, \gamma) &= \sum_{i=1}^3 \frac{d}{dv_i} D_3 h(\mathbf{v}, q_c, q'_c, \gamma) \\ \text{i.e., } \frac{\partial}{\partial q_c} h(\mathbf{v}, q_c, q'_c, \gamma) &= \sum_{j=1}^3 \frac{d}{dv_j} \frac{\partial}{\partial q'_c} h(\mathbf{v}, q_c, q'_c, \gamma). \end{aligned}$$

But, $h(\mathbf{v}, q_c, q'_c, \gamma)$ is independent of q'_c , so

$$\frac{\partial}{\partial q_c} h(\mathbf{v}, q_c, q'_c, \gamma) = 0.$$

This gives the following equation for the conservation correction in terms of the Lagrange multipliers:

$$\begin{aligned} 2(q_c - q_u) + \gamma_1 + \sum_{j=1}^3 \gamma_{j+1} v_j + \gamma_5 |\mathbf{v}|^2 &= 0 \\ \Rightarrow q_c(\mathbf{v}) &= q_u(\mathbf{v}) - \frac{1}{2}(\gamma_1 + \sum_{j=1}^3 \gamma_{j+1} v_j + \gamma_5 |\mathbf{v}|^2). \end{aligned} \quad (3.2.7)$$

Let $g(\mathbf{v}, \gamma) = \gamma_1 + \sum_{j=1}^3 \gamma_{j+1} v_j + \gamma_5 |\mathbf{v}|^2$. Substituting (3.2.7) into the constraints from (3.2.5) gives

$$\begin{aligned} \rho_u &:= \int_{\Omega_v} q_u(\mathbf{v}) d\mathbf{v} = \frac{1}{2} \int_{\Omega_v} g(\mathbf{v}, \gamma) d\mathbf{v} \\ \mu_u^j &:= \int_{\Omega_v} v_j q_u(\mathbf{v}) d\mathbf{v} = \frac{1}{2} \int_{\Omega_v} v_j g(\mathbf{v}, \gamma) d\mathbf{v}, \quad j = 1, 2, 3 \\ e_u &:= \int_{\Omega_v} |\mathbf{v}|^2 q_u(\mathbf{v}) d\mathbf{v} = \frac{1}{2} \int_{\Omega_v} |\mathbf{v}|^2 g(\mathbf{v}, \gamma) d\mathbf{v}. \end{aligned} \quad (3.2.8)$$

Identities (3.2.8) form a system of 5 linear equations in 5 unknown variables that can be solved. Solving for the critical $\gamma_j, j = 1, \dots, 5$, gives

$$\begin{aligned} \gamma_1 &= O_3 \rho_u + O_5 e_u, \\ \gamma_{j+1} &= O_5 \mu_u^j, \quad j = 1, 2, 3, \\ \gamma_5 &= O_5 \rho_u + O_7 e_u, \end{aligned} \quad (3.2.9)$$

where $O_r = O(\frac{1}{L^r})$ for $r \in \mathbb{Z}$ and O_r depends on $\Omega_v = [-L, L]^3$ defining the integration domain and also on the integrals of moment weights over Ω_v . In particular, O_r depends inversely on the volume of the domain $\Omega_v = [-L, L]^3$.

Substituting these values of critical Lagrange multipliers (3.2.9) into (3.2.7) gives the critical $q_c(\mathbf{v})$. But we are interested in the objective function $A^e(q_c)$ in (3.2.5)

$$\begin{aligned} A^e(q_c) = \|q_u - q_c\|_{L^2(\Omega_v)}^2 &= \int_{\Omega_v} (q_c(\mathbf{v}) - q_u(\mathbf{v}))^2 d\mathbf{v} \\ &= \frac{1}{4} \int_{\Omega_v} (\gamma_1 + \sum_{j=1}^3 \gamma_{j+1} v_j + \gamma_5 |\mathbf{v}|^2)^2 d\mathbf{v}. \end{aligned}$$

Upon simplification,

$$\|q_u - q_c\|_{L^2(\Omega_v)}^2 = 2L^3 \gamma_1^2 + \frac{2L^5(\gamma_2^2 + \gamma_3^2 + \gamma_4^2)}{3} + \gamma_5^2 \frac{38}{15} L^7 + \gamma_1 \gamma_5 4L^5, \quad (3.2.10)$$

where $\gamma_j, j = 1, \dots, 5$, as given by (3.2.9) are dependent on the moments of the unconserved collision integral. \square

Similar to (3.2.5), we now form the following optimization problem for the inelastic case

Inelastic Problem (IE):

$$\begin{aligned} \text{Minimize} \quad & A^{in}(q_c) : \int_{\Omega_v} (q_u(\mathbf{v}) - q_c(\mathbf{v}))^2 d\mathbf{v} \\ \text{Subject to} \quad & \psi_1(q_c) : \int_{\Omega_v} q_c(\mathbf{v}) d\mathbf{v} = 0; \\ & \psi_{j+1}(q_c) : \int_{\Omega_v} v_j q_c(\mathbf{v}) d\mathbf{v} = 0, \forall j = 1, 2, 3. \end{aligned} \quad (3.2.11)$$

Following the minimization process as given in the proof of Lemma 3.2.1, we get the following Lemma.

Lemma 3.2.2. (Inelastic Lagrange Estimate): *A solution to (3.2.5) exists and is given by*

$$q_c(\mathbf{v}) = q_u(\mathbf{v}) - \frac{1}{2}(\gamma_1 + \sum_{j=1}^3 \gamma_{j+1} v_j),$$

and the minimized objective function is given by

$$A^{in}(q_c) = \|q_u - q_c\|_{L^2(\Omega_v)}^2 = 2L^3 \gamma_1^2 + \frac{2L^5(\gamma_2^2 + \gamma_3^2 + \gamma_4^2)}{3}, \quad (3.2.12)$$

where γ_j for $j = 1, \dots, 4$, are Lagrange multipliers associated with the inelastic optimization problem given by

$$\begin{aligned} \gamma_1 &= O_3 \rho_u, \\ \gamma_{i+1} &= O_5 \mu_u^j, \quad j = 1, 2, 3, \end{aligned} \quad (3.2.13)$$

where $O_r = O(\frac{1}{L^r})$ for $r \in \mathbb{Z}$ and O_r depends on $\Omega_v = [-L, L]^3$ defining the integration domain and also on the integrals of moment weights on Ω_v . In particular, O_r depends inversely on the volume of the domain $\Omega_v = [-L, L]^3$.

Remark: Note that equation (3.2.6) in Lemma 3.2.1 (elastic optimization problem) indicates dependence only on the unconserved moments $\rho_u, \mu_u^1, \mu_u^2, \mu_u^3$, and e_u of $q_u(\mathbf{v})$. Ideally these are supposed to be zero. Similarly, (3.2.12) in Lemma 3.2.2 (inelastic optimization problem) indicates dependence on the unconserved moments ρ_u, μ_u^1, μ_u^2 , and μ_u^3 of $q_u(\mathbf{v})$. Also, $A^e(q_c)$ in (3.2.6) differs from $A^{in}(q_c)$ in (3.2.12) in the last two terms which correspond to the energy conservation constraint.

The next theorem shows the sharp control from the extended isoperimetric problem i.e. the conservation correction to the collision integral is spectrally accurate.

Theorem 3.2.3. (Conservation Correction Estimate): *The accuracy of the conservation scheme is directly proportional to the spectral accuracy of the method:*

$$\|Q_C^\Pi(f^\Pi, f^\Pi) - Q^\Pi(f^\Pi, f^\Pi)\|_{L^2(\Omega_v)} \leq \hat{C} \|Q(f, f) - Q^\Pi(f^\Pi, f^\Pi)\|_{L^2(\Omega_v)}, \quad (3.2.14)$$

where \hat{C} is a constant that is independent of the domain size L .

Proof. Let $\psi(\mathbf{v}) \in L^2(\Omega_v)$. As in the case of the classic space-homogeneous Boltzmann equation,

$$\frac{\partial}{\partial t} f(t, \mathbf{v}) = Q(f, f)(\mathbf{v}) \Rightarrow \langle Q(f, f), \psi \rangle = \langle \frac{\partial}{\partial t} f, \psi \rangle. \quad (3.2.15)$$

From (3.2.3), the space homogeneous Boltzmann equation for the truncated Fourier series is

$$\frac{\partial}{\partial t} f^\Pi(t, \mathbf{v}) = Q^\Pi(f^\Pi, f^\Pi)(\mathbf{v}) \Rightarrow \langle Q^\Pi(f^\Pi, f^\Pi), \psi \rangle = \langle \frac{\partial}{\partial t} f^\Pi, \psi \rangle. \quad (3.2.16)$$

For the elastic Boltzmann collision integral, $\langle Q(f, f), \psi \rangle = 0$ for $\psi(\mathbf{v}) = 1, v_1, v_2, v_3, |\mathbf{v}|^2$, and for the inelastic case, $\langle Q(f, f), \psi \rangle = 0$ for $\psi(\mathbf{v}) = 1, v_1, v_2, v_3$. From (3.2.15) - (3.2.16),

$$\begin{aligned} |\langle q_u, \psi \rangle| &= |\langle Q^\Pi(f^\Pi, f^\Pi), \psi \rangle| = |\langle \frac{\partial}{\partial t} f^\Pi, \psi \rangle - \langle \frac{\partial}{\partial t} f, \psi \rangle| \\ &= |\langle \frac{\partial}{\partial t} (f^\Pi - f), \psi \rangle| \\ &\leq \|\frac{\partial}{\partial t} (f^\Pi - f)\|_{L^2(\Omega_v)} \|\psi\|_{L^2(\Omega_v)} \\ &= \|Q(f, f) - Q^\Pi(f^\Pi, f^\Pi)\|_{L^2(\Omega_v)} \|\psi\|_{L^2(\Omega_v)}. \end{aligned} \quad (3.2.17)$$

For $\psi(\mathbf{v}) = 1, v_1, v_2, v_3, |\mathbf{v}|^2$, the $L^2(\Omega_v)$ norms can be explicitly computed and they are calculated to be proportional to powers of L . Exact calculations give

$$\begin{aligned} C^\rho &: \quad \|1\|_{L^2(\Omega_v)} = \sqrt{8L^3}, \\ C^\mu &: \quad \|v_j\|_{L^2(\Omega_v)} = \sqrt{\frac{8L^5}{3}}, \quad \text{for } j = 1, 2, 3, \\ C^e &: \quad \|\mathbf{v}^2\|_{L^2(\Omega_v)} = \sqrt{\frac{152L^7}{15}}. \end{aligned} \quad (3.2.18)$$

Using (3.2.18) in (3.2.18) gives estimates of the unconserved moments in terms of the domain size L :

$$\begin{aligned}
|\rho_u| &\leq C^\rho \|Q(f, f) - Q^\Pi(f^\Pi, f^\Pi)\|_{L^2(\Omega_v)}, \\
|\mu_u^j| &\leq C^\mu \|Q(f, f) - Q^\Pi(f^\Pi, f^\Pi)\|_{L^2(\Omega_v)}, \quad j = 1, 2, 3, \\
|e_u| &\leq C^e \|Q(f, f) - Q^\Pi(f^\Pi, f^\Pi)\|_{L^2(\Omega_v)}.
\end{aligned} \tag{3.2.19}$$

Elastic collisions:

We examine the individual terms of (3.2.6), by substituting in (3.2.9) and using (3.2.19). We find that all the factors with C^ρ , C^μ , and C^e cancel out exactly with the $O_r = O(\frac{1}{L^r})$, $r \in \mathbb{Z}$ terms with the appropriate values of r (recall that r depends on the v -space dimension in the domain Ω_v defining the integration domain and the integrals of the moment weights in Ω_v). The first term in (3.2.5) yields

$$\begin{aligned}
\gamma_1^2 2L^3 &= (O_6 \rho_u^2 + O_{10} e_u^2 + O_8 \rho_u e_u) 2L^3 \\
&= O_3 \rho_u^2 + O_7 e_u^2 + O_5 \rho_u e_u \\
&\leq (O_3 (C^\rho)^2 + O_7 (C^e)^2 + O_5 C^\rho C^e) \|Q(f, f) - Q^\Pi(f^\Pi, f^\Pi)\|_{L^2(\Omega_v)}^2 \\
&\leq \hat{C}_1 \|Q(f, f) - Q^\Pi(f^\Pi, f^\Pi)\|_{L^2(\Omega_v)}^2.
\end{aligned} \tag{3.2.20}$$

Similarly, using the definition of $O_r = O(\frac{1}{L^r})$, $r \in \mathbb{Z}$ and plugging in the values of ρ_u, e_u, μ_u^j , $j = 1, 2, 3$ into other terms of (3.2.6) we get

$$\begin{aligned}
\gamma_{j+1}^2 \frac{2L^5}{3} &= (\mu_u^j)^2 O_5 \\
&\leq \hat{C}_2 \|Q(f, f) - Q^\Pi(f^\Pi, f^\Pi)\|_{L^2(\Omega_v)}^2, \quad \text{for } j = 1, 2, 3, \\
\gamma_5^2 \frac{38L^7}{15} &= O_7 e_u^2 + O_3 \rho_u^2 + O_5 \rho_u e_u \\
&\leq \hat{C}_3 \|Q(f, f) - Q^\Pi(f^\Pi, f^\Pi)\|_{L^2(\Omega_v)}^2, \\
\gamma_1 \gamma_5 4L^5 &= O_3 \rho_u^2 + O_7 e_u^2 + O_5 \rho_u e_u \\
&\leq \hat{C}_4 \|Q(f, f) - Q^\Pi(f^\Pi, f^\Pi)\|_{L^2(\Omega_v)}^2,
\end{aligned} \tag{3.2.21}$$

where $\hat{C}_1, \hat{C}_2, \hat{C}_3, \hat{C}_4$ are constants independent of L and the order of moments. In order to estimate (3.2.14) for the elastic case by means of (3.2.4), we need to estimate $\|q_u - q_c\|_{L^2(\Omega_v)}$ where we use the estimates from (3.2.21) in (3.2.6):

$$\begin{aligned}
\|Q^\Pi(f^\Pi, f^\Pi) - Q_C^\Pi(f^\Pi, f^\Pi)\|_{L^2(\Omega_v)}^2 &= \|q_u - q_c\|_{L^2(\Omega_v)}^2 \\
&= 2L^3\gamma_1^2 + \frac{2L^5(\gamma_2^2 + \gamma_3^2 + \gamma_4^2)}{3} \\
&\quad + \gamma_5^2 \frac{38}{15}L^7 + \gamma_1\gamma_5 4L^5 \\
&\leq \hat{C}^2 \|Q(f, f) - Q^\Pi(f^\Pi, f^\Pi)\|_{L^2(\Omega_v)}^2,
\end{aligned}$$

where \hat{C} is a constant independent of L but depends on the dimension of the \mathbf{v} -space and the order of moments through $\hat{C}_1, \hat{C}_2, \hat{C}_3, \hat{C}_4$. This is the claimed result.

Inelastic collisions:

Next, we examine the individual terms of (3.2.12) (inelastic optimization problem), by plugging in (3.2.13) and using (3.2.19) and find that all the factors with C^ρ, C^μ cancel out exactly with the O_r terms with the appropriate values of r to give:

$$\begin{aligned}
\gamma_1^2 2L^3 &= O_3 \rho_u^2 \\
&\leq \|Q(f, f) - Q^\Pi(f^\Pi, f^\Pi)\|_{L^2(\Omega_v)}^2, \\
\gamma_{j+1}^2 \frac{2L^5}{3} &= (\mu_u^j)^2 O_5 \\
&\leq \|Q(f, f) - Q^\Pi(f^\Pi, f^\Pi)\|_{L^2(\Omega_v)}^2, \quad \text{for } j = 1, 2, 3. \quad (3.2.22)
\end{aligned}$$

In order to estimate (3.2.14) by means of (3.2.4), we need to estimate $\|q_u - q_c\|_{L^2(\Omega_v)}$ for the inelastic case where we use the estimates from (3.2.22) in (3.2.12)

$$\begin{aligned}
\|Q^\Pi(f^\Pi, f^\Pi) - Q_C^\Pi(f^\Pi, f^\Pi)\|_{L^2(\Omega_v)}^2 &= \|q_u - q_c\|_{L^2(\Omega_v)}^2 \\
&= 2L^3\gamma_1^2 + \frac{2L^5(\gamma_2^2 + \gamma_3^2 + \gamma_4^2)}{3} \\
&\leq 2\|Q(f, f) - Q^\Pi(f^\Pi, f^\Pi)\|_{L^2(\Omega_v)}^2.
\end{aligned}$$

This gives

$$\|Q^\Pi(f^\Pi, f^\Pi) - Q_C^\Pi(f^\Pi, f^\Pi)\|_{L^2(\Omega_v)} \leq \sqrt{2}\|Q(f, f) - Q^\Pi(f^\Pi, f^\Pi)\|_{L^2(\Omega_v)}$$

As expected, again this shows that the conservation error is directly proportional to the spectral approximation error and works for all finite domains $\Omega_v = [-L, L]^3$ of support of $f(t, \cdot)$ in \mathbf{v} .

Thus, we obtain the same conservation error (3.2.14) for both elastic and inelastic collisions and the theorem 3.2.3 is proven. \square

3.2.2 Discrete in Time Conservation Method: Lagrange Multiplier Method

In this subsection, we consider the discrete version of the conservation scheme. For such a discrete formulation, the conservation routine is implemented as a Lagrange multiplier method where the conservation properties of the discrete distribution are set as constraints. Let $M = N^d$, the total number of Fourier modes. For elastic collisions, $\rho = 0$, $\mathbf{m} = (m1, m2, m3) = (0, 0, 0)$ and $e = 0$ are conserved, and for inelastic collisions, $\rho = 0$ and $\mathbf{m} = (m1, m2, m3) = (0, 0, 0)$ are conserved. Let $\omega_j > 0$ be the integration weights for $j = 1, 2, \dots, M$. Let

$$\tilde{\mathbf{Q}} = (\tilde{Q}_1 \quad \tilde{Q}_2 \quad \dots \quad \tilde{Q}_M)^T$$

be the distribution vector at the computed time step and

$$\mathbf{Q} = (Q_1 \quad Q_2 \quad \dots \quad Q_M)^T$$

be the corrected distribution vector with the required moments conserved. For the elastic case, let

$$\mathbf{C}_{(d+2) \times M}^e = \begin{pmatrix} \omega_j \\ v_i \omega_j \\ |v_j|^2 \omega_j \end{pmatrix}$$

and correspondingly, let

$$\mathbf{a}_{(d+2) \times 1}^e = (\rho \quad m1 \quad m2 \quad m3 \quad e)^T$$

be the vector of conserved quantities. Using the above vectors, the conservation method can be written as a constrained optimization problem:

$$(*) \left\{ \min \|\tilde{\mathbf{Q}} - \mathbf{Q}\|_2^2 : \mathbf{C}^e \mathbf{Q} = \mathbf{a}^e; \mathbf{C}^e \in \mathbb{R}^{d+2 \times M}, \mathbf{Q} \in \mathbb{R}^M, \mathbf{a}^e \in \mathbb{R}^{d+2} \right\}$$

To solve (*), one can employ the Lagrange multiplier method. Let $\gamma \in \mathbb{R}^{d+2}$ be the Lagrange multiplier vector. Then the scalar objective function to be optimized is given by

$$L(\mathbf{Q}, \lambda) = \sum_{j=1}^M |\tilde{Q}_j - Q_j|^2 + \gamma^T (\mathbf{C}^e \mathbf{Q} - \mathbf{a}^e). \quad (3.2.23)$$

Equation (3.2.23) can be solved explicitly for the corrected distribution value and the resulting equation of correction be implemented numerically in the code. Taking the derivative of $L(\mathbf{Q}, \lambda)$ with respect to $f_j, j = 1, \dots, M$, and $\gamma_i, i = 1, \dots, d + 2$, i.e., gradients of L ,

$$\begin{aligned} \frac{\partial L}{\partial Q_j} &= 0 \quad j = 1, \dots, M, \\ \Rightarrow \\ \mathbf{Q} &= \tilde{\mathbf{Q}} + \frac{1}{2} (\mathbf{C}^e)^T \gamma. \end{aligned} \quad (3.2.24)$$

Moreover,

$$\begin{aligned} \frac{\partial L}{\partial \gamma_1} &= 0; i = 1, \dots, d + 2, \\ \Rightarrow \\ \mathbf{C}^e \mathbf{Q} &= \mathbf{a}^e, \end{aligned} \quad (3.2.25)$$

retrieves the constraints. Solving for γ ,

$$\mathbf{C}^e(\mathbf{C}^e)^T \gamma = 2(a^e - \mathbf{C}^e \tilde{\mathbf{Q}}). \quad (3.2.26)$$

Now $\mathbf{C}^e(\mathbf{C}^e)^T$ is symmetric and, because \mathbf{C}^e is the integration matrix, $\mathbf{C}^e(\mathbf{C}^e)^T$ is positive definite. By linear algebra, the inverse of $\mathbf{C}^e(\mathbf{C}^e)^T$ exists. In particular one can compute the value of λ by

$$\gamma = 2(\mathbf{C}^e(\mathbf{C}^e)^T)^{-1}(a^e - \mathbf{C}^e \tilde{\mathbf{Q}}).$$

Substituting γ into (3.2.24), since $\mathbf{a}^e = \mathbf{0}$,

$$\begin{aligned} \mathbf{Q} &= \tilde{\mathbf{Q}} + (\mathbf{C}^e)^T (\mathbf{C}^e(\mathbf{C}^e)^T)^{-1} (a^e - \mathbf{C}^e \tilde{\mathbf{Q}}) \\ &= [\mathbb{I} - (\mathbf{C}^e)^T (\mathbf{C}^e(\mathbf{C}^e)^T)^{-1} \mathbf{C}^e] \tilde{\mathbf{Q}} \\ &= \Lambda_N(\mathbf{C}^e) \tilde{\mathbf{Q}}, \end{aligned} \quad (3.2.27)$$

where $\mathbb{I} = N \times N$ identity matrix and we define $\Lambda_N(\mathbf{C}^e) : \mathbb{I} - (\mathbf{C}^e)^T (\mathbf{C}^e(\mathbf{C}^e)^T)^{-1} \mathbf{C}^e$. For the future sections, define this conservation routine as *Conserve*. So,

$$\text{Conserve}(\tilde{\mathbf{Q}}) = \mathbf{Q} = \Lambda_N(\mathbf{C}^e) \tilde{\mathbf{Q}}. \quad (3.2.28)$$

Define $D_t \mathbf{f}$ to be any order time discretization of $\frac{\partial \mathbf{f}}{\partial t}$. Then we have:

$$D_t \mathbf{f} = \Lambda_N(\mathbf{C}^e) \tilde{\mathbf{Q}}, \quad (3.2.29)$$

where we expect the required observables are conserved and the solution approaches a stationary state for the elastic space homogeneous Boltzmann equation, since $\lim_{n \rightarrow \infty} \|\Lambda_N(C) \mathbf{Q}(f_j^n, f_j^n)\|_\infty = 0$ [52]. Identity (3.2.29) summarizes the whole conservation process. As described previously, setting the conservation properties as constraints to a Lagrange multiplier optimization problem ensures that the required observables are conserved.

3.3 Accuracy and Consistency

In this section, we prove the accuracy of the artificial conservation property imposed and the spectral accuracy of approximating the classic collision integral with the projected version. Define $H^{\alpha,0}(\Omega_v) = \{g \in L^2(\Omega_v) | D^\beta g \in L^2(\Omega_v) \forall |\beta| \leq |\alpha|; \text{supp}[g] \subset \Omega_v\}$.

The following result is an extension of the standard approximation estimate for regular functions by Fourier series expansions to $H^{\alpha,0}(\Omega_v)$ space. We include here that result for completeness of the reading.

Lemma 3.3.1. (Fourier Approximation Estimate I): *Let $g \in H^{\alpha,0}(\Omega_v)$, $g_N = \Pi g = \sum_k \hat{g}_N(\zeta_k) e^{i\zeta_k \cdot \mathbf{v}}$ and $\alpha = (\alpha_1, \alpha_2, \alpha_3)$ be a multi-index. Then*

$$\|g - g_N\|_{L^2(\Omega_v)} \leq \frac{C}{N^{\alpha_1 + \alpha_2 + \alpha_3}} \|g\|_{H^{\alpha,0}(\Omega_v)}, \quad (3.3.1)$$

where C is a constant that depends on the Fourier space (ζ) discretization, h_ζ .

Proof. From the definition of $g(\mathbf{v})$ as a full Fourier series

$$g(\mathbf{v}) = \sum_{k=-\infty}^{\infty} \hat{g}_N(\zeta_k) e^{i\zeta_k \cdot \mathbf{v}},$$

and using the definition of $g_N(\mathbf{v})$, we get:

$$g(\mathbf{v}) - g_N(\mathbf{v}) = \sum_{|k| > N/2} \hat{g}_N(\zeta_k) e^{i\zeta_k \cdot \mathbf{v}}. \quad (3.3.2)$$

Parseval's relation gives

$$\|g - g_N\|_{L^2(\Omega_v)} = \sqrt{\sum_{|k| > N/2} |\hat{g}_N(\zeta_k)|^2}.$$

For g a periodic function or $g \in H^{\alpha,0}(\Omega_v)$, we have

$$\begin{aligned}
|\hat{g}(\zeta_k)| &= \frac{1}{(\sqrt{2\pi})^3} \frac{1}{\prod_{j=1}^3 |(\zeta_k^j)^{\alpha_j}|} |(\widehat{D^\alpha g})(\zeta_k)| \\
\Rightarrow \sum_{|\mathbf{k}| > N/2} |\hat{g}_N(\zeta_k)|^2 &= \frac{1}{(2\pi)^3} \sum_{|\mathbf{k}| > N/2} \frac{1}{\prod_{j=1}^3 |(\zeta_k^j)^{\alpha_j}|^2} |(\widehat{D^\alpha g})(\zeta_k)|^2 \\
&\leq \frac{1}{(2\pi)^3} \frac{1}{\prod_{j=1}^3 |(\zeta_{N/2}^j)^{\alpha_j}|^2} \sum_{|\mathbf{k}| > N/2} |(\widehat{D^\alpha g})(\zeta_k)|^2 \\
&\leq \frac{1}{(2\pi)^3} \frac{1}{\prod_{j=1}^3 |(\zeta_{N/2}^j)^{\alpha_j}|^2} \sum_{\mathbf{k}} |(\widehat{D^\alpha g})(\zeta_k)|^2.
\end{aligned}$$

So

$$\begin{aligned}
\int_{\Omega_v} |g(\mathbf{v}) - g_N(\mathbf{v})|^2 d\mathbf{v} &= \sum_{|\mathbf{k}| > N/2} |\hat{g}_N(\zeta_k)|^2 = \frac{1}{(2\pi)^3} \frac{1}{\prod_{j=1}^3 |(\zeta_{N/2}^j)^{\alpha_j}|^2} \int_{\Omega_v} |D^\alpha g(\mathbf{v})|^2 d\mathbf{v} \\
&= \frac{1}{(2\pi)^3} \frac{1}{\prod_{j=1}^3 |(\zeta_{N/2}^j)^{\alpha_j}|^2} \|D^\alpha g\|_{L^2(\Omega_v)}^2 \\
&\leq \frac{1}{(2\pi)^3} \frac{1}{\prod_{j=1}^3 |(\zeta_{N/2}^j)^{\alpha_j}|^2} \|g\|_{H^{\alpha,0}(\Omega_v)}^2.
\end{aligned}$$

We use the definition of $\zeta_{N/2}^\alpha = \frac{Nh_\zeta}{2}$. This gives the error in projection

$$\begin{aligned}
\|g - g_N\|_{L^2(\Omega_v)} &\leq \frac{C}{\prod_{j=1}^3 N^{\alpha_j}} \|g\|_{H^{\alpha,0}} \\
&\leq \frac{C}{N^{\alpha_1 + \alpha_2 + \alpha_3}} \|g\|_{H^{\alpha,0}} \\
&= \frac{C}{N^{|\alpha|}} \|g\|_{H^{\alpha,0}}, \tag{3.3.3}
\end{aligned}$$

where C is a constant that depends on the Fourier space (ζ) discretization, h_ζ . Note that α is the degree of regularity of g as a multi-index. \square

Define $\|g\|_{L_m^p(\Omega_v)} := (\int_{\Omega_v} (1 + |\mathbf{v}|^2)^{m/2} |g(\mathbf{v})|^p d\mathbf{v})^{1/p}$. We now extend the above result (3.3.3) to a weighted $L_m^2(\Omega_v)$ norm.

Corollary 3.3.2. (Fourier Approximation Estimate II): Let $g \in H^{\alpha,0}(\Omega_v)$, $g_N = \Pi g = \sum_k \hat{u}_N(\zeta_k) e^{i\zeta_k \cdot v}$ and $\alpha = (\alpha_1, \alpha_2, \alpha_3)$ be a multi-index. Then,

$$\|g - g_N\|_{L_m^2(\Omega_v)} \leq \frac{C}{N^{\alpha_1 + \alpha_2 + \alpha_3}} \|g\|_{H_m^{\alpha,0}(\Omega_v)}, \quad (3.3.4)$$

where C is a constant that depends on the Fourier space (ζ) discretization, h_ζ .

Proof. Let $U(\mathbf{v}) = (1 + |\mathbf{v}|^2)^{m/2} (g - g_N)(\mathbf{v})$ and apply Lemma 3.3.1 to it. Hence the corollary. \square

Next, we derive an estimate on the classic collision integral $Q(f, f)$. The following theorem draws from the estimates for variable hard potentials for the collision integrals originally derived in [48] for elastic and inelastic hard sphere interactions in the whole velocity space \mathbb{R}^3 . In the sequel, the following notation is used

$$\|\cdot\|_{L_l^k(\mathbb{R}^3)} = \|\cdot\|_{L_l^k}.$$

Theorem 3.3.3. (Collision Integral Estimate for Elastic/ Inelastic Collisions): For $f, g \in L_{m+\lambda}^2$,

$$\|Q(f, g)\|_{L_m^2} \leq C^{\lambda, \beta} (\|f\|_{L_{m+\lambda}^2} \|g\|_{L_{m+\lambda}^1} + \|f\|_{L_{m+\lambda}^1} \|g\|_{L_{m+\lambda}^2}), \quad (3.3.5)$$

where $C^{\lambda, \beta}$ is a constant that depends on the collision cross-section, mass and energy of the initial state, λ and $\beta = \frac{1+e}{2}$; e is the restitution coefficient.

Proof. In Lemma 4.1 in [48], we have proven the above estimate for $\lambda = 1$ for both elastic and inelastic collisions for the whole velocity domain \mathbb{R}^3 . However a thorough calculation shows that it is valid for any $0 \leq \lambda \leq 1$. Consider $Q(f, g) = Q_+(f, g) - Q_-(f, g)$, the asymmetric form of the collision operator. For an estimate

on the loss part of the collision integral, consider that:

$$\begin{aligned}
Q_-(f, g) &= f(\mathbf{v}) \left(\int_{\mathbb{R}^3} B(|\mathbf{v} - \mathbf{v}_*|, \theta) g(\mathbf{v}_*) d\mathbf{v}_* \right) \\
&= f(\mathbf{v}) [B(|\cdot|, \theta) * g(\cdot)](\mathbf{v}) \\
&= f(\mathbf{v}) [B(|\mathbf{u}|, \theta) * g(\mathbf{u})](\mathbf{v}),
\end{aligned}$$

which gives [48]

$$\begin{aligned}
\|Q_-(f, g)\|_{L_m^1} &\leq C_1 C_\lambda \|f\|_{L_{m+\lambda}^1} \|g\|_{L_{m+\lambda}^2} \\
&\leq C_2 C_\lambda \|f\|_{L_{m+\lambda}^2} \|g\|_{L_{m+\lambda}^2}.
\end{aligned} \tag{3.3.6}$$

Using the weak form of the collision integral, we reduce the $L_t^2(\mathbb{R}^3)$ bound of the asymmetric collision integral $Q(f, g)$ to $L^1(\mathbb{R}^3)$ bounds on the operator $S[\psi](\mathbf{v}, \mathbf{v}_*)$ on the unit sphere S^2 , defined as follows from [48], where $B(\mathbf{u}, \sigma) = |u|^\lambda b(\mathbf{u}, \sigma)$,

$$\begin{aligned}
S[\psi](\mathbf{v}, \mathbf{v}_*) &= \int_{\sigma \in S^2} \psi' b(\mathbf{u}, \sigma) d\sigma \\
&= \int_{\mathbf{u} \cdot \sigma > 0} \psi' b(\mathbf{u}, \sigma) d\sigma - \int_{-\mathbf{u} \cdot \sigma > 0} \psi' b(\mathbf{u}, \sigma) d\sigma \\
&= S_+[\psi](\mathbf{v}, \mathbf{v}_*) - S_-[\psi](\mathbf{v}, \mathbf{v}_*).
\end{aligned} \tag{3.3.7}$$

The $\|S_\pm[\psi](\mathbf{v}, \mathbf{v}_*)\|_{L^1}$ estimate from Proposition 4.2 in [48] gives

$$\begin{aligned}
\int_{\mathbf{v}_*} S_+[\psi](\mathbf{v}, \mathbf{v}_*) d\mathbf{v}_* &\leq \left(\frac{\beta}{2}\right)^{-3} \|\psi\|_{L^1}, \\
\int_{\mathbf{v}} S_-[\psi](\mathbf{v}, \mathbf{v}_*) d\mathbf{v} &\leq \left(\frac{2-\beta}{2}\right)^{-3} \|\psi\|_{L^1}.
\end{aligned} \tag{3.3.8}$$

Next, we bound $Q(f, g)$ with (3.3.8) using the definition $\langle \mathbf{v} \rangle^m := (1 + |\mathbf{v}|^2)^{m/2}$.

Let $\Lambda(\mathbf{v}, \mathbf{v}_*) = \langle \mathbf{v} \rangle^{m+\lambda} + \langle \mathbf{v}_* \rangle^{m+\lambda}$, then:

$$\begin{aligned}
\int_{\mathbf{v} \in \mathbb{R}^3} Q(f, g) \psi d\mathbf{v} &\leq C_m \int_{\mathbf{v}_* \in \mathbb{R}^3} f(\mathbf{v}_*) \int_{\mathbf{v} \in \mathbb{R}^3} g(\mathbf{v}) (\Lambda(\mathbf{v}, \mathbf{v}_*)) S_+[\psi](\mathbf{v}, \mathbf{v}_*) d\mathbf{v} d\mathbf{v}_* \\
&\quad + C_m \int_{\mathbf{v}_* \in \mathbb{R}^3} g(\mathbf{v}_*) \int_{\mathbf{v} \in \mathbb{R}^3} f(\mathbf{v}) (\Lambda(\mathbf{v}, \mathbf{v}_*)) S_-[\psi](\mathbf{v}, \mathbf{v}_*) d\mathbf{v}_* d\mathbf{v}.
\end{aligned} \tag{3.3.9}$$

Using (3.3.8) in (3.3.9) and simplifying the resulting expression gives the following with $\psi = Q(f, g)$

$$\|Q(f, g)\|_{L_m^2} \leq C^{\lambda, \beta} (\|f\|_{L_{m+\lambda}^2} \|g\|_{L_{m+\lambda}^1} + \|f\|_{L_{m+\lambda}^1} \|g\|_{L_{m+\lambda}^2}) \quad (3.3.10)$$

where $C^{\lambda, \beta}$ is a constant that depends on the collision cross-section, mass and energy of the initial state, λ and $\beta = \frac{1+e}{2}$; e is the restitution coefficient. \square

Define

$$\begin{aligned} H_m^\alpha &: \{g \in L_m^2 | D^\beta g \in L_m^2 \forall |\beta| \leq |\alpha|\}, \\ \|g\|_{H_m^\alpha}^2 &: \sum_{\forall \beta, |\beta| \leq |\alpha|} \|\partial^\beta g\|_{L_m^2}^2. \end{aligned} \quad (3.3.11)$$

Next, we prove a Sobolev class regularity bound for the collision integral based on the technique outlined in Lemma 4.6 in [48] and the Leibniz formula

$$\partial^j Q(f, g) = \sum_{0 \leq l \leq j} \binom{j}{l} Q(\partial^{j-l} f, \partial^l g), \quad (3.3.12)$$

where j and l are multi-indices, $j = (j_1, j_2, j_3)$, $l = (l_1, l_2, l_3)$, $\partial^j = \partial_{v_1}^{j_1} \partial_{v_2}^{j_2} \partial_{v_3}^{j_3}$ and $\binom{j}{l}$ are multinomial coefficients.

Theorem 3.3.4. (Sobolev Bound Estimate): *For $f, g \in H_{m+\lambda}^\alpha \cap H_{m+\mu}^\alpha$, we have the following bound on the assymetric collision integral $Q(f, g)$ in H_m^α :*

$$\|Q(f, g)\|_{H_m^\alpha}^2 \leq \hat{C}^{\lambda, \beta, \mu} \sum_{1 \leq l \leq \alpha} \binom{\alpha}{l} (\|f\|_{H_{m+\lambda}^{\alpha-l}}^2 \|g\|_{H_{m+\mu}^l}^2 + \|f\|_{H_{m+\mu}^{\alpha-l}}^2 \|g\|_{H_{m+\lambda}^l}^2), \quad (3.3.13)$$

where $\hat{C}^{\lambda, \beta, \mu}$ is a constant that depends on $\mu > \frac{3}{2} + \lambda$, λ, β , and the mass and energy of the initial state.

Proof. We now get the H_m^α estimate of the asymmetric collision integral $Q(f, g)$ using the methodology outlined in lemma 4.6 in [48]. From (3.3.11) and (3.3.12),

we know

$$\begin{aligned}
\|Q(f, g)\|_{H_m^\alpha}^2 &= \sum_{1 \leq j \leq \alpha} \|\partial^j Q(f, g)\|_{L_m^2}^2 \\
&= \sum_{1 \leq j \leq \alpha} \left\| \sum_{1 \leq l \leq j} \binom{j}{l} Q(\partial^{j-l} f, \partial^l g) \right\|_{L_m^2}^2 \\
&\leq \sum_{1 \leq j \leq \alpha} \sum_{1 \leq l \leq j} \binom{j}{l} \|Q(\partial^{j-l} f, \partial^l g)\|_{L_m^2}^2. \tag{3.3.14}
\end{aligned}$$

We then use Theorem 3.3.3 in the summand of (3.3.14)

$$\begin{aligned}
\|Q(\partial^{j-l} f, \partial^l g)\|_{L_m^2}^2 &\leq (C^{\lambda, \beta})^2 (\|\partial^{j-l} f\|_{L_{m+\lambda}^2} \|\partial^l g\|_{L_{m+\lambda}^1} + \|\partial^{j-l} f\|_{L_{m+\lambda}^1} \|\partial^l g\|_{L_{m+\lambda}^2})^2 \\
&\leq 2(C^{\lambda, \beta})^2 (\|\partial^{j-l} f\|_{L_{m+\lambda}^2}^2 \|\partial^l g\|_{L_{m+\lambda}^1}^2 \\
&\quad + \|\partial^{j-l} f\|_{L_{m+\lambda}^1}^2 \|\partial^l g\|_{L_{m+\lambda}^2}^2). \tag{3.3.15}
\end{aligned}$$

Note that

$$\|\partial^j f\|_{L_{m+\lambda}^1} \leq \| \langle \mathbf{v} \rangle^{\lambda-\mu} \|_{L^2} \|\partial^j f\|_{L_{m+\mu}^2}, \tag{3.3.16}$$

so if $\mu > \frac{3}{2} + \lambda$, we get

$$\|\partial^j f\|_{L_{m+\lambda}^1} \leq \hat{C}_{\mu, \lambda} \|\partial^j f\|_{L_{m+\mu}^2}, \tag{3.3.17}$$

where $\hat{C}_{\mu, \lambda}$ is a bounded constant that depends on λ and μ . Equation (3.3.16) can be simplified using (3.3.17) to

$$\|Q(\partial^{j-l} f, \partial^l g)\|_{L_m^2}^2 \leq \hat{C}^{\lambda, \beta, \mu} (\|\partial^{j-l} f\|_{L_{m+\lambda}^2}^2 \|\partial^l g\|_{L_{m+\mu}^2}^2 + \|\partial^{j-l} f\|_{L_{m+\mu}^2}^2 \|\partial^l g\|_{L_{m+\lambda}^2}^2). \tag{3.3.18}$$

Next we finish the proof by substituting in (3.3.18) into (3.3.14) and simplifying the

expression to get

$$\begin{aligned}
\|Q(f, g)\|_{H_m^\alpha}^2 &\leq \hat{C}_1^{\lambda, \beta, \mu} \sum_{1 \leq j \leq \alpha} \sum_{1 \leq l \leq j} \binom{j}{l} (\|\partial^{j-l} f\|_{L_{m+\lambda}^2}^2 \|\partial^l g\|_{L_{m+\mu}^2}^2 \\
&\quad + \|\partial^{j-l} f\|_{L_{m+\mu}^2}^2 \|\partial^l g\|_{L_{m+\lambda}^2}^2) \\
&\leq \hat{C}_2^{\lambda, \beta, \mu} \sum_{1 \leq l \leq \alpha} \binom{\alpha}{l} (\|\partial^{\alpha-l} f\|_{L_{m+\lambda}^2}^2 \|\partial^l g\|_{L_{m+\mu}^2}^2 \\
&\quad + \|\partial^{\alpha-l} f\|_{L_{m+\mu}^2}^2 \|\partial^l g\|_{L_{m+\lambda}^2}^2) \\
&\leq \hat{C}^{\lambda, \beta, \mu} \sum_{1 \leq l \leq \alpha} \binom{\alpha}{l} (\|f\|_{H_{m+\lambda}^{\alpha-l}}^2 \|g\|_{H_{m+\mu}^l}^2 \\
&\quad + \|f\|_{H_{m+\mu}^{\alpha-l}}^2 \|g\|_{H_{m+\lambda}^l}^2), \quad (3.3.19)
\end{aligned}$$

where $\hat{C}^{\lambda, \beta, \mu}$ is a constant that depends on $\mu > \frac{3}{2} + \lambda$, λ, β , and the mass and energy of the initial state. Thus we have proved the theorem. \square

From the estimate (3.3.19) in Theorem 3.3.4, we now prove a useful result for the symmetric collision integral $Q(f, f)$

Corollary 3.3.5. *For $f \in H_{m+\lambda}^\alpha \cap H_{m+\mu}^\alpha$*

$$\|Q(f, f)\|_{H_m^\alpha} \leq \hat{C}^{\lambda, \beta, \mu} \|f\|_{H_{m+\lambda+\mu}^\alpha}^2, \quad (3.3.20)$$

where $\mu > \frac{3}{2} + \lambda$, $\hat{C}^{\lambda, \beta, \mu}$ depends on the mass and energy of initial state, λ, β , and μ .

Proof. Note that

$$\|f\|_{H_{m+\lambda}^\alpha} \leq C^{\lambda, \mu} \|f\|_{H_{m+\lambda+\mu}^\alpha}, \quad (3.3.21)$$

where $C^{\lambda, \mu}$ depends on $\mu > \frac{3}{2} + \lambda$, the dimension of the \mathbf{v} -space, mass and energy of the initial state.

Then we use (3.3.21) in (3.3.19) of the proof of Theorem 3.3.4 for $g = f$ to get

$$\begin{aligned} \|Q(f, f)\|_{H_m^\alpha}^2 &\leq \hat{C}^{\lambda, \beta, \mu} \sum_{1 \leq l \leq \alpha} \binom{\alpha}{l} (\|f\|_{H_{m+\lambda}^{\alpha-l}}^2 \|f\|_{H_{m+\mu}^l}^2 + \|f\|_{H_{m+\mu}^{\alpha-l}}^2 \|f\|_{H_{m+\lambda}^l}^2) \\ &\leq \hat{C}_2^{\lambda, \beta, \mu} \sum_{1 \leq l \leq \alpha} \binom{\alpha}{l} \|f\|_{H_{m+\lambda+\mu}^\alpha}^4. \end{aligned} \quad (3.3.22)$$

Upon simplification of (3.3.22), we get the corollary. \square

Remarks:

(i) From [36] and bilinearity of the $Q(f, f)$,

$$Q(f, f) - Q(g, g) = Q(f + g, f - g). \quad (3.3.23)$$

(ii) If it has a regularity $\alpha = (\alpha_1, \alpha_2, \alpha_3)$, multi-index $\forall |\alpha| \geq 0$ then, $Q(f^\Pi, f^\Pi) \in H^{\alpha, 0}(\Omega_v)$.

(iii) Computational velocity domain: The choice of truncation, L in the velocity domain $(\Omega_v = [-L, L]^3)$ is based on two factors:

- The velocity domain is restricted to $\Omega_v = [-L, L]^3$. The choice of L is done in such a way that $\text{supp}[f] = [-L_f, L_f]^3 \subset \Omega_v$. From [81], it is known that for such a choice of f , $\text{supp}[Q(f, f)] \subset [-\sqrt{2}L_f, \sqrt{2}L_f]^3$. In order for the support relations of Q and f to hold good in the estimates, the value of L is chosen in such a way that Ω_v contains the supports of both Q and f , i.e., $L > \sqrt{2}L_f$. So, $Q(f^\Pi, f^\Pi) \in L^2(\Omega_v)$ and $\text{supp}[Q(f^\Pi, f^\Pi)] \subset \Omega_v$.
- Long time behavior of f :

* If there is a steady state solution, \mathcal{M} to the problem, then given any ϵ , $\exists \Omega_\epsilon$ such that

$$\|\mathcal{M}\|_{L_t^k(\mathbb{R}^3 \setminus \Omega_\epsilon)} \leq O(\epsilon).$$

* For $k = 1, 2; l \in [0, 1]$, from the work of Bobylev, Cercignani and Gamba [26] for Maxwell type interactions,

$$\text{supp } f_0 \subset \Omega_\epsilon, \text{ and } \|f - \mathcal{M}\|_{L_t^k(\mathbb{R}^3)} \leq e^{-\mu t} \|f_0 - \mathcal{M}\|_{L_t^k(\mathbb{R}^3)}.$$

* So, uniformly in time

$$\begin{aligned} \|f\|_{L_t^k(\mathbb{R}^3 \setminus \Omega_\epsilon)} &\leq \|f - \mathcal{M}\|_{L_t^k(\mathbb{R}^3 \setminus \Omega_\epsilon)} + \|\mathcal{M}\|_{L_t^k(\mathbb{R}^3 \setminus \Omega_\epsilon)} \\ &\leq \|f - \mathcal{M}\|_{L_t^k(\mathbb{R}^3)} + O(\epsilon) \\ &\leq e^{-\mu t} \|f_0 - \mathcal{M}\|_{L_t^k(\mathbb{R}^3)} + O(\epsilon). \end{aligned}$$

Since $\|f_0 - \mathcal{M}\|_{L_t^k(\mathbb{R}^3)}$ is known and time independent,

$$\|f\|_{L_t^k(\mathbb{R}^3 \setminus \Omega_\epsilon)} \leq O(\epsilon) \quad \text{for any } t > T_* = |\log(\epsilon + \|f_0 - \mathcal{M}\|_{L_t^k(\mathbb{R}^3)})/\mu|.$$

Then,

$$\begin{aligned} \|f\|_{L_t^k(\mathbb{R}^3)} &\leq \|f\|_{L_t^k(\Omega_\epsilon)} + \|f\|_{L_t^k(\mathbb{R}^3 \setminus \Omega_\epsilon)} \\ &\leq \|f\|_{L_t^k(\Omega_\epsilon)} + O(\epsilon) \quad \text{for any } t > T_*. \end{aligned} \quad (3.3.24)$$

Note: ϵ is seen as the mass lost due to truncation of the computed distribution functions.

Theorem 3.3.6. (Convergence Estimate): For $f \in H_{\lambda+\mu}^\alpha(\Omega_v)$, and $f^\Pi \in H_{\lambda+\mu}^\gamma(\Omega_v)$,

$$\|Q(f, f) - Q_C^\Pi(f^\Pi, f^\Pi)\|_{L^2(\Omega_v)} \leq \hat{C}^{\lambda, \beta, \mu} \frac{\|f\|_{H_{\lambda+\mu}^\alpha(\Omega_v)}^2}{N^{|\alpha|}} + \hat{C}^{\lambda, \beta, \mu} \frac{\|f^\Pi\|_{H_{\lambda+\mu}^\gamma(\Omega_v)}}{N^{|\gamma|}} + O(\epsilon) + O(\epsilon^2), \quad (3.3.25)$$

where $\hat{C}^{\lambda,\beta,\mu}$ is a constant that depends on λ, β, L , and the Fourier space (ζ) discretization, h_ζ ; $C^{\lambda,\beta,L}$ is a constant that depends on λ, β , and μ ; and α, γ are the degrees of regularity of f and Q , respectively, as multi-indices. ϵ is the error due to velocity truncation.

Proof. The proof of (3.3.25) is straightforward due to Theorems 3.2.3 and 3.3.3 and Corollary 3.3.2. The first step in proving (3.3.25) is rewriting its left hand side using the transitive property and the bilinearity property of $Q(f, g)$ from (3.3.23). For brevity, let $Q(f) = Q(f, f)$, $Q(f^\Pi) = Q(f^\Pi, f^\Pi)$, $Q^\Pi(f^\Pi) = Q^\Pi(f^\Pi, f^\Pi)$, and $Q_C^\Pi(f^\Pi) = Q_C^\Pi(f^\Pi, f^\Pi)$. Then

$$\begin{aligned}
\|Q(f) - Q_C^\Pi(f^\Pi)\|_{L^2(\Omega_v)} &\leq \|Q(f) - Q^\Pi(f^\Pi)\|_{L^2(\Omega_v)} + \|Q^\Pi(f^\Pi) - Q_C^\Pi(f^\Pi)\|_{L^2(\Omega_v)} \\
&\leq (1 + \hat{C})(\|Q(f) - Q^\Pi(f^\Pi)\|_{L^2(\Omega_v)}) \\
&\leq C_1(\|Q(f) - Q(f^\Pi)\|_{L^2(\Omega_v)} + \|Q(f^\Pi) - Q^\Pi(f^\Pi)\|_{L^2(\Omega_v)}) \\
&\leq C_1(\|Q(f + f^\Pi, f - f^\Pi)\|_{L^2(\Omega_v)} \\
&\quad + \|Q(f^\Pi) - Q^\Pi(f^\Pi)\|_{L^2(\Omega_v)})
\end{aligned} \tag{3.3.26}$$

where Theorem 3.2.3 was used in the second line. Now,

$$\|Q(f + f^\Pi, f - f^\Pi)\|_{L^2(\Omega_v)} \leq \|Q(f + f^\Pi, f - f^\Pi)\|_{L^2}. \tag{3.3.27}$$

We then use Theorem 3.3.3 with $m = 0$ and (3.3.27) in the first term of the last line of (3.3.26):

$$\|Q(f + f^\Pi, f - f^\Pi)\|_{L^2(\Omega_v)} \leq C^{\lambda,\beta}(\|f + f^\Pi\|_{L_\lambda^2} \|f - f^\Pi\|_{L_\lambda^1} + \|f + f^\Pi\|_{L_\lambda^1} \|f - f^\Pi\|_{L_\lambda^2}).$$

Using (3.3.24) in the above equation,

$$\begin{aligned}
\|Q(f + f^\Pi, f - f^\Pi)\|_{L^2(\Omega_v)} &\leq \tilde{C}^{\lambda,\beta}(\|f\|_{L_\lambda^2(\Omega_v)} \|f - f^\Pi\|_{L_\lambda^1(\Omega_v)} \\
&\quad + \|f\|_{L_\lambda^1(\Omega_v)} \|f - f^\Pi\|_{L_\lambda^2(\Omega_v)} + O(\epsilon) + O(\epsilon^2)).
\end{aligned} \tag{3.3.28}$$

For $g \in L^2_{m+\mu}(\Omega_v)$, it is straightforward to see that

$$\begin{aligned} \|g\|_{L^1_m(\Omega_v)} &\leq C_1^\mu \|g\|_{L^2_{m+\mu}(\Omega_v)}, \\ \|g\|_{L^2_m(\Omega_v)} &\leq C_2^\mu \|g\|_{L^2_{m+\mu}(\Omega_v)}, \end{aligned} \quad (3.3.29)$$

where C_1^μ, C_2^μ are bounded constants that depend on $\mu > \frac{3}{2}$. Using (3.3.29) and (3.3.4) from Corollary 3.3.2 in (3.3.28), we get

$$\begin{aligned} \|Q(f + f^\Pi, f - f^\Pi)\|_{L^2(\Omega_v)} &\leq \tilde{C}^{\lambda, \beta} (C_2^\mu \|f\|_{L^2_{\lambda+\mu}(\Omega_v)} C_1^\mu \|f - f^\Pi\|_{L^2_{\lambda+\mu}(\Omega_v)} \\ &\quad + C_1^\mu \|f\|_{L^2_{\lambda+\mu}(\Omega_v)} C_2^\mu \|f - f^\Pi\|_{L^2_{\lambda+\mu}(\Omega_v)}) \\ &\leq \hat{C}^{\lambda, \beta, \mu} \|f\|_{L^2_{\lambda+\mu}(\Omega_v)} \|f - f^\Pi\|_{L^2_{\lambda+\mu}(\Omega_v)} \\ &\leq \hat{C}_1^{\lambda, \beta, \mu} \frac{\|f\|_{L^2_{\lambda+\mu}(\Omega_v)} \|f\|_{H^{\alpha, 0}_{\lambda+\mu}(\Omega_v)}}{N^{|\alpha|}} \\ &\leq \hat{C}_2^{\lambda, \beta, \mu} \frac{\|f\|_{H^{\alpha, 0}_{\lambda+\mu}(\Omega_v)} \|f\|_{H^{\alpha, 0}_{\lambda+\mu}(\Omega_v)}}{N^{|\alpha|}} \\ &\leq \hat{C}^{\lambda, \beta, \mu} \frac{\|f\|_{H^{\alpha}_{\lambda+\mu}(\Omega_v)}^2}{N^{|\alpha|}}, \end{aligned} \quad (3.3.30)$$

where α gives the degree of regularity of f in \mathbf{v} as a multi-index. Lets consider the second term in the last line of (3.3.26). This term can be bounded using the projection approximation estimate from Corollary 3.3.2. This gives

$$\begin{aligned} \|Q(f^\Pi) - Q^\Pi(f^\Pi)\|_{L^2(\Omega_v)} &\leq \hat{C}_4 \frac{\|Q(f^\Pi)\|_{H^{\gamma, 0}(\Omega_v)}}{N^{|\gamma|}} \\ &\leq \hat{C} \frac{\|Q(f^\Pi)\|_{H^\gamma(\Omega_v)}}{N^{|\gamma|}}, \end{aligned} \quad (3.3.31)$$

where γ gives the degree of regularity of Q in \mathbf{v} as a multi-index. We combine the results from (3.3.30) and (3.3.31) and absorbing C into $\hat{C}^{\lambda, \beta, L}$ and \hat{C} in the appropriate terms to give

$$\|Q(f, f) - Q_C^\Pi(f^\Pi, f^\Pi)\|_{L^2(\Omega_v)} \leq \hat{C}^{\lambda, \beta, \mu} \frac{\|f\|_{H^{\alpha}_{\lambda+\mu}(\Omega_v)}^2}{N^{|\alpha|}} + \hat{C} \frac{\|Q(f^\Pi)\|_{H^\gamma(\Omega_v)}}{N^{|\gamma|}} + O(\epsilon) + O(\epsilon^2), \quad (3.3.32)$$

where \hat{C} is a constant that depends on v - space dimension and the Fourier space (ζ) discretization, h_ζ ; $C^{\lambda,\beta,L}$ is a constant that depends on λ, β , and μ ; and α, γ are the degrees of regularity of f and Q respectively as multi-indices.

Finally, we finish proving (3.3.25) from (3.3.33) by using $k = 0$ in Corollary 3.3.5 and using (3.3.24) to get

$$\|Q(f, f) - Q_C^\Pi(f^\Pi, f^\Pi)\|_{L^2(\Omega_v)} \leq \hat{C}^{\lambda,\beta,\mu} \frac{\|f\|_{H_{\lambda+\mu}^\alpha(\Omega_v)}^2}{N^{|\alpha|}} + \hat{C}^{\lambda,\beta,\mu} \frac{\|f^\Pi\|_{H_{\lambda+\mu}^\gamma(\Omega_v)}}{N^{|\gamma|}} + O(\epsilon) + O(\epsilon^2) \quad (3.3.33)$$

where $\hat{C}^{\lambda,\beta,\mu}$ and $C^{\lambda,\beta,L}$ are as required. \square

Chapter 4

Self-Similar Asymptotics for the Space Homogeneous Problem with Maxwell Type Interactions

As mentioned in the introduction, a new interesting benchmark problem for our scheme is that of a dynamically scaled solution involving self-similar asymptotics. More precisely, we present a simulation where the computed solution, in properly scaled time, approaches a self similar solution. This is of interest because of the power tail behavior, i.e., higher order moments of the computed solution are unbounded. The content of the current chapter is inspired by the work of Gamba and Bobylev [17]. For completeness of this presentation, the analytical description of such asymptotics is given here.

4.1 Self-Similar Solution for a Non-negative Thermostat Temperature

We consider the Maxwell type equation from (2.2.12) related to a space homogeneous model for a weakly coupled mixture modeling a slowdown process. The content of this section is dealt in detail in [17] for a particular choice of zero background temperature (cold thermostat). For the sake of brevity, we refer to [17] for certain details. However, a slightly more general form of the self-similar solution for non zero background temperature is derived here from the zero background temperature solution. Without loss of generality for our numerical test, we assume the differential cross sections for the collision kernel, b_L of the linear part and corresponding nonlinear part, b_N are the same, both denoted by $b(\frac{\zeta \cdot \sigma}{|\zeta|})$, satisfying the *Grad cut-off*

conditions (2.1.6). In particular, condition (2.2.14) is automatically satisfied.

Taking the Fourier Transform of the initial value problem (2.2.12) with respect to the velocity variable \mathbf{v} (for a general velocity dimension d) yields

$$\begin{aligned}\hat{f}_t &= \hat{Q}(\hat{f}, \hat{f}) + \Theta \int_{\sigma \in S^{d-1}} b\left(\frac{\zeta \cdot \sigma}{|\zeta|}\right) [\hat{f}(\zeta_+) \hat{M}_{\mathcal{T}}(\zeta_-) - \hat{f}(\zeta) \hat{M}_{\mathcal{T}}(0)] d\sigma \\ &= \hat{Q}(\hat{f}, \hat{f}) + \Theta \hat{L}(\hat{f}, \hat{M}_{\mathcal{T}}), \\ \hat{f}(\zeta, 0) &= \hat{f}_0(\zeta),\end{aligned}\tag{4.1.1}$$

where $\hat{f}(0) = 1$ and $\hat{M}_{\mathcal{T}}(\zeta) = e^{-\frac{\mathcal{T}|\zeta|^2}{2m}}$. The first collisional integral is

$$\begin{aligned}\hat{Q}(\hat{f}, \hat{f}) &= \int_{\omega \in S^{d-1}} \left[\hat{f}(\zeta_+) \hat{f}(\zeta_-) - \hat{f}(0) \hat{f}(\zeta) \right] b\left(\frac{\zeta \cdot \sigma}{|\zeta|}\right) d\sigma, \\ \zeta_{\pm} &= \frac{1}{2}(\zeta \pm |\zeta|\omega),\end{aligned}\tag{4.1.2}$$

corresponding to the transformed elastic collisions of particles with mass equal to unity in spectral space. The corresponding exchange of coordinates in the second linear integral \hat{L} in (4.1.1) is given by

$$\zeta_+ = \frac{\zeta + m|\zeta|\omega}{1+m} \quad \text{and} \quad \zeta_- = \zeta - \zeta_+, \tag{4.1.3}$$

corresponding to those exchanging collisions with particles of mass m .

In order to benchmark our calculation we use a particular case of model (4.1.1) for a choice of parameters where explicit solution formulae in Fourier space were constructed in [17]. In particular, in order to find a solvable equation (4.1.1), we set both sets of particles to have equal mass, that is $m = 1$ in (4.1.3). First, rescale (4.1.1) with the Fourier transform equilibrium distribution (i.e., Maxwellian),

$$\hat{f}(\zeta, t) = \tilde{f}(\zeta, t) \exp\left(\frac{-\mathcal{T}|\zeta|^2}{2}\right),$$

so it follows

$$\begin{aligned}\tilde{f}_t &= \widehat{Q}(\tilde{f}, \tilde{f}) + \Theta \int_{\sigma \in S^{d-1}} b\left(\frac{\zeta \cdot \sigma}{|\zeta|}\right) [\tilde{f}(\zeta_+) - \tilde{f}(\zeta)] d\sigma \\ &= \widehat{Q}(\tilde{f}, \tilde{f}) + \Theta \widehat{L}(\tilde{f}).\end{aligned}\tag{4.1.4}$$

Notice that this last equation is equivalent to (4.1.1) for $\mathcal{T} = 0$. Next, we will look for isotropic solutions to the initial value problem. Let the initial states be isotropic with bounded energy whose Fourier transform belongs to the unit ball of continuous bounded functions with the L^∞ -norm. Set

$$x = \frac{|\zeta|^2}{2}, \quad \phi(x, t) = \tilde{f}(\zeta, t),\tag{4.1.5}$$

and $\zeta \cdot \sigma / |\zeta| = \cos \theta = 2s - 1$, where the differential cross section function b is renormalized such that

$$\int_{S^{d-1}} b\left(\frac{\zeta \cdot \sigma}{|\zeta|}\right) d\sigma = 2^{d-1} \omega_{d-2} \int_0^1 b(2s-1)(s(1-s))^{\frac{d-3}{2}} ds = \int_0^1 G(s) ds = 1,$$

where the constant ω_{d-2} is the measure of the $d-2$ dimensional sphere. Then using (4.1.5), the transformed and rescaled initial value problem (4.1.4) becomes

$$\begin{aligned}\phi_t &= \int_0^1 \phi((1-s)x) [\phi(sx) + \Theta] G(s) ds - (1 + \Theta) \phi(x), \\ \phi(x, 0) &= 1 - x + O(x^{1+\varepsilon}) \quad \text{for } \varepsilon \geq 0, |x| < 1.\end{aligned}\tag{4.1.6}$$

Note that $\phi(0, t) = 1$ for all $t \geq 0$. For our simulations we take $d = 3$ and $b(\cos \theta) = G(s) = (4\omega_1)^{-1} = 1/4\pi$. However, it is possible to compute more general cross sections satisfying the integrability condition in s . In what follows, the only important assumption is that $b(\cos \theta)$ satisfies the *Grad cut-off* assumption (2.1.6).

Further, in order to construct self-similar solutions with finite energy, one starts by looking for solutions of (4.1.6) with the form

$$\phi(x, t) = \psi(xe^{-\mu t}) = 1 - a(xe^{-\mu t})^p, \quad \text{as } xe^{-\mu t} \rightarrow 0, \quad \text{with } p \leq 1, \tag{4.1.7}$$

Note that $p = 1$ corresponds to initial states with finite energy. We shall see that it is possible to choose a value of μ and Θ for which one can find explicit solutions in Fourier space with a very peculiar behavior: they decay power like for large velocities, and are unbounded at zero velocity. Equivalently, set

$$\eta = a^{\frac{1}{p}} x e^{-\mu t},$$

and substitute $\phi(x, t)$ by $\psi(\eta)$ in (4.1.6) to obtain

$$-\psi'(\eta)\mu\eta + (1 + \Theta)\psi(\eta) = \int_0^1 \psi((1-s)\eta)[\psi(s\eta) + \Theta] ds. \quad (4.1.8)$$

Next, set the change of coordinates $s\eta = y$ with its corresponding differentials $ds = \frac{dy}{\eta}$ and replace in (4.1.8) to obtain

$$\begin{aligned} -\mu\eta\psi'(\eta) + (1 + \Theta)\psi(\eta) &= \int_0^\eta \psi(\eta - y)[\psi(y) + \Theta] \frac{dy}{\eta} \\ &= \frac{1}{\eta} [\psi * (\psi + \Theta)](\eta). \end{aligned} \quad (4.1.9)$$

In order to construct an explicit solution to (4.1.9), one needs to examine its Laplace transform. Define the Laplace transform as

$$w(z) = L(\psi)(z) = \int_0^\infty \psi(\eta) e^{-z\eta} d\eta; \quad \text{Re}(z) > z_0.$$

Recalling the Laplace transform properties $L(\eta^2\psi'(\eta))(z) = (zw(z))''$ and $L(\eta\psi(\eta))(z) = -w'(z)$, the corresponding Laplace transformed equation computed from (4.1.9) reads

$$\mu(zw(z))'' + (1 + \Theta)w'(z) + w(z)(w(z) + \frac{\Theta}{z}) = 0, \quad (4.1.10)$$

or equivalently, for $u(z) = zw(z)$, satisfies the equation

$$\mu z^2 u'' + (1 + \Theta)z u' + u(u - 1) = 0. \quad (4.1.11)$$

Next, for a parameter q to be conveniently determined below, set $\bar{u}(\mathbf{z}) = u(z) = u(\mathbf{z}^{\frac{1}{q}})$, with $\mathbf{z} = z^q$. Then rewrite (4.1.11) in terms of $\bar{u}(\mathbf{z})$ in order to obtain

$$\mu q^2 \mathbf{z}^2 \bar{u}'' + q[\mu(q-1) + (1+\Theta)] \mathbf{z} \bar{u}' + \bar{u}^2 - \bar{u} = 0. \quad (4.1.12)$$

To this end, for a parameter B , also to be conveniently determined below, set $\bar{u}(\mathbf{z}) = \mathbf{z}^2 y(\mathbf{z}) + B$, so (4.1.12) is transformed into a solvable second order ODE for $y(\mathbf{z})$. That is

$$\mu q^2 \mathbf{z}^4 y'' + \mathbf{z}^4 y^2 + \alpha \mathbf{z}^3 y' + \beta \mathbf{z}^2 y + B(B-1) = 0,$$

where the coefficients α and β satisfy

$$\alpha = (5\mu q + 1 + \Theta - \mu)q \quad \text{and} \quad \beta = 4\mu q^2 + 2B - 1 + 2q(1 + \Theta - \mu), \quad (4.1.13)$$

and setting both α and β to vanish, equation (4.1.13) is of Painlevé type. If in addition, B is taken to be 0 or 1, the solutions of (4.1.13) are rational functions of \mathbf{z} depending on the parameter q .

The particular choice of $B = 1$ results in a self-similar solution with finite energy, which is the case of interest for our benchmarking calculations. In particular, $B = 1$, combined with the α and β vanishing conditions of (4.1.13), yields that q must satisfy $6\mu q^2 = 1$. The corresponding reduced equation (4.1.13) is the simple ODE $y'' = -6y^2$, whose solution is expressed in terms of the Weierstrass elliptic function $y(\mathbf{z}) = -(c + \mathbf{z})^{-2}$, with the constant c determined below by the appropriate boundary conditions at infinity given in (4.2.1) in the next section. We remark that the particular choice of $B = 0$ yields

$$\begin{aligned} \mu(p) &= -\frac{1}{6p^2}, \\ \Theta &= \frac{(3p-1)(1-2p)}{6p^2}. \end{aligned} \quad (4.1.14)$$

In particular, for $B = 1$ and choosing q such that α and β vanish, the solutions to (4.1.11) are of the form

$$u(z) = 1 - (1 + c z^{-q})^{-2}$$

with

(4.1.15)

$$6\mu q^2 = 1 \quad \text{and} \quad \Theta = \mu[1 - 5q] - 1 ,$$

where c is determined from the boundary conditions (4.2.1), which must satisfy

$$u(z) \cong 1 - \frac{1}{z^q}, \quad \text{as } z \rightarrow \infty .$$

Since this condition at infinity is satisfied for the choice of $q = -\frac{p}{2}$, then the vanishing conditions on (4.1.13) results in the constraint that both μ and Θ are related to the solution of the problem as follows

$$u(z) = 1 - (1 + z^{\frac{p}{2}})^{-2}$$

with

$$\mu = \frac{2}{3p^2} \quad \text{and} \quad \Theta = \frac{(3p+1)(2-p)}{3p^2} .$$

In order to recover the corresponding self-similar solution in the space of probability distributions with finite energy, one chooses $p = 1$, which forces from the above identity $\mu = \frac{2}{3}$. To complete the discussion of finite background temperatures, we denote the self-similar solution for the original equilibrium positive temperature \mathcal{T} (i.e., the hot thermostat case) for the linear collisional term (including time dependence for convenience) by

$$\phi_0(x, t) = \phi(x, t) \quad \text{for } \mathcal{T} = 0 \quad \text{and} \quad \phi_{\mathcal{T}}(x, t) = \phi(x, t) \quad \text{for } \mathcal{T} > 0$$

so that $\phi_{\mathcal{T}}(x, t) = \phi_0(x, t)e^{-\mathcal{T}x} .$

(4.1.16)

Note that the solution constructed in (4.2.2) in the next section is actually $\phi_0(x, t)$. Then the self-similar solution for non zero background temperature, denoted by

$\phi_{\mathcal{T}}(x, t)$, satisfies

$$\begin{aligned}\phi_{\mathcal{T}}(\zeta, t) &= \frac{4}{\pi} \int_0^\infty e^{-|\zeta|^2 e^{-2t/3} a s^2 / 2} \frac{1}{(1+s^2)^2} e^{-|\zeta|^2 \mathcal{T} / 2} ds \\ &= \frac{4}{\pi} \int_0^\infty e^{-|\zeta|^2 [e^{-2t/3} a s^2 + \mathcal{T}] / 2} \frac{1}{(1+s^2)^2} ds,\end{aligned}\quad (4.1.17)$$

where $x = |\zeta|^2 / 2$ has been used. In particular, let $\bar{T} = e^{-2t/3} a s^2 + \mathcal{T}$. Taking the inverse Fourier Transform, we obtain the corresponding self-similar state, according to (2.2.9), in probability space

$$f_{\mathcal{T}}^{ss}(|\mathbf{v}|, t) = e^t F_{\mathcal{T}}(|\mathbf{v}| e^{t/3}) \text{ with } F_{\mathcal{T}}(|\mathbf{v}|) = \frac{4}{\pi} \int_0^\infty \frac{1}{(1+s^2)^2} \frac{e^{-|\mathbf{v}|^2 / 2\bar{T}}}{(2\pi\bar{T})^{\frac{3}{2}}} ds. \quad (4.1.18)$$

As $t \rightarrow \infty$, $\bar{T} = \mathcal{T} + a s^2 e^{-\frac{2t}{3}} \rightarrow \mathcal{T}$. This yields

$$F_{\mathcal{T}}(|\mathbf{v}|) \rightarrow_{t \rightarrow \infty} \frac{4}{\pi} \frac{1}{(2\pi\mathcal{T})^{\frac{3}{2}}} e^{-|\mathbf{v}|^2 / 2\mathcal{T}} \int_0^\infty \frac{1}{(1+s^2)^2} ds = M_{\mathcal{T}}(\mathbf{v}), \quad (4.1.19)$$

$$\text{since} \quad \frac{4}{\pi} \int_0^\infty \frac{1}{(1+s^2)^2} ds = \frac{2}{\pi} \left(\frac{s}{1+s^2} + \arctan(s) \right) \Big|_0^\infty = 1. \quad (4.1.20)$$

So, the self-similar particle distribution $f_{\mathcal{T}}^{ss}(\mathbf{v}, t)$ approaches a rescaled Maxwellian distribution with the background temperature \mathcal{T} , that is according to (2.2.9),

$$f_{\mathcal{T}}^{ss}(|\mathbf{v}|, t) = e^t F_{\mathcal{T}}(|\mathbf{v}| e^{t/3}) \approx \frac{e^t}{(2\pi\mathcal{T})^{\frac{3}{2}}} e^{-(|\mathbf{v}|^2 e^{2t/3}) / 2\mathcal{T} + t}, \quad \text{as } t \rightarrow \infty. \quad (4.1.21)$$

Remark: Such an asymptotic behavior, for finite initial energy, is due to the balance of the binary term and the linear collisional term in (2.2.12).

4.2 Self Similar Asymptotics for Cold Thermostat

In order to complete the argument, we need the inverse Laplace transforms from Bobylev and Cercignani [12], where it was shown that the inversion by Laplace transform of $u(z)$, the solution of (4.1.8) for $p = 1$ and $\mu = \frac{2}{3}$, satisfies

$$\psi(\eta) = \frac{4}{\pi} \int_0^\infty \frac{s^2}{(1+s^2)^2} e^{-\eta} ds.$$

The Fourier transform of the isotropic self-similar solution associated to the problem in (2.2.12) will take the form

$$\phi(x, t) = \psi(xe^{-\mu t}) = 1 - a(xe^{-\mu t})^p, \quad \text{as } xe^{-\mu t} \rightarrow 0, \quad \text{with } p \leq 1, \quad (4.2.1)$$

where $x = |\zeta|^2/2$ and μ and Θ are related by

$$\mu = \frac{2}{3p^2} \quad \text{and} \quad \Theta = \frac{(3p+1)(2-p)}{3p^2}.$$

Note that $p = 1$ in (4.2.1) corresponds to initial states with finite energy. It was shown in [17] for $\mathcal{T} = 0$ (i.e., cold thermostat), the Fourier transform of the self-similar, isotropic solutions of (2.2.12) is given by

$$\phi(x, t) = \frac{4}{\pi} \int_0^\infty \frac{1}{(1+s^2)^2} e^{-xe^{-\frac{2t}{3}} s^2} ds, \quad (4.2.2)$$

and its corresponding inverse Fourier transform for $p = 1$, $\mu = \frac{2}{3}$ and $\Theta = \frac{4}{3}$ (as computed in [17]) is given by

$$f_0^{ss}(|\mathbf{v}|, t) = e^t F_0(|\mathbf{v}| e^{t/3}) \quad \text{with} \quad F_0(|\mathbf{v}|) = \frac{4}{\pi} \int_0^\infty \frac{1}{(1+s^2)^2} \frac{e^{-|\mathbf{v}|^2/2s^2}}{(2\pi s^2)^{\frac{3}{2}}} ds. \quad (4.2.3)$$

Remark: It is interesting to observe that, as computed originally in [12], for $B = 0$ in (4.1.14), letting $p = \frac{1}{3}$ or $p = \frac{1}{2}$ in (4.2.2) yields $\Theta = 0$, and one can construct explicit solutions to the elastic BTE with infinite initial energy. It is clear now that in order to have self-similar explicit solutions with finite energy, one needs to have this weakly couple mixture model for slowdown processes, or bluntly speaking, the linear collisional term added to the elastic energy conservative operator.

In addition, very interesting behavior is seen on $F_{\mathcal{T}}(|\mathbf{v}|)$ as $\mathcal{T} \rightarrow 0$ (cold thermostat problem), where the particle distribution approaches a distribution with power-like tails (i.e., a power law decay for large values of $|\mathbf{v}|$) and an integral singularity at

the origin. Indeed, in [17] an asymptotic behavior is derived for $F_0(|\mathbf{v}|)$ from (4.2.3), for large and small values of $|\mathbf{v}|$, leading to

$$\begin{aligned} F_0(|\mathbf{v}|) &= 2\left(\frac{2}{\pi}\right)^{5/2} \frac{1}{|\mathbf{v}|^6} [1 + O(\frac{1}{|\mathbf{v}|})], \quad \text{for } |\mathbf{v}| \rightarrow \infty, \\ F_0(|\mathbf{v}|) &= \frac{2^{1/2}}{\pi^{5/2}} \frac{1}{|\mathbf{v}|^2} [1 + 2|\mathbf{v}|^2 \ln(|\mathbf{v}|) + O(|\mathbf{v}|^2)], \quad \text{for } |\mathbf{v}| \rightarrow 0. \end{aligned} \quad (4.2.4)$$

In particular, the self-similar particle distribution function $F(|\mathbf{v}|)$, $\mathbf{v} \in \mathbb{R}^3$, behaves like $\frac{1}{|\mathbf{v}|^6}$ as $|\mathbf{v}| \rightarrow \infty$, and as $\frac{1}{|\mathbf{v}|^2}$ as $|\mathbf{v}| \rightarrow 0$, which indicates a very anomalous, non-equilibrium behavior as a function of velocity, but, nevertheless, remains with finite mass and kinetic temperature. This asymptotic effect can be described as an overpopulated (with respect to Maxwellian), large energy tails and infinitely many particles at zero energy. This interesting, unusual behavior is observed in problems of soft condensed matter [54].

We shall see, then in the following section, that our solver captures these states with spectral accuracy and, consequently, the self similar solutions are attractors for a large class of initial states. These numerical tests are a crucial aspect of the spectral Lagrangian deterministic solver used to simulate this type of non-equilibrium phenomena, where all these explicit formulas for our probability distributions allow us to carefully benchmark the proposed numerical scheme.

4.3 Self-Similar Asymptotics for a General Problem

The self-similar nature of the solutions $F(|\mathbf{v}|)$ for a general class of problems, for a wide range of values for the parameters β , p , μ and Θ , was addressed in [15] with much detail. Three different behaviors have been clearly explained. Of particular interest for our present numerical study are the mixture problem with a cold background and the inelastic Boltzmann cases.

For the purpose of our presentation, let $\phi = \mathcal{F}[f]$ be the Fourier transform of the probability distribution function satisfying the initial value problem (2.1.1)-(2.1.5) or (2.2.3). Let's denote by $\Gamma(\phi) = \mathcal{F}[Q^+(f, f)]$ the Fourier transform of the gain part of the collisional term associated with the initial value problem. It was shown that the operator $\Gamma(\phi)$, defined over the Banach space of continuous bounded functions with the L^∞ -norm (i.e., the space of characteristic functions or the space of Fourier transforms of probability distributions), satisfies the following three properties:

- 1 -** $\Gamma(\phi)$ preserves the unit ball in the Banach space;
- 2 -** $\Gamma(\phi)$ is an L -Lipschitz operator, i.e., there exists a bounded linear operator L in the Banach space, such that

$$|\Gamma(u_1) - \Gamma(u_2)|(x, t) \leq L(|u_1 - u_2|(x, t)) \quad \forall \quad \|u_i\| \leq 1, i = 1, 2; .$$

- 3 -** $\Gamma(\phi)$ is invariant under the transformations (dilations)

$$e^{\tau \mathcal{D}} \Gamma(u) = \Gamma(e^{\tau \mathcal{D}} u) , \quad \mathcal{D} = x \frac{\partial}{\partial x} , \quad e^{\tau \mathcal{D}} u(x) = u(xe^\tau), \quad \tau \in \mathbb{R}^+ . \quad (4.3.1)$$

In the particular case of the initial value problem associated to Boltzmann type equations for Maxwell type interactions, the bounded linear operator that satisfies Property **2** is the one that linearizes the Fourier transform of the gain operator about the state $u = 1$.

Let x^p be the eigenfunction corresponding to the eigenvalue $\lambda(p)$ of the linear operator L associated to Γ , i.e., $L(x^p) = \lambda(p)x^p$. Define the *spectral function associated to Γ* as $\mu(p) = \frac{\lambda(p)-1}{p}$, defined for $p > 0$. It can be shown that $\mu(0+) = +\infty$ (i.e. $p = 0$ is a vertical asymptote) and that for the problems associated to the initial

value problems (2.1.1)-(2.1.5) or (2.2.3), there exists a unique minimum for $\mu(p)$ localized at $p_0 > 1$, and that $\mu(p) \rightarrow 0^-$ as $p \rightarrow +\infty$.

The existence of self-similar states and convergence of the solution to the initial value problem to such self-similar distribution function is described in the following four statements.

(i) *Existence:* [15] - Lemma 5.1 There exists a unique isotropic solution $f(|\mathbf{v}|, t)$ to the initial value problem (2.1.1)-(2.1.5) or (2.2.3) for Maxwell type interactions in the class of probability measures, satisfying $f(|\mathbf{v}|, 0) = f_0(|\mathbf{v}|) \geq 0$, $\int_{\mathbb{R}^d} f_0(|\mathbf{v}|) d\mathbf{v} = 1$, and such that for the Fourier transform problem $x = \frac{|\zeta|^2}{2}$, $u_0 = \mathcal{F}[f_0(|\mathbf{v}|)] = 1 + O(x)$, as $x \rightarrow 0$.

(ii) *Self similar states:* [15] - Theorem 7.2: $f(|\mathbf{v}|, t)$ has self-similar asymptotics in the following sense.

Taking the Fourier transform of the initial state to satisfy

$$u_0 + \mu(p) x^p u'_0 = \Gamma(u_0) + O(x^{p+\epsilon}) \quad \text{such that } p + \epsilon < p_0 \quad (4.3.2)$$

(i.e., $\mu'(p) < 0$). Then, there exists a unique, non-negative, self-similar solution

$$f^{ss}(|\mathbf{v}|, t) = e^{-\frac{d}{2}\mu(p)t} F_p(|\mathbf{v}| e^{-\frac{1}{2}\mu(p)t}),$$

with $\mathcal{F}(F_p(|\mathbf{v}|)) = w(x)$, $x = |\zeta|^2/2$, such that $\mu(p)x^p w'(x) + w(x) = \Gamma(w)$.

(iii) *Self similar asymptotics* - Section 9 and Theorem 11.1 in [15]: In the class of probability measures, there exists a unique solution $f(|\mathbf{v}|, t)$ satisfying $f(|\mathbf{v}|, 0) =$

$f_0(|\mathbf{v}|) \geq 0$, with $\int_{\mathbb{R}^d} f(|\mathbf{v}|) d\mathbf{v} = 1$, such that, for $x = \frac{|\zeta|^2}{2}$,

$$\mathcal{F}[f_0(|\mathbf{v}|)] = 1 - a x^p + O(x^{p+\epsilon}), x \rightarrow 0, 0 \leq p \leq 1 \quad \text{with } p + \epsilon < p_0 .$$

Then, for any given $0 \leq p \leq 1$, there exists a unique non-negative self-similar solution $f_{ss}^{(p)}(|\mathbf{v}|, t) = e^{-\frac{d}{2}\mu(p)t} F_p(|\mathbf{v}| e^{-\frac{1}{2}\mu(p)t})$ such that

$$f(|\mathbf{v}|, t) \rightarrow_{t \rightarrow \infty} e^{-\frac{d}{2}\mu(p)t} F_p(|\mathbf{v}| e^{-\frac{1}{2}\mu(p)t}) , \quad (4.3.3)$$

or, equivalently,

$$e^{\frac{d}{2}\mu(p)t} f(|\mathbf{v}| e^{\frac{1}{2}\mu(p)t}, t) \rightarrow_{t \rightarrow \infty} F_p(|\mathbf{v}|) , \quad (4.3.4)$$

where $\mu(p)$ is the value of the spectral function associated to the linear bounded operator L as described above.

(iv) *Power tail behavior of the asymptotic limit:* If $\mu(p) < 0$, then the self-similar limiting function $F_p(|\mathbf{v}|)$ does not have finite moments of all orders. In addition, if $0 \leq p \leq 1$ then all moments of order less than p are bounded; i.e., $m_q = \int_{\mathbb{R}^d} F_p(|\mathbf{v}|) |\mathbf{v}|^{2q} d\mathbf{v} \leq \infty$ for $0 \leq q \leq p$. However, if $p = 1$ (the finite energy case), then the boundedness of moments of any order larger than 1 depend on the conjugate value of $\mu(1)$ by the spectral function $\mu(p)$. That means $m_q < \infty$ only for $0 \leq q \leq p_*$, where $p_* \geq p_0 > 1$ is the unique maximal root of the equation $\mu(p_*) = \mu(1)$.

Remark 1: When $p = 1$, $\mu(1)$ is the energy dissipation rate, and $\mathcal{E}(t) = e^{\mu(1)t}$ is the kinetic energy evolution function. So, $\mathcal{E}(t)^{d/2} f(\mathbf{v}\mathcal{E}(t), t) \rightarrow F_1(|\mathbf{v}|)$.

Remark 2: We point out that condition (4.3.2) on the initial state is easily satisfied by taking a sufficiently concentrated Maxwellian distribution, as shown in [15], and

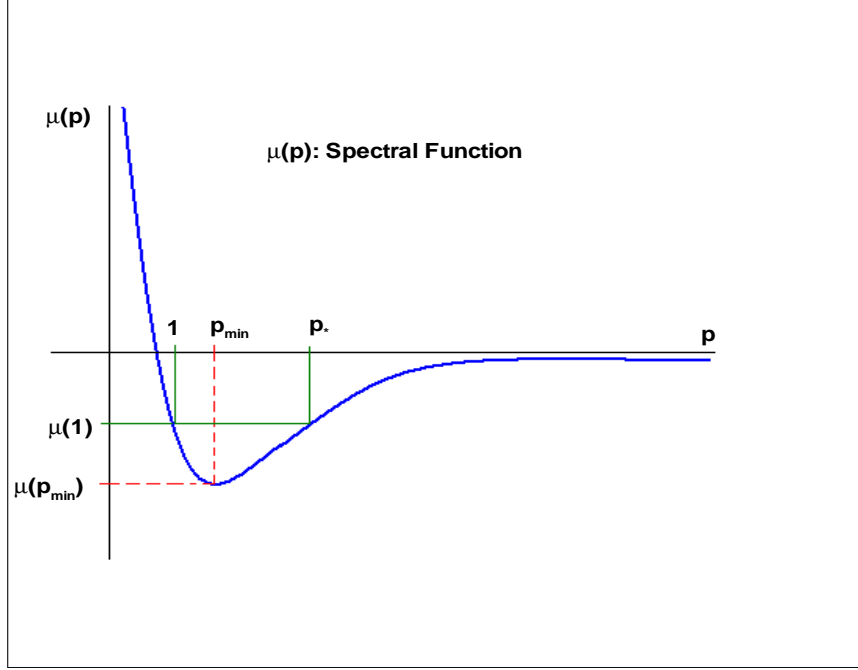


Figure 4.1: Spectral Function $\mu(p)$ for a general homogeneous Boltzmann collisional problem of Maxwell type interactions.

as done for our simulations in the next section.

However, rescaling with a different rate, it is not possible to pick up the non-trivial limiting state f^{ss} , since

$$f(|\mathbf{v}|e^{\frac{1}{2}\eta t}, t) \rightarrow_{t \rightarrow \infty} e^{-\frac{d}{2}\eta t} \delta_0(|\mathbf{v}|) \quad \eta > \mu(1), \quad (4.3.5)$$

and

$$f(|v|e^{\frac{1}{2}\eta t}, t) \rightarrow_{t \rightarrow \infty} 0 \quad \mu(p_{min}) < \mu(1 + \delta) < \eta < \mu(1). \quad (4.3.6)$$

These results are also true for any $p \leq 1$. For the general space homogeneous (elastic or inelastic) Boltzmann model of Maxwell type or the corresponding mixture

problem, the spectral function $\mu(p)$ is given in Figure 4.1.

Chapter 5

Numerical Results

In this chapter, the numerical analysis of the proposed spectral scheme is performed and the results benchmarked. The velocity space discretization is shown in Section 5.1. Since the collision integral computation is an important component in modeling physical processes in rarefied gas dynamics, the algorithm used to compute it is described in Section 5.2. Several test cases for the space homogeneous Boltzmann are performed in Section 5.4. An interesting self-similar solution is computed in Section 5.4. As described in the introduction, the Boltzmann equation is an important tool in the analysis of shock structures. Recognizing this, such a study is done for $1D(\mathbf{x}) \times 3D(\mathbf{v})$ in Section 5.5. The classic Riemann problem is numerically analyzed for Knudsen numbers close to continuum. The shock tube problem of Sone and Aoki [85], where the wall temperature is suddenly increased or decreased, is also studied. We consider the problem of heat transfer between two parallel plates with diffusive boundary conditions for a range of Knudsen numbers from close to continuum to a highly rarefied state. Finally, the classical infinite shock tube problem that generates a non-moving shock wave is studied. The point worth noting in this example is that the flow in the final case turns from a supersonic flow to a subsonic flow across the shock.

5.1 Velocity and Fourier Space Discretization

The distribution function is generally not compactly supported in \mathbf{v} but is usually negligible outside of a small ball

$$B_L(\mathbf{V}) = \{\mathbf{v} \in \mathbb{R}^3 : |\mathbf{v} - \mathbf{V}| \leq L\},$$

where \mathbf{V} is the flow velocity. As mentioned in the description of the spectral method, we restrict to distribution functions that are compactly supported, i.e.,

$$\text{supp} f(\mathbf{x}, \cdot, t) = B_L(\mathbf{V}), \quad \forall \mathbf{x} \in \Omega_x, \quad t \geq 0.$$

It is numerically much more convenient to consider a cube instead of a ball $B_L(\mathbf{V})$

$$C_L(\mathbf{V}) = \{\mathbf{v} \in \mathbb{R}^3 : |v_j - V_j| \leq L, \quad j = 1, 2, 3\}.$$

It is easy to see that $B_L(\mathbf{V}) \subset C_L(\mathbf{V})$, and such a discretization is used for all velocity variables \mathbf{v}, \mathbf{v}_* . This yields the following discretization space for the relative velocity $\mathbf{u} = \mathbf{v} - \mathbf{v}_*$

$$\mathbf{u} \in C_{2L}(\mathbf{0}).$$

Let $N \in \mathbb{N}$ be a natural number. Then we denote by C_N the following three-dimensional indices

$$C_N = \{\mathbf{k} \in \mathbb{Z}^3 : 0 \leq k_m < N, \quad m = 1, 2, 3\}.$$

Introducing the velocity mesh size $h_v = \frac{2L}{N}$, we get the following discrete velocities

$$C_v = \{\mathbf{v}_j = \mathbf{V} + (h_v - \frac{N}{2})\mathbf{j}, \quad \mathbf{j} \in C_N\} \subset C_L(\mathbf{V}).$$

Similarly, the appropriate set for the relative velocity \mathbf{u} is

$$C_u = \{\mathbf{v}_j = (h_v - \frac{N}{2})\mathbf{j}, \quad \mathbf{j} \in C_N\} \subset C_{2L}(\mathbf{0}).$$

Because, an FFT package is used, the discrete velocity space then requires the Fourier space mesh size $h_\zeta = \frac{2L_\zeta}{N}$ to be given from h_v as

$$h_v h_\zeta = \frac{2\pi}{N}, \quad \text{i.e.,} \quad h_\zeta = \frac{\pi}{L},$$

and the discrete Fourier variable set is given by

$$C_\zeta = \{\zeta = h_\zeta \mathbf{j}, \quad \mathbf{j} \in C_N\}.$$

5.2 Collision Integral Algorithm

The collision integral is given by (3.1.8) and (3.1.9) in Section 3.1. $\bar{G}_{\lambda,\beta}(\xi, \zeta)$ from (3.1.9) can be computed either in advance and stored or at run time. Depending on the computing strategy employed, a operation efficient (former) or a memory efficient (latter) approach can be implemented. Define $\bar{G}_{\mathbf{l},\mathbf{m}} := \bar{G}_{\lambda,\beta}(\xi_{\mathbf{l}}, \zeta_{\mathbf{m}})$ for a particular choice of λ and β . Then the process of computing the collision integral can be summarized into the following algorithm, wherein $\omega[\mathbf{l}]$ are the integration weights. For the purpose of numerical analysis in the rest of the chapter, trapezoidal rule

weights are used.

```

[1] ( $O(N^3 \log(N))$ )       $\hat{f}(\zeta_{\mathbf{m}}) = \text{FFT}_{\mathbf{v}_{\mathbf{k}} \rightarrow \zeta_{\mathbf{m}}} [f(\mathbf{v}_{\mathbf{k}})]$ 
[2] ( $O(N^3)$ )              For  $\zeta_{\mathbf{m}} \in C_u$ , Do

[2.1]       $\hat{Q}(\zeta_{\mathbf{m}}) = 0$ 
[2.2] ( $O(N^3)$ )      For  $\xi_{\mathbf{l}} \in C_u$ , Do

[2.2.1]  $g(\xi_{\mathbf{l}}) = \hat{f}(\xi_{\mathbf{l}}) \times \hat{f}(\zeta_{\mathbf{m}} - \xi_{\mathbf{l}})$ 
[2.2.2]  $\hat{Q}(\zeta_{\mathbf{m}}) = \hat{Q}(\zeta_{\mathbf{m}}) + \bar{G}_{\mathbf{l}, \mathbf{m}} \times \omega[\mathbf{l}] \times g(\xi_{\mathbf{l}})$ 

[2.2]*      End Do

[2]*      End Do

[3] ( $O(N^3 \log(N))$ )       $Q(\mathbf{v}_k) = \text{IFFT}_{\zeta_{\mathbf{m}} \rightarrow \mathbf{v}_{\mathbf{k}}} [\hat{Q}(\zeta_{\mathbf{m}})]$ 

```

5.3 Temporal and Advection Approximation

After the discretization of the collision integral, the problem of numerically solving the Boltzmann equation reduces to approximating the time derivative $\frac{\partial}{\partial t}$ and the advection term $\mathbf{v} \cdot \nabla_{\mathbf{x}} f(\mathbf{x}, \mathbf{v}, t) + \nabla_{\mathbf{v}} \cdot (\mathbf{F} f(\mathbf{x}, \mathbf{v}, t))$ in (2.1.1). The current section describes a standard way of dealing with the advection term in the space inhomogeneous Boltzmann equation. A description of the time and space discretizations which are employed is also given.

5.3.1 Time Splitting

When computing the space inhomogeneous Boltzmann transport equation with zero force field, i.e., $\mathbf{F} = (0, 0, 0)$, a reliable way of devising a numerical approximation is to employ an efficient time-splitting method. The problem of solving equation (2.1.1) with $\mathbf{F} = (0, 0, 0)$ is divided into two smaller subproblems. We discretize time into discrete values $t_n = t_0 + n * dt$, where $dt > 0$ is the time step size. Denote $f(\mathbf{x}, \mathbf{v}, t_n)$ by $f_n(\mathbf{x}, \mathbf{v})$. Using a first order time-splitting scheme, in a small time interval $[t_n, t_{n+1}]$, the two subproblems are given by

(1) The Advection (Collisionless) Problem

$$\begin{aligned} \frac{\partial}{\partial t} g(\mathbf{x}, \mathbf{v}, t) + \mathbf{v} \cdot \nabla_{\mathbf{x}} g(\mathbf{x}, \mathbf{v}, t) &= 0, \\ g(\mathbf{x}, \mathbf{v}, 0) &= f_n(\mathbf{x}, \mathbf{v}), \end{aligned} \quad (5.3.1)$$

and

(2) The Homogenous (Collision) Problem

$$\begin{aligned} \frac{\partial}{\partial t} \tilde{f}(\mathbf{x}, \mathbf{v}, t) &= Q(\tilde{f}, \tilde{f}), \\ \tilde{f}(\mathbf{x}, \mathbf{v}, 0) &= g(\mathbf{x}, \mathbf{v}, dt). \end{aligned} \quad (5.3.2)$$

Let $A(dt)$ and $H(dt)$ be solution operators corresponding to (5.3.1) and (5.3.2), respectively. Then the solutions for (5.3.1) and (5.3.2) can be rewritten as

$$\begin{aligned} g(\mathbf{x}, \mathbf{v}, dt) &= A(dt) f_n(\mathbf{x}, \mathbf{v}), \\ \tilde{f}(\mathbf{x}, \mathbf{v}, dt) &= H(dt) g(\mathbf{x}, \mathbf{v}, dt), \end{aligned} \quad (5.3.3)$$

and the computed solution at time step t_{n+1} is given by

$$f_{n+1}(\mathbf{x}, \mathbf{v}) = f(\mathbf{x}, \mathbf{v}, t_{n+1}) = H(dt) A(dt) f_n(\mathbf{x}, \mathbf{v}). \quad (5.3.4)$$

This is a time-splitting method that is first order in time. Equation (5.3.4) is usually good enough for kinetic problems. Nevertheless, for non-stiff problems a second order time-splitting method (*Strang splitting*) can be employed:

$$f_{n+1}(\mathbf{x}, \mathbf{v}) = f(\mathbf{x}, \mathbf{v}, t_{n+1}) = A\left(\frac{dt}{2}\right)H(dt)A\left(\frac{dt}{2}\right)f_n(\mathbf{x}, \mathbf{v}). \quad (5.3.5)$$

Using *Strang splitting* to separate the advection and homogenous calculations, the overall finite difference scheme is second order in time provided that a second order in time scheme is used in each of the subproblems.

5.3.2 Space Discretization

We now turn to finite differences schemes for the advection operator. This is the first step in time splitting procedure mentioned above, i.e., collisionless step. For simplicity, only 1D flows (say in the x direction) are considered. So (5.3.1) reduces to

$$\frac{\partial}{\partial t}g(x, \mathbf{v}, t) + v_1 \frac{\partial}{\partial x}g(x, \mathbf{v}, t) = 0,$$

where $\mathbf{v} = (v_1, v_2, v_3)$ is used. A first order scheme that is used is the standard upwind scheme. Let $x_j = x_0 + jdx$ and $g_n^j(\mathbf{v}) = g(x_j, \mathbf{v}, t_n)$. Then

$$\begin{aligned} \frac{g_{n+1}^j(\mathbf{v}) - g_n^j(\mathbf{v})}{dt} + v_1 \frac{g_n^j(\mathbf{v}) - g_n^{j-1}(\mathbf{v})}{dx} &= 0, \quad v_1 \geq 0 \\ \frac{g_{n+1}^j(\mathbf{v}) - g_n^j(\mathbf{v})}{dt} + v_1 \frac{g_n^{j+1}(\mathbf{v}) - g_n^j(\mathbf{v})}{dx} &= 0, \quad v_1 < 0, \end{aligned} \quad (5.3.6)$$

gives the upwind scheme for appropriate signs of v_1 . As is the case with explicit finite difference schemes, (5.3.6) is restricted by the CFL condition which guarantees that the numerical domain of dependence includes the analytical domain of dependence. For (5.3.6), the CFL condition is given by $|\max(v_1) \frac{dt}{dx}| \leq 1$. When necessary, the

following second order upwind scheme is used:

$$\begin{aligned} \frac{g_{n+1}^j(\mathbf{v}) - g_n^j(\mathbf{v})}{dt} + v_1 \frac{g_n^{j-2}(\mathbf{v}) - 4g_n^{j-1}(\mathbf{v}) + 3g_n^j(\mathbf{v})}{2dx} &= 0, \quad v_1 \geq 0 \\ \frac{g_{n+1}^j(\mathbf{v}) - g_n^j(\mathbf{v})}{dt} + v_1 \frac{-g_n^{j+2}(\mathbf{v}) + 4g_n^{j+1}(\mathbf{v}) - 3g_n^j(\mathbf{v})}{2dx} &= 0, \quad v_1 < 0. \end{aligned} \quad (5.3.7)$$

Again, (5.3.7) is restricted by the CFL condition $|\max(v_1) \frac{dt}{dx}| \leq 1$.

When using finite differences, it is desirable to use an implicit scheme which is unconditionally stable. But there are some difficulties when using the splitting process with implicit schemes. The total approximation is guaranteed as well as for the explicit scheme; however the influence of the implicit scheme can result in smoothing the profiles of desired quantities. Indeed, the solutions at a given time level of an implicit scheme at any point of the computational domain depend on the boundary values at the previous time level. So, the adoption of an implicit scheme is connected with the type of problem under consideration. In some problems the fact that particles from the boundary would influence an interior point without undergoing collisions during the single time step in the splitting process can lead to large errors of approximation. For the physical processes considered in this dissertation, an explicit scheme does a good job in terms of convergence and order of error.

5.3.3 Time Discretization

The simplest time discretization that is employed for (5.3.2) is the *Euler scheme*. The collision integral computation in (5.3.2) is not conservative as noted in the introduction. So, the correction mentioned in Section 3.2 is done at this step to the computed collision integral $Q(f_n f_n)$. This gives in the time interval $[t_n, t_{n+1}]$

$$\begin{aligned} Q_n &= \text{Conserve}(Q(f_n, f_n)), \\ \tilde{f}(\mathbf{x}, \mathbf{v}, dt) &= f_n(\mathbf{x}, \mathbf{v}) + dt Q_n. \end{aligned} \quad (5.3.8)$$

The Euler scheme is formally first order in time. For higher order accuracy, a second order Runge Kutta scheme is used whenever necessary:

$$\begin{aligned}
\tilde{Q}_n &= \text{Conserve}(Q(f_n, f_n)), \\
f_{n+1/2}(\mathbf{x}, \mathbf{v}) &= f_n(\mathbf{x}, \mathbf{v}) + \frac{dt}{2} \tilde{Q}_n, \\
Q_n &= \text{Conserve}(Q(f_{n+1/2}, f_{n+1/2})), \\
f_{n+1}(\mathbf{x}, \mathbf{v}) &= f_n(\mathbf{x}, \mathbf{v}) + dt Q_n.
\end{aligned} \tag{5.3.9}$$

The *Conserve* routine used in (5.3.8) and (5.3.9) is described in (3.2.28). In the rest of this chapter, appropriate reference quantities are chosen and the non-dimensional Boltzmann equation (2.4.2) with (2.4.3) is used. The “hats” are intentionally dropped in the sequel for simplicity.

5.4 The Space Homogenous Boltzmann Equation

The proposed numerical method is benchmarked to compute several examples of 3D in velocity and time for initial value problems associated with non-conservative models where some analysis is available. The exact moment formulae for Maxwell type of interactions as well as qualitative analysis for solutions of VHS models are available and these results are numerically validated. We plot our numerical results versus the exact available solutions in several cases. Because, all the computed problems converge to an isotropic long time state, we choose to plot the distribution function in only one direction, which is chosen to be the one with the initial anisotropies. All examples considered in this chapter are assumed to have isotropic, VHS collision kernels, i.e., the differential cross section is independent of the scattering angle. We simulate the homogeneous problem associated to the following problems for different choices of the parameters β and λ , and the Jacobian J_β and heating force term $\mathcal{G}(f)$. Let $x_r = l_0$ be the mean free time, T_r be the equilibrium temperature, $t_r = t_0$

be the mean free time and $v_r = v_{th}$ be the thermal velocity; these are the reference quantities in (2.4.1) for all space homoeogenous numerical computations.

5.4.1 Maxwell Type Elastic Collisions

Consider the initial value problem (2.2.1), with $B(|\mathbf{u}|, \mu) = \frac{1}{4\pi}|\mathbf{u}|^\lambda$. In (2.1.1), (2.1.5), the value of the parameters are $\beta = 1, J_\beta = 1$ and $\lambda = 0$ with the pre-collision velocities defined from (2.1.5). In this case, for a general initial state with finite mass, flow velocity and kinetic energy, there is no exact expression for the evolving distribution function. However, there are exact expressions for all the statistical moments (observables). Thus, the numerical method is compared with the known analytical moments for different discretizations in the velocity space.

The initial states we take are convex combinations of two shifted Maxwellian distributions. So consider the following case of initial states with unit mass $\int_{\mathbb{R}^3} f_0(\mathbf{v}) d\mathbf{v} = 1$ given by

$$f(\mathbf{v}, 0) = f_0(t) = \gamma M_{T_1}(\mathbf{v} - \mathbf{V}_1) + (1 - \gamma) M_{T_2}(\mathbf{v} - \mathbf{V}_2); \text{ with } 0 \leq \gamma \leq 1, \quad (5.4.1)$$

where $M_T(\mathbf{v} - \mathbf{V}) = \frac{1}{(2\pi T)^{3/2}} e^{-\frac{|\mathbf{v} - \mathbf{V}|^2}{(2T)}}$. Taking $\gamma = 0.5$ and flow velocity fields for the initial state determined by

$$\mathbf{V}_1 = [-2, 2, 0]^T, \quad \mathbf{V}_2 = [2, 0, 0]^T, \quad T_1 = 1, \quad T_2 = 1,$$

enables the first five moment equations corresponding to the collision invariants to be computed from those of the initial state. All higher order moments are computed using the classical moments recursion formulas for Maxwell type interactions (2.2.2). In particular, it is possible to obtain the exact evolution of moments as functions of time. Thus

$$\rho(t) = \rho_0 = 1 \quad \text{and} \quad \mathbf{V}(t) = \mathbf{V}_0 = [0, 1, 0]^T.$$

By a corresponding moment calculation as in (2.2.2), the complete evolution of the second moment tensor (2.1.10) is given by

$$M(t) = \begin{pmatrix} 5 & -2 & 0 \\ -2 & 3 & 0 \\ 0 & 0 & 1 \end{pmatrix} e^{-t/2} + \frac{1}{3} \begin{pmatrix} 8 & 0 & 0 \\ 0 & 11 & 0 \\ 0 & 0 & 8 \end{pmatrix} (1 - e^{-t/2}),$$

and the energy flow (2.1.10)

$$r(t) = \frac{1}{2} \begin{pmatrix} -4 \\ 13 \\ 0 \end{pmatrix} e^{-t/3} + \frac{1}{6} \begin{pmatrix} 0 \\ 43 \\ 0 \end{pmatrix} (1 - e^{-t/3}) - \frac{1}{6} \begin{pmatrix} 12 \\ 4 \\ 0 \end{pmatrix} (e^{-t/2} - e^{-t/3}),$$

and the kinetic temperature is conserved, so

$$T(t) = T_0 = \frac{8}{3}. \quad (5.4.2)$$

The above moments along with their numerical approximations for different discretizations in velocity space are shown in Figure 5.4.1. There is a good agreement of the computed moments with the corresponding analytical quantities except for energy flow for larger time. This is due to the fact that r_1 and r_2 are third order moments and that a smaller number of Fourier modes are taken for the simulation. Also, such higher order moments are not enforced as part of the conservation routine.

In Figure 5.2, the evolution of the computed distribution function into a Maxwellian is shown for $N = 40$.

5.4.2 Maxwell Type Elastic Collisions: Bobylev-Krook-Wu (BKW) Solution

An explicit solution to the initial value problem (2.1.1) for elastic, Maxwell type interactions ($\beta = 1, \lambda = 0$) was derived in [4] and independently in [67] for initial states that have at least $2 + \delta$ bounded moments. It is not of self-similar type, but

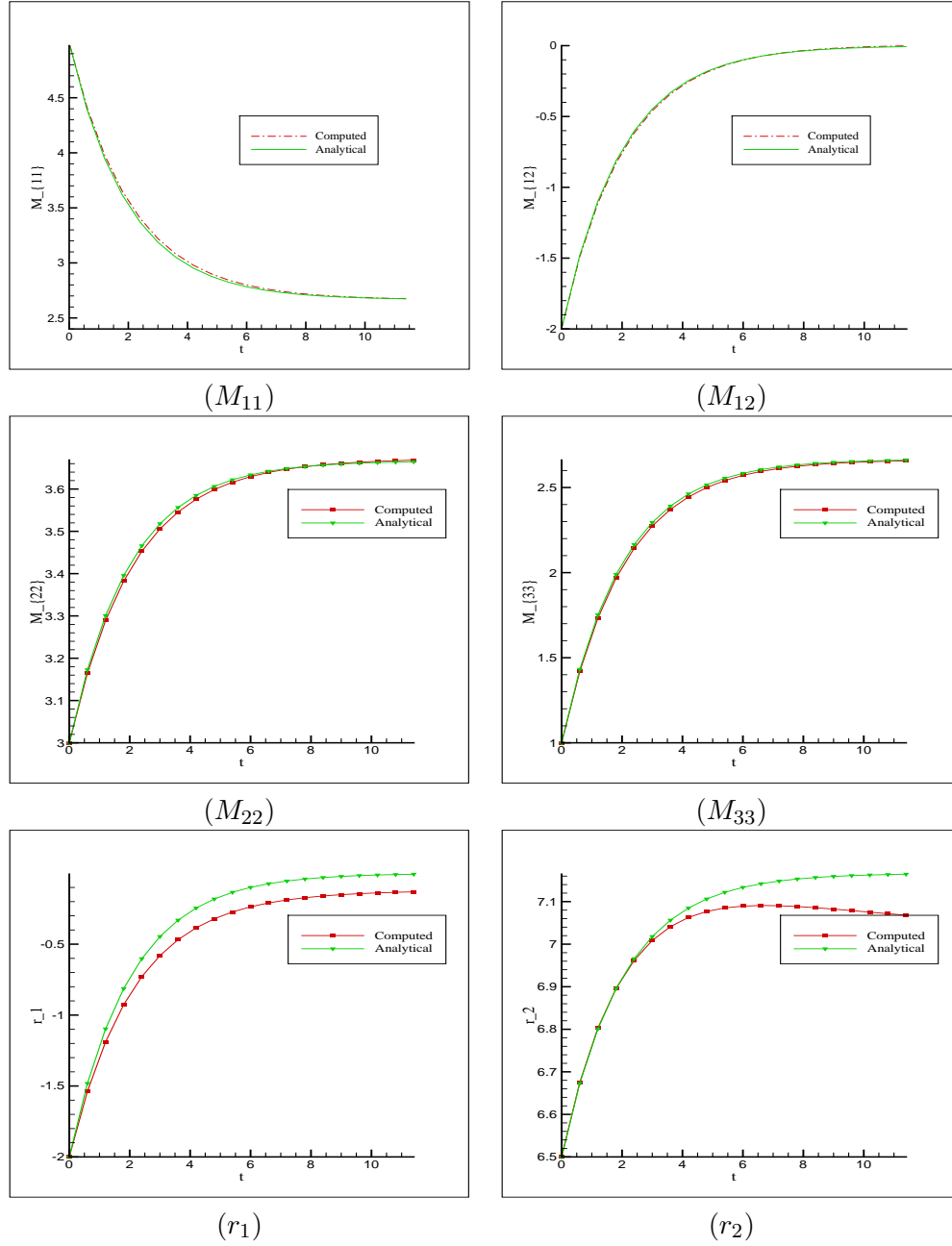


Figure 5.1: Maxwell type elastic collisions: Momentum flow M_{11} , M_{12} , M_{22} , M_{33} and energy flow r_1 , r_2 .

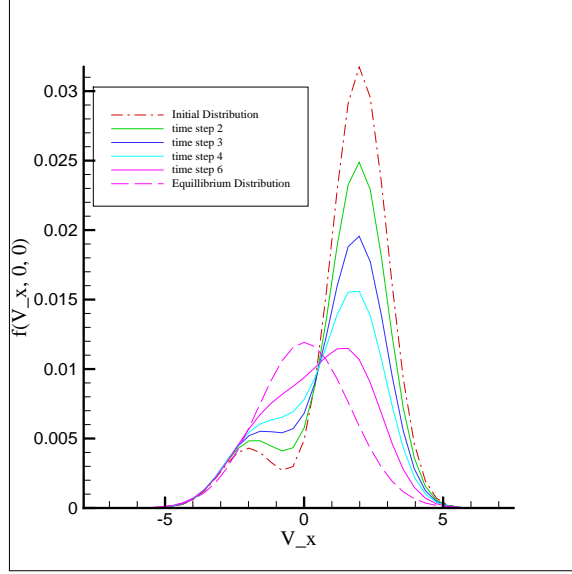


Figure 5.2: Maxwell type elastic collisions: Evolution of the distribution function

it can be shown to converge to a Maxwellian distribution. This solution takes the form

$$f(\mathbf{v}, t) = \frac{e^{-|\mathbf{v}|^2/(2K\eta^2)}}{2(2\pi K\eta^2)^{3/2}} \left(\frac{5K-3}{K} + \frac{1-K}{K^2} \frac{|\mathbf{v}|^2}{\eta^2} \right), \quad (5.4.3)$$

where $K = 1 - e^{-t/6}$ and η is the initial distribution temperature. It is interesting that it is negative for small values of t . So in order to obtain a physically meaning probability distribution, f must be non-negative. This is indeed the case for any $K \geq \frac{3}{5}$ or $t \geq t_0 \equiv 6 \ln(\frac{5}{2}) \sim 5.498$. In order to test the accuracy of the proposed solver, we set the initial distribution function to be the BKW solution at rescaled initial time. The numerical approximation to the BKW solution and the exact solution are shown for different values of N at various time steps in Figure 5.3. As can be seen in the figure, there is a good agreement.

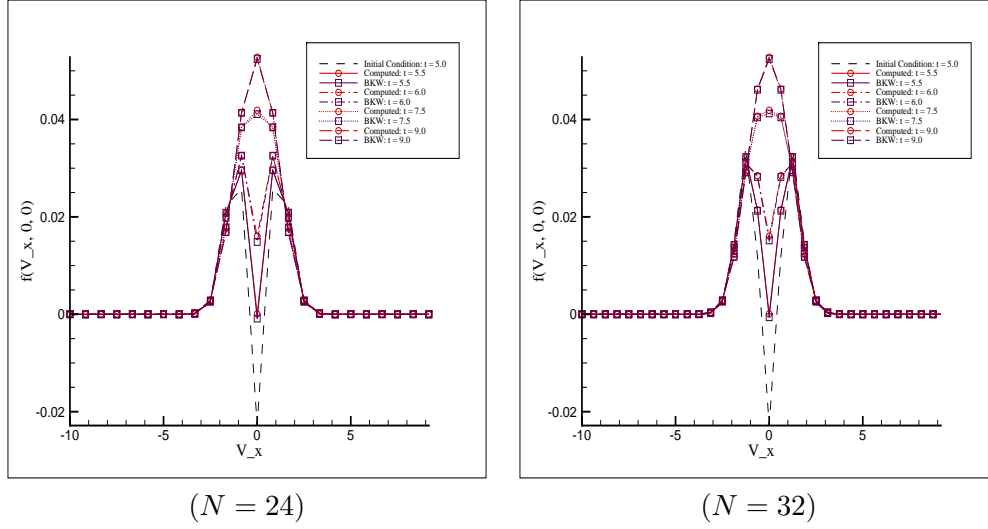


Figure 5.3: BKW, $\rho, E(t)$ conserved.

5.4.3 Hard-Sphere Elastic Collisions

In (2.1.1), we have $\beta = 1, J_\beta = 1$ and $\lambda = 1$ with the post-collision velocities defined from (2.1.1). Unlike Maxwell type interactions, there is neither an explicit expression for the moment equations nor are any explicit solution expression, as opposed to the BKW scenario. For Hard Sphere isotropic collisions, the expected behavior of the moments is similar to that of the Maxwell type interactions case, except that in this case, the moments evolve to the equilibrium faster than in the former case (see Figure 5.4 and compare to Figure 5.4.1).

Also shown is the time evolution of the distribution function starting from the convex combination of Maxwellians as described (5.4.1) in Figure 5.5.

5.4.4 Inelastic Collisions

Inelastic collisions is the scenario wherein the utility of the proposed method is clearly seen. No other spectral deterministic method can compute the distribution

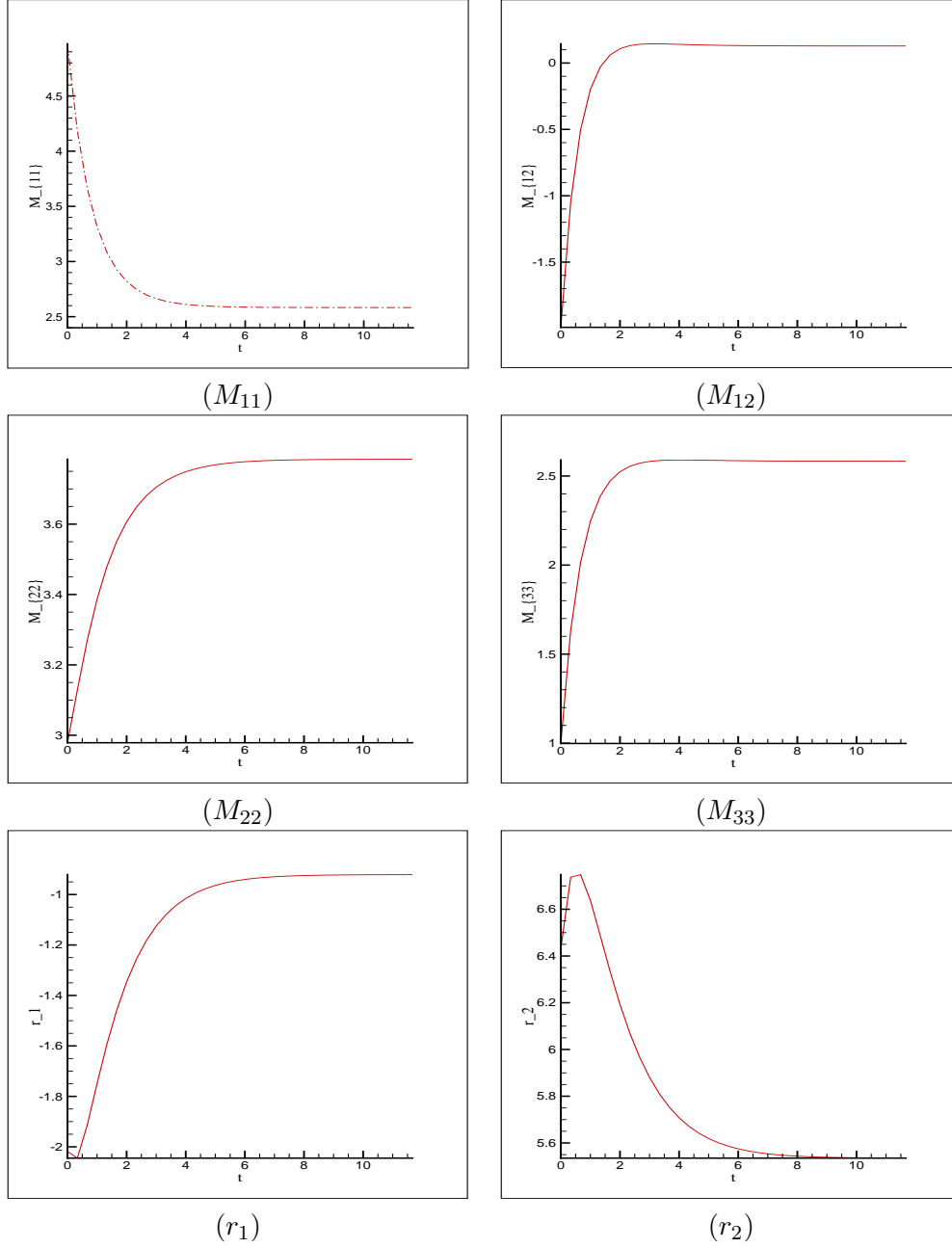


Figure 5.4: Hard sphere, elastic: Momentum flow $M_{11}, M_{12}, M_{22}, M_{33}$, energy flow r_1, r_2 .

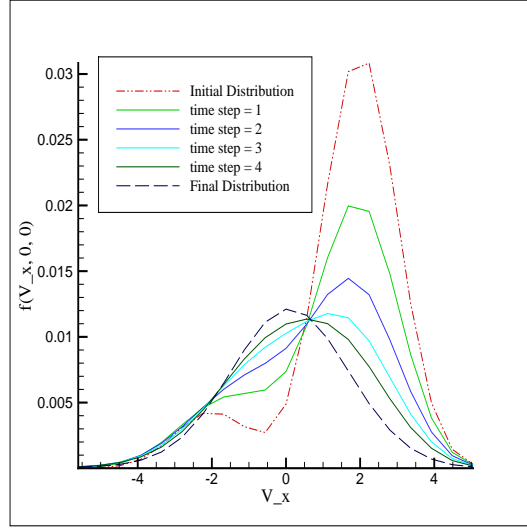


Figure 5.5: Hard sphere, elastic: Evolution of the distribution function, $N = 32$.

function in the case of inelastic collisions, but the current method computed $3 - D$ evolution examples without much complication and with exactly the same number of operations as used in an elastic collision case. This model works for variable hard potential (VHP) interactions. Consider the special case of Maxwell ($\lambda = 0$) type inelastic ($\beta \neq 1$) collisions in a space homogeneous Boltzmann Equation in (2.1.1), (2.1.5). Let $\phi(\mathbf{v}) = |\mathbf{v}|^2$ be a smooth enough test function. Using the weak form of the Boltzmann equation with such a test function, one can obtain the ODE governing the evolution of the kinetic energy $K(t)$. In general

$$\begin{aligned} \int_{\mathbf{v} \in \mathbb{R}^3} Q(f, f) \phi(\mathbf{v}) d\mathbf{v} &= \frac{1}{2} \int_{\mathbf{v} \times \mathbf{w} \in \mathbb{R}^6} \int_{\sigma \in S^2} B(|\mathbf{u}|, \mu) f(\mathbf{v}, t) f(\mathbf{w}, t) [\phi(\mathbf{v}') + \phi(\mathbf{w}')] d\sigma d\mathbf{w} d\mathbf{v} \\ &\quad - \frac{1}{2} \int_{\mathbf{v} \times \mathbf{w} \in \mathbb{R}^6} \int_{\sigma \in S^2} B(|\mathbf{u}|, \mu) f(\mathbf{v}, t) f(\mathbf{w}, t) [\phi(\mathbf{w}) + \phi(\mathbf{v})] d\sigma d\mathbf{w} d\mathbf{v}, \end{aligned} \quad (5.4.4)$$

and $\phi(\mathbf{v}) = |\mathbf{v}|^2$ gives the kinetic energy estimate. Using the definition of the post-collisional velocities from (2.1.1) and $\nu = \frac{\mathbf{u}}{|\mathbf{u}|}$ and $\mu = \sigma \cdot \nu$,

$$\begin{aligned}
|\mathbf{v}'|^2 + |\mathbf{w}'|^2 &= |\mathbf{v}|^2 + \beta(|\mathbf{u}|\sigma - \mathbf{u}) \cdot \mathbf{v} + \frac{\beta^2}{4}||\mathbf{u}|\sigma - \mathbf{u}|^2 + |\mathbf{w}|^2 \\
&\quad - \beta(|\mathbf{u}|\sigma - \mathbf{u}) \cdot \mathbf{w} + \frac{\beta^2}{4}||\mathbf{u}|\sigma - \mathbf{u}|^2 \\
&= |\mathbf{v}|^2 + |\mathbf{w}|^2 + \frac{\beta^2}{2}||\mathbf{u}|\sigma - \mathbf{u}|^2 + \beta(|\mathbf{u}|\sigma - \mathbf{u}) \cdot \mathbf{u} \\
&= |\mathbf{v}|^2 + |\mathbf{w}|^2 + \frac{\beta^2}{2}[2|\mathbf{u}|^2 - 2|\mathbf{u}|\sigma \cdot \mathbf{u}] + \beta(|\mathbf{u}|\sigma \cdot \mathbf{u} - |\mathbf{u}|^2)
\end{aligned}$$

So,

$$\begin{aligned}
|\mathbf{v}'|^2 + |\mathbf{w}'|^2 &= |\mathbf{v}|^2 + |\mathbf{w}|^2 + \beta^2|\mathbf{u}|[|\mathbf{u}| - \sigma \cdot \mathbf{u}] + \beta|\mathbf{u}|(\sigma \cdot \mathbf{u} - |\mathbf{u}|) \\
&= |\mathbf{v}|^2 + |\mathbf{w}|^2 + \beta|\mathbf{u}|[\beta(|\mathbf{u}| - \sigma \cdot \mathbf{u}) + (\sigma \cdot \mathbf{u} - |\mathbf{u}|)] \\
&= |\mathbf{v}|^2 + |\mathbf{w}|^2 + \beta|\mathbf{u}|(\sigma \cdot \mathbf{u} - |\mathbf{u}|)[- \beta + 1] \\
&= |\mathbf{v}|^2 + |\mathbf{w}|^2 + \beta|\mathbf{u}|^2\left(\frac{\sigma \cdot \mathbf{u}}{|\mathbf{u}|} - 1\right)[- \beta + 1] \\
&= |\mathbf{v}|^2 + |\mathbf{w}|^2 + \beta(1 - \beta)|\mathbf{u}|^2(\sigma \cdot \nu - 1),
\end{aligned}$$

which gives

$$|\mathbf{v}'|^2 + |\mathbf{w}'|^2 - |\mathbf{v}|^2 - |\mathbf{w}|^2 = \beta(1 - \beta)|\mathbf{u}|^2(\mu - 1). \quad (5.4.5)$$

Multiplying (2.1.1) with $\phi(\mathbf{v}) = |\mathbf{v}|^2$ and using (5.4.4), (5.4.5) and

$$K(t) = \frac{1}{2} \left(\int_{\mathbf{v} \in \mathbb{R}^3} |\mathbf{v}|^2 f(\mathbf{v}, t) d\mathbf{v} \right),$$

we get

$$\begin{aligned}
K'(t) &= \frac{1}{2} \frac{d}{dt} \left(\int_{\mathbf{v} \in \mathbb{R}^6} |\mathbf{v}|^2 f(\mathbf{v}, t) d\mathbf{v} \right) \\
&= \frac{1}{2} \int_{\mathbf{v} \in \mathbb{R}^3} \int_{\mathbf{w} \in \mathbb{R}^3} \int_{\sigma \in S^2} C_\lambda |\mathbf{u}|^\lambda f(\mathbf{v}, t) f(\mathbf{w}, t) [\beta(1 - \beta) |\mathbf{u}|^2 (1 - \mu)] d\sigma d\mathbf{w} d\mathbf{v} \\
&= \frac{C_\lambda \beta(1 - \beta)}{2} \int_{\mathbf{v} \in \mathbb{R}^3} \int_{\mathbf{w} \in \mathbb{R}^3} |\mathbf{u}|^{\lambda+2} f(\mathbf{v}, t) f(\mathbf{w}, t) d\mathbf{w} d\mathbf{v} \underbrace{\int_{\sigma \in S^2} (1 - \mu) d\sigma}_{-4\pi}.
\end{aligned}$$

Let $\lambda = 0$ and $C_\lambda = \frac{1}{4\pi}$, i.e., Maxwell type interactions. Then

$$\begin{aligned}
K'(t) &= \frac{\beta(\beta - 1)}{4} \int_{\mathbf{v} \in \mathbb{R}^3} \int_{\mathbf{w} \in \mathbb{R}^3} |\mathbf{v} - \mathbf{w}|^2 f(\mathbf{v}, t) f(\mathbf{w}, t) d\mathbf{w} d\mathbf{v} \\
&= \frac{\beta(\beta - 1)}{4} \int_{\mathbf{v} \in \mathbb{R}^3} \int_{\mathbf{w} \in \mathbb{R}^3} (|\mathbf{v}|^2 + |\mathbf{w}|^2 - 2\mathbf{v} \cdot \mathbf{w}) f(\mathbf{v}) f(\mathbf{w}) d\mathbf{w} d\mathbf{v} \\
&= \frac{\beta(\beta - 1)}{4} [2K(t) + 2K(t) - 2 \int_{\mathbf{v} \in \mathbb{R}^3} \int_{\mathbf{w} \in \mathbb{R}^3} \mathbf{v} \cdot \mathbf{w} f(\mathbf{v}, t) f(\mathbf{w}, t) d\mathbf{w} d\mathbf{v}] \\
&= \beta(1 - \beta) \left[\frac{1}{2} \int_{\mathbf{v} \in \mathbb{R}^3} \int_{\mathbf{w} \in \mathbb{R}^3} \mathbf{v} \cdot \mathbf{w} f(\mathbf{v}, t) f(\mathbf{w}, t) d\mathbf{w} d\mathbf{v} - K(t) \right]
\end{aligned}$$

Using the fact that $\mathbf{v} = (v_1, v_2, v_3)$, $\mathbf{w} = (w_1, w_2, w_3)$, then the integral above can be simplified as follows

$$\begin{aligned}
\int_{\mathbf{v} \in \mathbb{R}^3} \int_{\mathbf{w} \in \mathbb{R}^3} \mathbf{v} \cdot \mathbf{w} f(\mathbf{v}, t) f(\mathbf{w}, t) d\mathbf{w} d\mathbf{v} &= \sum_{i=1}^3 \left(\int_{\mathbf{v} \in \mathbb{R}^3} v_i f(\mathbf{v}, t) d\mathbf{v} \right) \left(\int_{\mathbf{w} \in \mathbb{R}^3} w_i f(\mathbf{w}, t) d\mathbf{w} \right) \\
&= \sum_{i=1}^3 \rho(t)^2 V_i^2(t) \\
&= |\rho(t) \mathbf{V}(t)|^2,
\end{aligned}$$

where $\rho(t) \mathbf{V}(t)$ is the momentum of the distribution function. Since this is conserved, it remains constant, i.e., $\rho(t) \mathbf{V}(t) = \rho \mathbf{V}$. So

$$K'(t) = \beta(1 - \beta) \left(\frac{|\rho \mathbf{V}|^2}{2} - K(t) \right). \quad (5.4.6)$$

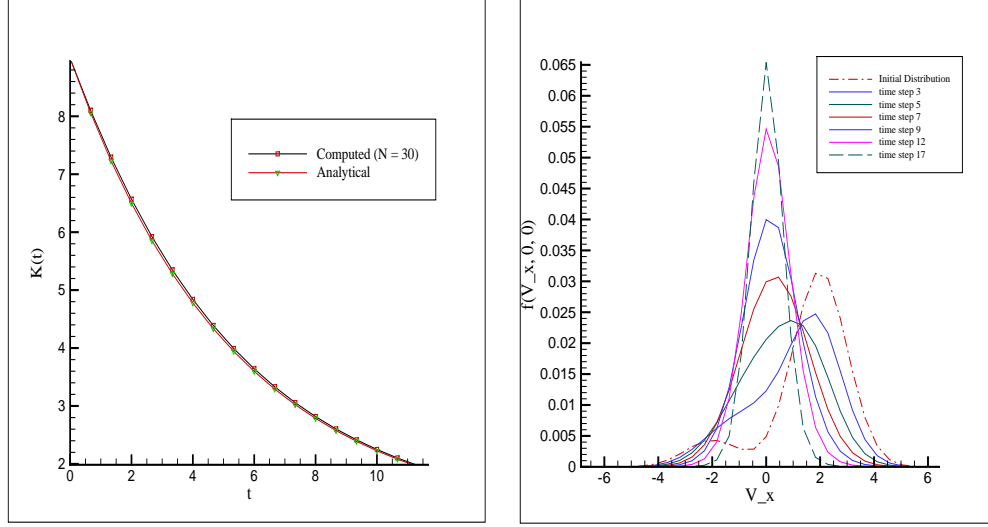


Figure 5.6: Inelastic: Kinetic energy (left) and $f(\mathbf{v}, t)$ (right).

This gives the following solution for the kinetic energy as computed in (2.2.2):

$$K(t) = K(0)e^{-\beta(1-\beta)t} + \frac{|\rho \mathbf{V}|^2}{2}(1 - e^{-\beta(1-\beta)t}), \quad (5.4.7)$$

where $K(0)$ is the kinetic energy at time $t = 0$. As we have an explicit expression for the kinetic energy evolving in time, this analytical moment can be compared with its numerical approximation for accuracy and the corresponding graph is given in Figure 5.6. The general evolution of the distribution in an inelastic collision environment is also shown in Figure 5.6. In the conservation routine (constrained Lagrange multiplier method), energy is not used as a constraint and just density and momentum equations are used for constraints. Figure 5.6 shows the numerical accuracy of the method even though the energy (plotted quantity) is not being conserved as part of the constrained optimization method.

5.4.5 Inelastic Collisions with Diffusion Term

Here we simulate for (2.2.3) and (2.2.4), a model corresponding to inelastic interactions in a randomly excited heat bath with constant temperature η . Following the procedure in Section 5.4.4, the evolution equation for kinetic temperature as a function of time is given by

$$\frac{dT}{dt} = 2\eta - \zeta \frac{1-e^2}{24} \int_{\mathbf{v} \in \mathbb{R}^3} \int_{\mathbf{w} \in \mathbb{R}^3} \int_{\sigma \in S^2} (1-\mu) B(|\mathbf{u}|, \mu) |\mathbf{u}|^2 f(\mathbf{v}) f(\mathbf{w}) d\sigma d\mathbf{w} d\mathbf{v}, \quad (5.4.8)$$

which, in the case of inelastic Maxwell type interactions according to (2.2.2), becomes

$$\frac{dT}{dt} = 2\eta - \zeta \pi C_0 (1-e^2) T. \quad (5.4.9)$$

The above equation gives a closed form expression for the time evolution of the kinetic temperature and can be expressed as

$$T(t) = T_0 e^{-\zeta \pi C_0 (1-e^2)t} + T_\infty^{MM} [1 - e^{-\zeta \pi C_0 (1-e^2)t}], \quad (5.4.10)$$

where

$$T_0 = \frac{1}{3} \int_{\mathbf{v} \in \mathbb{R}^3} |\mathbf{v}|^2 f(\mathbf{v}, 0) d\mathbf{v} \quad \text{and} \quad T_\infty^{MM} = \frac{2\eta}{\zeta \pi C_0 (1-e^2)}.$$

From (5.4.10), it can be seen that in the absence of the diffusion term (i.e., $\eta = 0$) and for $e \neq 1$ (inelastic collisions), the kinetic temperature of the distribution function decays like an exponential, just like in the previous section. So, the presence of the diffusion term pushes the temperature to an equilibrium value of $T_\infty^{MM} > 0$, though the collisions are locally inelastic. Also note that if the interactions were elastic and the diffusion coefficient positive then, $T_\infty^{MM} = +\infty$, so there would be no equilibrium states with finite kinetic temperature. These properties were shown in [47] and similar time asymptotic behavior is expected in the case of hard-sphere interactions where $T_\infty^{HS} > 0$ is shown to exist. However, the time evolution of the

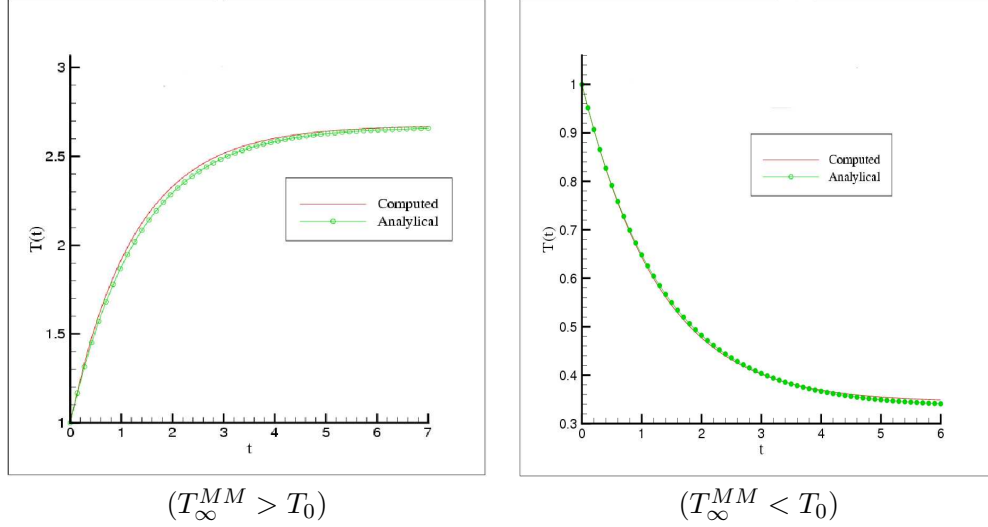


Figure 5.7: Maxwell type inelastic collisions, diffusion term for $N = 16$.

kinetic temperature is a non-local integral (5.4.8) does not satisfy a closed ODE form (5.4.9). The proposed numerical method for the calculation of the collision integral is tested for these two cases. We compare with the analytical expression (5.4.10) for different initial data and show the corresponding computed kinetic temperatures for Maxwell type interactions in Figure 5.7. The asymptotic behavior is observed in the case of hard-sphere interactions in Figure 5.8. The conservation properties for this case of inelastic collisions with a diffusion term are set exactly like in the previous Section 5.4.4 (no energy constraint).

5.4.6 Maxwell Type Elastic Collisions: Slow Down Process Problem

Next, consider (2.2.12) with $\beta = 1$, $J_{\beta} = 1$ and $B(|\mathbf{u}|, \mu) = \frac{1}{4\pi}$, i.e., isotropic collisions. The second term is the linear collision integral which conserves only density and the first term is the classical collision integral from (2.2.12) conserving density,

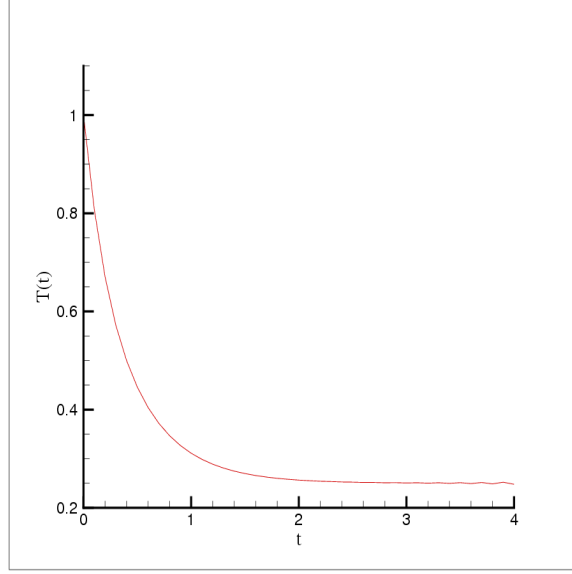


Figure 5.8: Hard sphere, inelastic collisions, diffusion term, $T_\infty^{HS} < T_0$ for $N = 16$.

momentum and energy. $M(\mathbf{v})$ in (2.2.12) refers to the Maxwellian defined by

$$M_{\mathcal{T}}(\mathbf{v}) = e^{\frac{-|\mathbf{v}|^2}{(2\mathcal{T})}} \frac{1}{(2\pi\mathcal{T})^{3/2}},$$

with \mathcal{T} the constant thermostat temperature. In particular, any initial distribution function converges to the background distribution $M_{\mathcal{T}}$. Such behavior is well captured by the numerical method. Indeed, Figure 5.9 corresponds to an initial state of a convex combination of two Maxwellians. In addition, from (4.1.18),

$$f_{\mathcal{T}}^{ss}(\mathbf{v}, t) = \frac{\sqrt{2}}{\pi^{5/2}} \int_0^\infty \frac{1}{(1+s^2)^2} \frac{e^{-|\mathbf{v}|^2/2\bar{T}}}{\bar{T}^{3/2}} ds \quad \text{where} \quad \bar{T} = \mathcal{T} + as^2 e^{\frac{-2t}{3}},$$

which is the finite energy solution for $p = 1, a = 1, \mu = \frac{2}{3}$, and $\theta = \frac{4}{3}$ in (4.2.2), i.e., $p = 1$ in (4.3.3) and (4.3.4). As $t \rightarrow \infty$, the time rescaled numerical distribution is compared with the analytical solution $f_{\mathcal{T}}^{ss}$ for a positive background temperature \mathcal{T} and it converges to a Maxwellian $M_{\mathcal{T}}$. From Figure 5.9, it can be seen that the numerical method is quite accurate and the computed distribution is in very good agreement with the analytical self-similar distribution $f_{\mathcal{T}}^{ss}$ from (4.1.18).

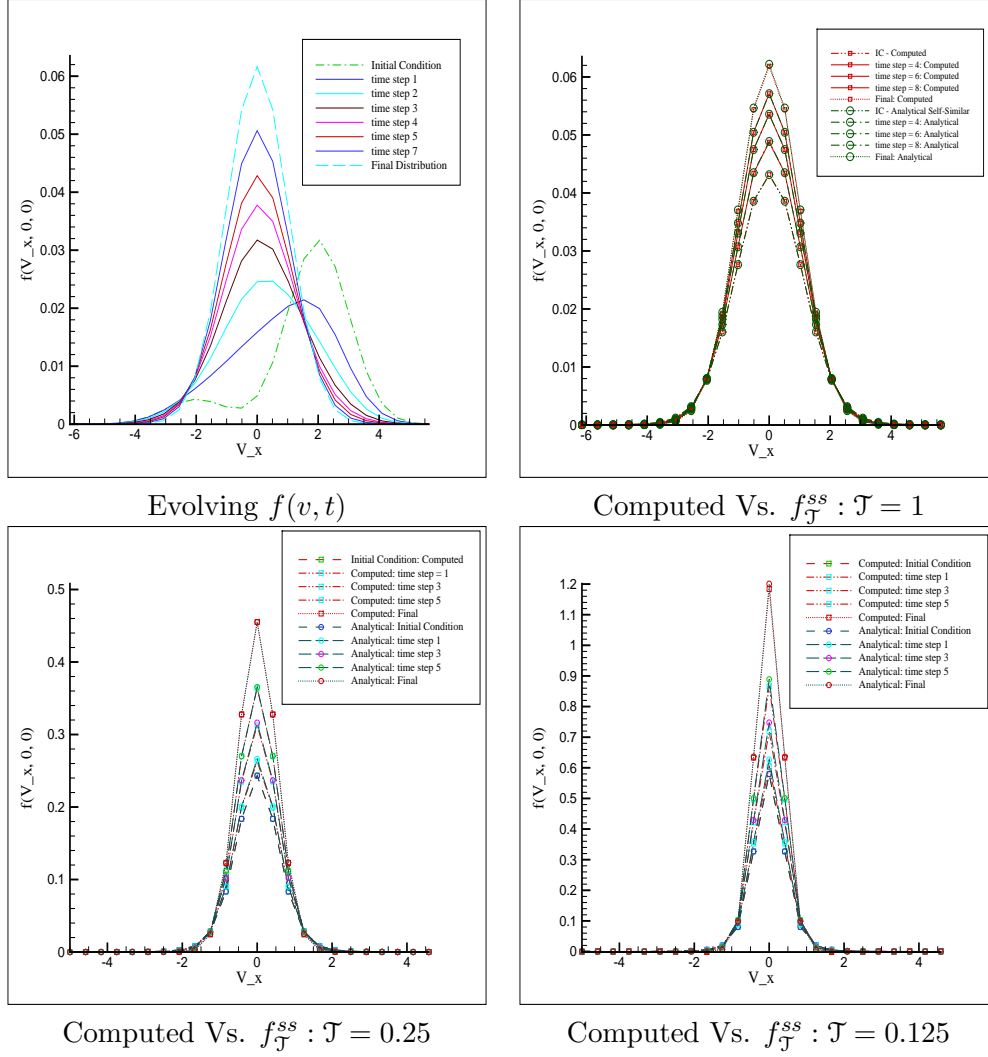


Figure 5.9: Maxwell type collisions, slow down process with $\Theta = 4/3, \mu = 2/3, N = 24$.

Similar agreement is observed for different constant values of \mathcal{T} approaching 0 (Figure 5.9). The interesting asymptotics (4.2.4) corresponding to power-like tails and infinitely many particles at zero energies occur only when $\mathcal{T} = 0$ as shown in (4.2.4) and (4.2.4). Since letting $\mathcal{T} = 0$ in the scheme created an instability, we proposed the following new methodology to counter this effect. We let, instead, $\mathcal{T} = \gamma e^{-\alpha t}$ ensuring that the thermostat temperature vanishes for large time, and set

$$\bar{T} = \gamma e^{-\alpha t} + a s^2 e^{\frac{-2t}{3}}, \quad (5.4.11)$$

where the role of α is very important and a proper choice needs to be made. A choice of $\alpha < 2/3$ would result in \mathcal{T} converging to 0 more slowly than required to guarantee power tail behavior; while $\alpha > 2/3$ results in $\mathcal{T} \rightarrow 0$ faster than non-equilibrium distribution temperature. Such a rapid decay is not required, but is only an essential condition, and would require better spectral accuracy, i.e., larger N . The condition $\alpha = 2/3$ is the necessary condition. In our simulations, we take $\gamma = 0.25$ and the values of α need to be chosen exactly as $\alpha = \mu(1) = 2/3$, the energy dissipation rate as described in Section 4.2 to recover the asymptotics as in (4.2.4).

Remark: *Due to the exponential time rescaling of Fourier modes, our procedure to compute self-similar solutions in free space may also be viewed as a non-uniform grid of Fourier modes that are distributed according to the continuum spectrum of the associated problem. This choice plays the equivalent role to the corresponding spectral approximation of the free space problem of the heat kernel, that is, the Green's function for the heat equation, which happens to be a similarity solution as well, due to the linearity of the problem in this case. In particular, we expect optimal algorithm complexity using such non-equispaced Fast Fourier Transform, as obtained by Greengard and Lin [55] for spectral approximation of the free space*

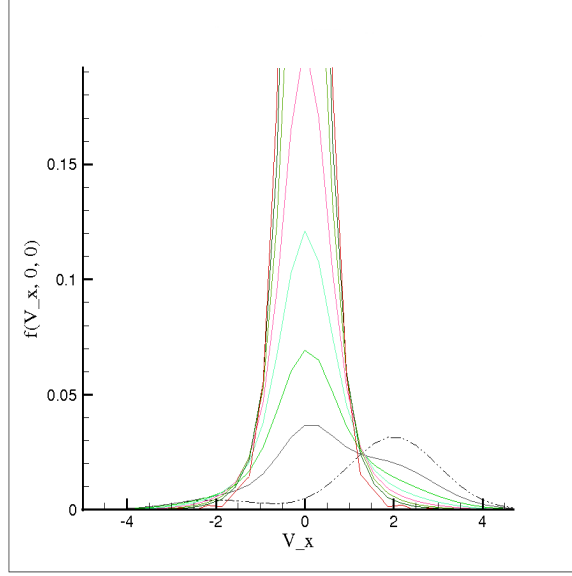


Figure 5.10: Slow down process: $N = 32$, $\mathcal{T} = \frac{1}{4}e^{-2t/3}$.

heat kernel. This problem will be addressed in a forthcoming paper. The following plots, Figures 5.10, 5.11, elucidate the fact that power-like tails are achieved asymptotically with a decaying \mathcal{T} .

For a decaying background temperature as in (5.4.11), Figure 5.10 shows evolution of a convex combination of Maxwellians to a self-similar (blow up for zero energies and power-like heavy tails for high energies) behavior. Figure 5.11 plots the computed distribution along with a Maxwellian with temperature of the computed solution. This illustrates that the computed self-similar solution deviates strongly from a Maxwellian equilibrium.

In order to better capture the power-law effect using this numerical method, we set $\mathcal{T} = \zeta e^{-2t/3} = \zeta e^{-\mu t}$, see (5.4.11), where μ is related the spectral properties of the Fourier transformed equation as described previously in Chapter 4 on the slow down process problem with $\mu = \mu(1)$, the energy dissipation rate. Thus, as it was

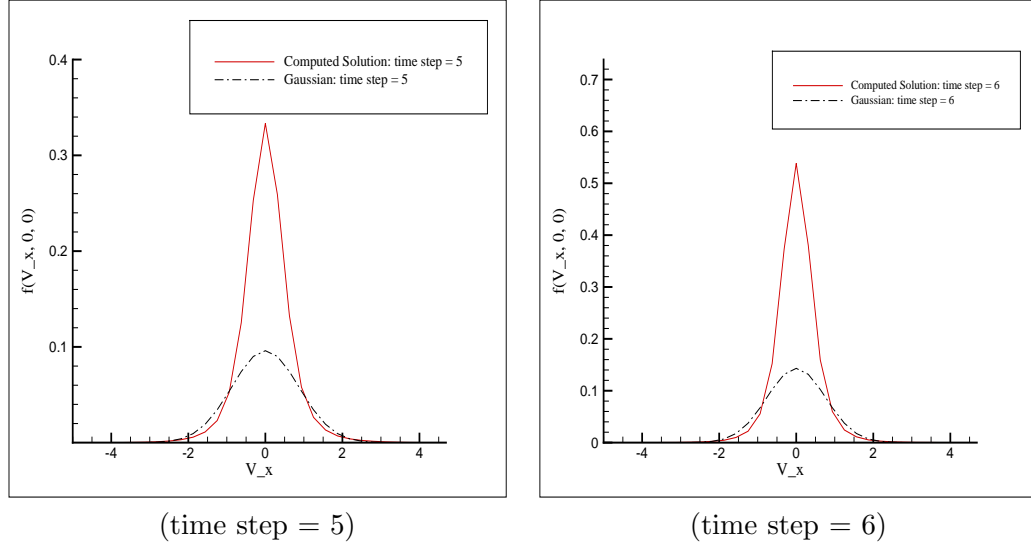


Figure 5.11: Computed distribution Vs. Maxwellian with temperature of the computed distribution.

computed in [17] and revised in Chapter 4, we know that for initial states with finite energy, $p = 1$ and the corresponding energy dissipation rate is $\mu(1) = \mu = 2/3$ is positive. In particular $p_* = 1.5$ is the conjugate of $p = 1$ of the spectral curve m_q in Theorem 4.1 Part (i). In addition, the rescaled probability will converge to the moments of the self-similar state (4.3.3), (4.3.4), that is,

$$e^{-qt^{2/3}} \int_{\mathbf{v} \in \mathbb{R}^3} f(\mathbf{v}) |\mathbf{v}|^{2q} d\mathbf{v} \rightarrow m_q,$$

and we know any moment m_q is unbounded for $q > p_* = 1.5$. We show in figure 5.12, the evolution of $e^{-qt^{2/3}} \int_{\mathbf{v} \in \mathbb{R}^3} f(\mathbf{v}) |\mathbf{v}|^{2q} d\mathbf{v}$ for $q = 1, 1.3, 1.45, 1.5, 1.55, 1.7$, and 2.0, computed for $N = 10, 14, 22$, and 26. It can be seen that as time progresses (and as the thermostat temperature \mathcal{T} decreases to 0), the approximated numerically computed moments $m_q, q \geq 1.5$ start to blow up as predicted. The value $q = 1.5$ is the threshold value, as any moment $m_{q>1.5}(t) \rightarrow \infty$. The expected spectral accuracy, as the value of N increases, improves the growth zone of such moments for larger final

times. The reason for such an effect is because the velocity domain is truncated and we use only a finite number of Fourier modes. This makes the computed distribution function take small negative values for large velocities, contributing to numerical errors that may cause m_q to peak and then relax back. In particular, larger order moments of the computed self-similar asymptotics with the negative oscillating parts on large energy tails, result in the large negative moment values for the above mentioned values of N creating large negative errors. However it is noticed that the negative oscillation values of $f(t, \mathbf{v})$ coincide with large velocity values used in getting its q -moments approximating m_q , for $q > 1.5$, and that such error is reduced in time for larger number of Fourier modes. Typically, it is easier to see the power-law tails in the distribution function when plotted in a semilog scale. But, in the current simulations because of the negative distribution values for large velocities, we show the power-law effect using higher order moments of the distribution function.

Finally, we point out that the FFTW [44] package is used to compute the fast fourier transform (FFT). We have noticed in our numerics that for the specific choice of values $N \neq 6, 10, 14, 18, 22, 26, \dots, 6 + 4k$ for $k = 0, 1, 2, 3, \dots$, the approximating moments to $m_q(t)$ start to take negative values very quickly, as seen in Figure 5.13 for $N = 16$ and 20 , making the numerical solution inadmissible, since analytically $m_q(t) > 0, \forall t$. To see this trend of moments becoming negative for the above mentioned values of N , we show the moments only for a smaller duration of time. For larger time, the moments take large negative values.

5.5 The Space Inhomogeneous Boltzmann Equation

In this section, several physical examples of $1D$ in \mathbf{x} are modelled using (2.1.1). When solving the inhomogeneous Boltzmann equation, the choice of reference quantities plays an important role. These reference quantities are dictated by the under-

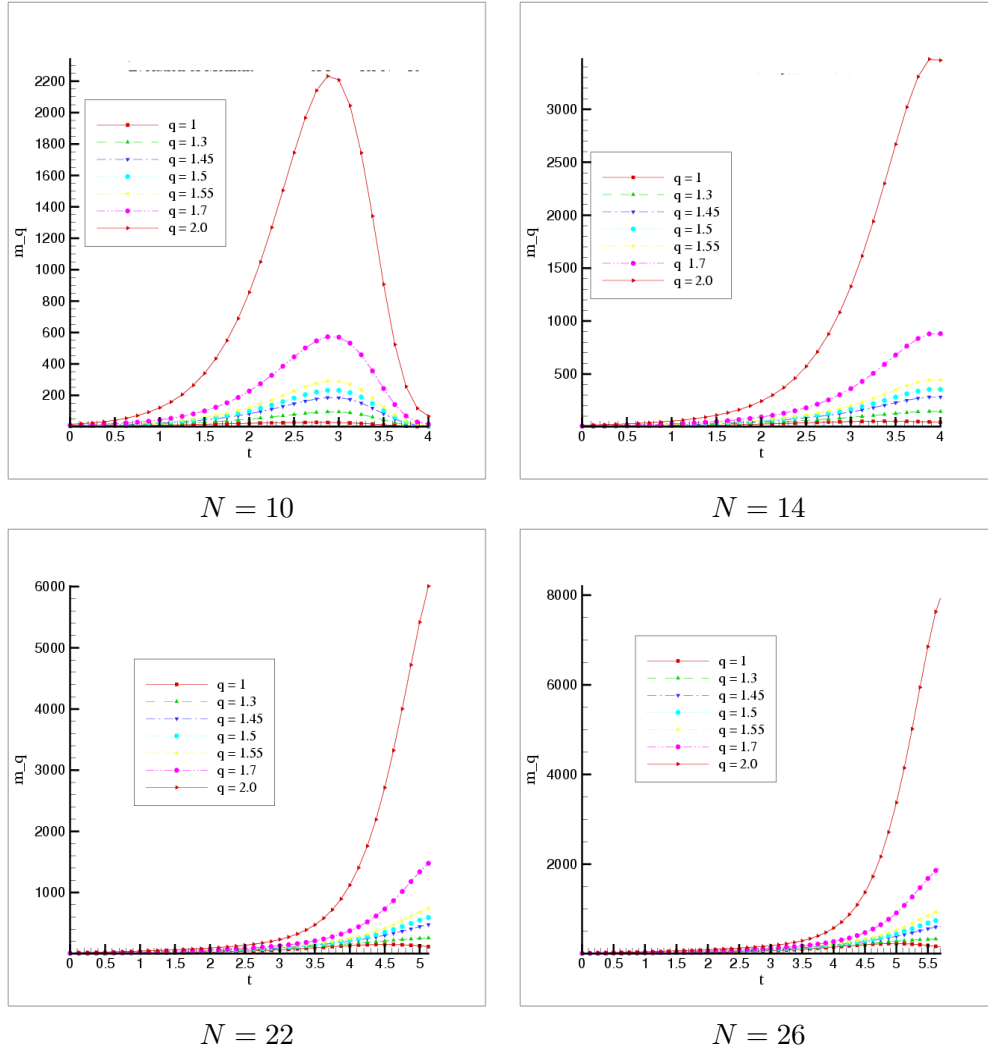


Figure 5.12: $m_q(t)$ for $\mathcal{T} = \frac{1}{4}e^{-2t/3}$.

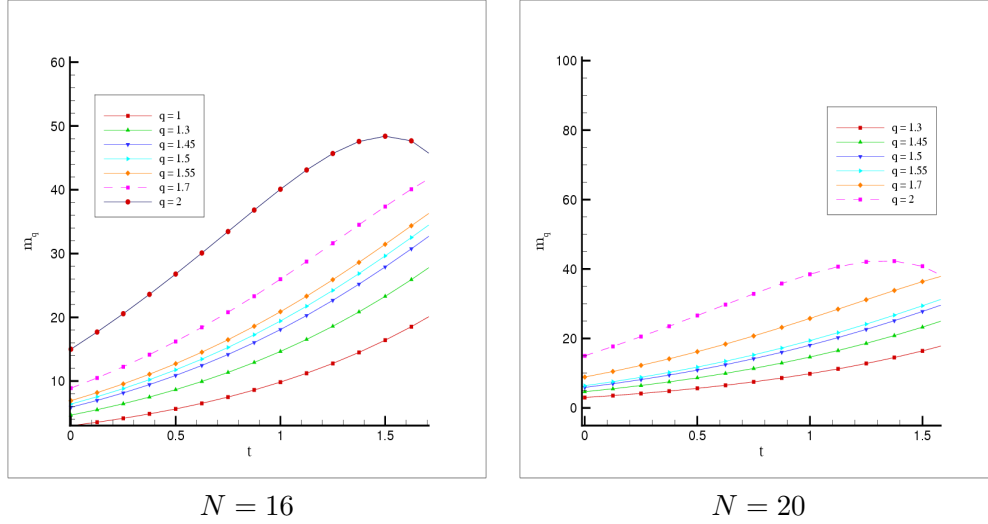


Figure 5.13: $m_q(t)$ for $\mathcal{T} = \frac{1}{4}e^{-2t/3}$.

lying physics and scales of the problem. In the sequel, depending on the problem being modelled, the reference quantities will be specified and (2.4.2) will be used with the scaled variables in (2.4.1).

The splitting approach as mentioned in Section 5.3 is used to numerically compute the inhomogeneous Boltzmann equation. A scheme that is first order in time and space is used for the advection part and also the homogeneous part of the split problem. When a higher order splitting scheme is used then, higher order approximations are employed for the time and space derivatives.

In shock structure problems, it is convenient to look at the conservation equations (2.3.5) in a divergence form. A typical scenario of a $1-D$ flow in an infinite expanse of a gas is when we have a monatomic gas at two uniform states at infinities. The states at infinities being uniform are described by Maxwellian distribution functions with parameters $\rho_l, T_l, \mathbf{V}_l = (V_l, 0, 0)$ for $x_1 \rightarrow -\infty$, and ρ_r, T_r , and $\mathbf{V}_r = (V_r, 0, 0)$

for $x_1 \rightarrow \infty$. The two states at infinities cannot be chosen arbitrarily, but their macroscopic quantities have to satisfy the *Rankine-Hugoniot* relations. For a steady state, the *Rankine-Hugoniot* relations can be derived from (2.3.5):

$$\begin{aligned}\rho_l V_l &= \rho_r V_r, \\ \rho_l V_l^2 + \rho_l T_l &= \rho_r V_r^2 + \rho_r T_r, \\ \rho_l V_l(T_l + 5V_l^2) &= \rho_r V_r(T_r + 5V_r^2).\end{aligned}\tag{5.5.1}$$

Our interest is in understanding the solution that connects these two states at infinities, i.e., *shock wave analysis*.

5.5.1 The Riemann Problem

The Riemann problem is a fundamental tool for studying the interaction between waves. It has played a central role both in the theoretical analysis of systems of hyperbolic conservation laws and in the development and implementation of practical numerical solutions of such systems. The Riemann problem describes the micro structure of the shock wave.

This test deals with the numerical solution of the inhomogeneous $1D \times 3D$ Boltzmann equation for hard sphere molecules ($\lambda = 1$). In this section, we present some results for the one dimensional Riemann problem. Numerical solutions are obtained for a Knudsen number closed the fluid limit ($Kn \leq 0.01$). The macroscopic initial conditions satisfying the Rankine-Hugoniot relations (5.5.1) are given by

$$\begin{aligned}(\rho_l, V_l, T_l) &= (1, 0, 1) \quad \text{if } 0 \leq x \leq 0.5, \\ (\rho_r, V_r, T_r) &= (0.125, 0, 0.25) \quad \text{if } 0.5 < x \leq 1.0.\end{aligned}\tag{5.5.2}$$

Let t_0 the mean free time, and T_l , ρ_l , and $V_{th} = \sqrt{2RT_l}$ be the reference quantities. Recall that L is the domain size parameter of \mathbf{v} i.e. $\mathbf{v} \in \Omega_v = [-L, L]^3$. Then the

CFL condition gives $\frac{dt}{t_0} \leq \frac{dx}{L}$ mean free times.

The flow becomes stationary by a smaller final time of 0.2 mean free times. In this case, a choice of $dx = 0.5l_0$ is made. For smaller values of $Kn \leq 0.01$, i.e., close to continuum flow, the numerical method is noticeably slow. In order to maintain good accuracy and to reduce the effect of the splitting error for close to stiff problems, a smaller value of dt is taken than required by the CFL condition. This results in a slow march in time, and thus it typically takes longer to reach the stationary state. The density, flow velocity and temperature profiles are shown in Figure 5.5.1. It can be seen that for $Kn = 0.01$, the profiles approach the shapes typical of continuum flows.

5.5.2 Shock Due to a Sudden Change in Wall Temperature

As an example showing the formation of a shock wave and its propagation, we consider a semi-infinite expanse ($x_1 > 0$) of a gas bounded by a plane wall at rest with temperature T_0 at $x_1 = 0$. Initially, the gas is at equilibrium with the wall at pressure p_0 and temperature T_0 . At time $t = 0$, the temperature of the wall is suddenly changed to another value T_1 and is kept at T_1 for subsequent time. The time evolution of the behavior of the gas is studied numerically on the basis of the fully nonlinear Boltzmann equation and the diffuse-reflection condition (full accommodation) on the wall.

As the reference length X_r , we take l_0 the mean free path of the gas in the equilibrium state at rest with density $\rho_0 = p_0/RT_0$ and temperature T_0 . We take $l_0/\sqrt{2RT_0}$ as the reference time t_r and use Equation (2.4.2). Typically, when considering a flow that is uniform in a particular velocity direction, the Boltzmann equation can be reduced to a system of equations by integrating the distribution function in respective

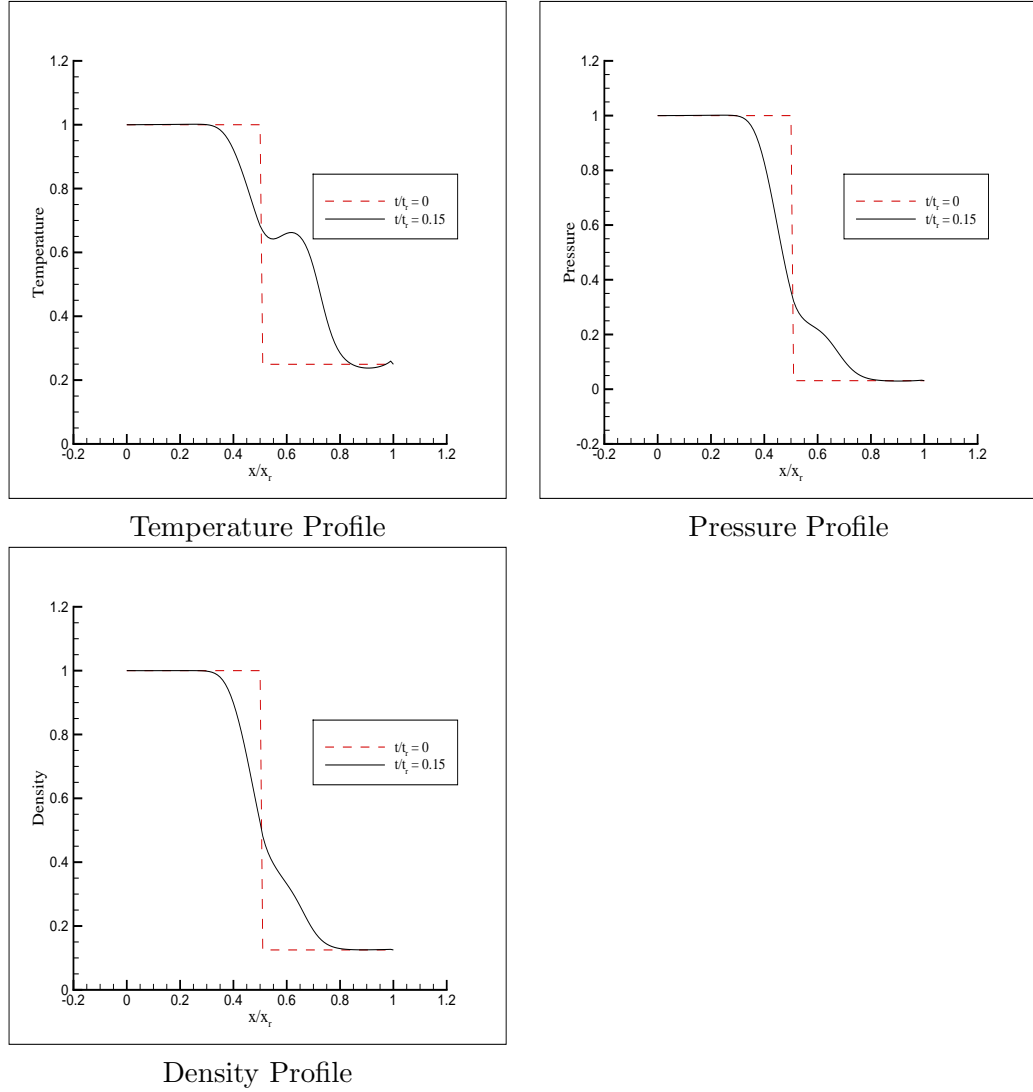
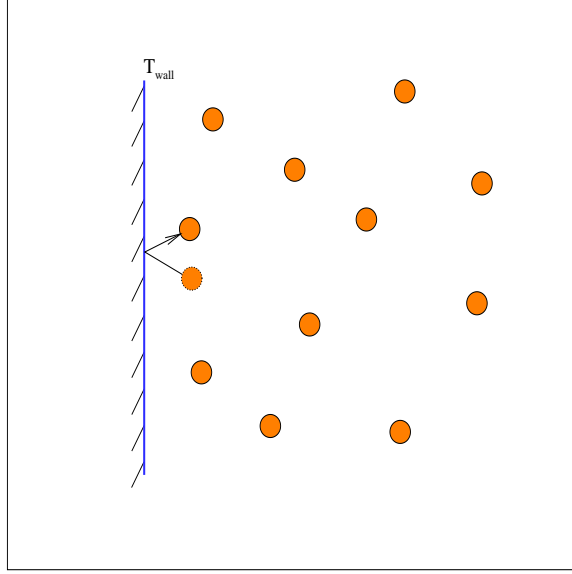


Figure 5.14: Riemann problem: Stationary profiles for $Kn = 0.01$ at $t = 0.15$.



velocity direction(s) to get a set of marginal distributions. The proposed algorithm in this dissertation relies on the weak form for its derivation. But, such a weak form is not available for the marginal distribution. Moreover, it is a difficult task to eliminate a velocity component in the nonlinear collision integral. It is for these reasons that the conservative spectral method cannot be reduced in velocity components and the full $3 - D$ computation in \mathbf{v} has to be performed. For the purpose of analysis, the marginal distribution function ($g(x_1, v_1, t) = \int_{v_2, v_3} f(x_1, \mathbf{v}, t) dv_2 dv_3$) is calculated from the three dimensional velocity distribution.

The marginal velocity distribution function g has a discontinuity at the corner $(x_1, t) = (0, 0)$ of the domain $(x_1 > 0, t > 0)$ for $v_1 > 0$. This discontinuity in g propagates in the direction of characteristic $x_1 - v_1 t = 0$, and subsequently decays owing to the collision integral on the right hand side. The direction of propagation depends on v_1 . For $v_1 < 0$, the characteristic starts from infinity where g is continuous and thus for all x_1, t remains continuous. For numerical calculations, typically

a modified scheme is devised to account for this. But, it has been observed that for the fully nonlinear Boltzmann equation, the standard finite-difference scheme with time splitting does an extremely good job of capturing this discontinuity.

There are two cases of interest in the numerical experiment, $T_1 = 0.5T_0$ and $T_1 = 2T_0$. For the first case where $T_1 = 0.5T_0$, in the numerical computation of the time-evolution problem the temperature, pressure and density profiles have been shown in Figure 5.5.2. By sudden cooling of the wall temperature, the gas near the wall is suddenly cooled resulting in a pressure decrease there and an expansion wave propagates into the gas. The expansion wave accelerates gas towards the wall initially. As time goes on, with the decrease of temperature of gas near the wall, the suction of heat from the gas by the wall decreases and pressure becomes weaker. Thus, the gas begins to accumulate near the wall, because there is no suction on the wall. The pressure drop by cooling of the gas is not enough to compensate the gas flow. As the gas equilibrates with the wall, in the absence of condensation (no sink of mass), a compression wave develops that propagates outward and attenuates the initial expansion wave. Then, a compression wave chases the expansion wave to attenuate. This phenomenon occurs in long time. The main temperature drop of the gas occurs gradually, well after the expansion wave is passed.

Next, we consider the case where $T_1 = 2T_0$. With the sudden rise of wall temperature, the gas close to the wall is heated and accordingly the pressure rises sharply near the wall, which pushes the gas away from the wall and a shock wave (or compression wave) propagates into the gas. As time goes on, the gas moves away from the wall but there is no gas supply from the wall and the heat transferred from the wall to the gas decreases owing to the rise of gas temperature near the wall. Accordingly, the pressure decrease due to escape of the gas is not compensated by the heating and

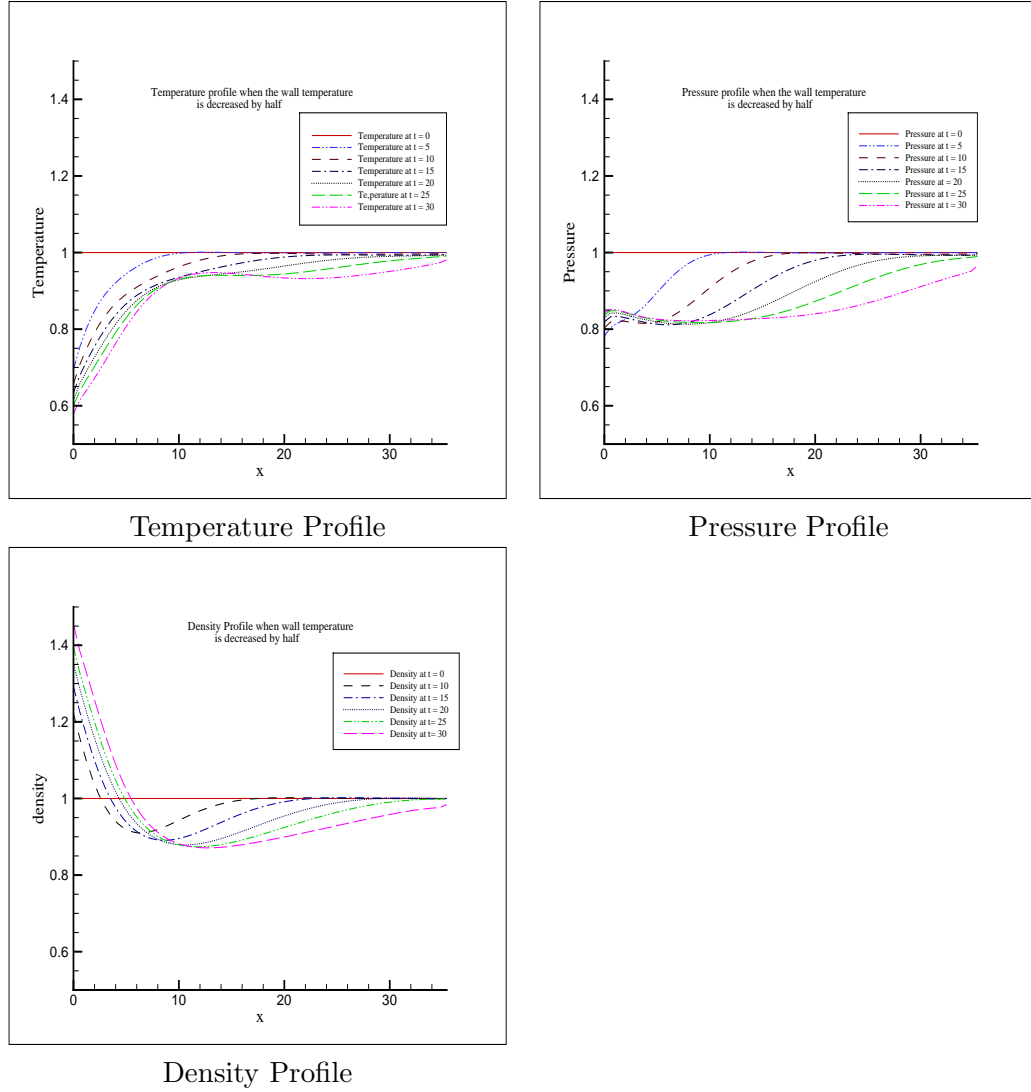


Figure 5.15: Formation of an expansion wave by an initial sudden change of wall temperature from T_0 to $T_0/2$.

the pressure gradually decreases. As a result, an expansion wave propagates toward the shock wave from behind and attenuates the shock wave together with another dissipation effect. The main temperature rise of the gas occurs gradually well after the shock wave passed. This process is due to the conduction of heat. In the numerical computation of the time-evolution problem, the temperature, pressure and density profiles have been shown in Figure 5.5.2 for the region of a few mean free paths close to the wall. In Figure 5.5.2, the marginal velocity distribution function g is plotted for various times t/t_r . We let $Kn = 1$, $dx = 0.01l_0$, $dt = 0.75dx/L$, and $N = 16$. We see that g has a discontinuity at (x_1, t) . As time goes on, the position of discontinuity shifts to $x_1 = v_1 t/t_r$, and the size of this discontinuity decreases due to molecular collisions (collision integral). All of the above numerical results agree extremely well with the ones obtained by Aoki, Sone, Nishino and Sugimoto [85]. In both cases of wall temperature change, the second wave (compression wave for $T_{wall} = 0.5T_0$ and expansion wave for $T_{wall} = 2T_0$) attenuates the first wave (expansion wave for $T_{wall} = 0.5T_0$ and compression wave for $T_{wall} = 2T_0$) only because the wall temperature is suddenly changed. If the wall temperature is changed gradually in proportion to the collision parameters i.e., the mean free path and mean free time then, we speculate that only the first wave would be propagating into the gas and there would be no ensuing second wave.

5.5.3 Heat transfer Between Two Parallel Plates

We consider the case of a rarefied gas between two parallel plane walls at rest: one with temperature T_0 at $x_1 = 0$ and the other with a temperature $T_1 = 2T_0$ at $x_1 = 1$. Note that, in this case the distance between the two plates is taken as the reference length. The gas molecules make diffuse reflection on the walls. The state of the gas or the velocity distribution function can be considered to be uniform with respect to x_2 and x_3 . Note that when considering a highly rarefied gas ($Kn \rightarrow \infty$),

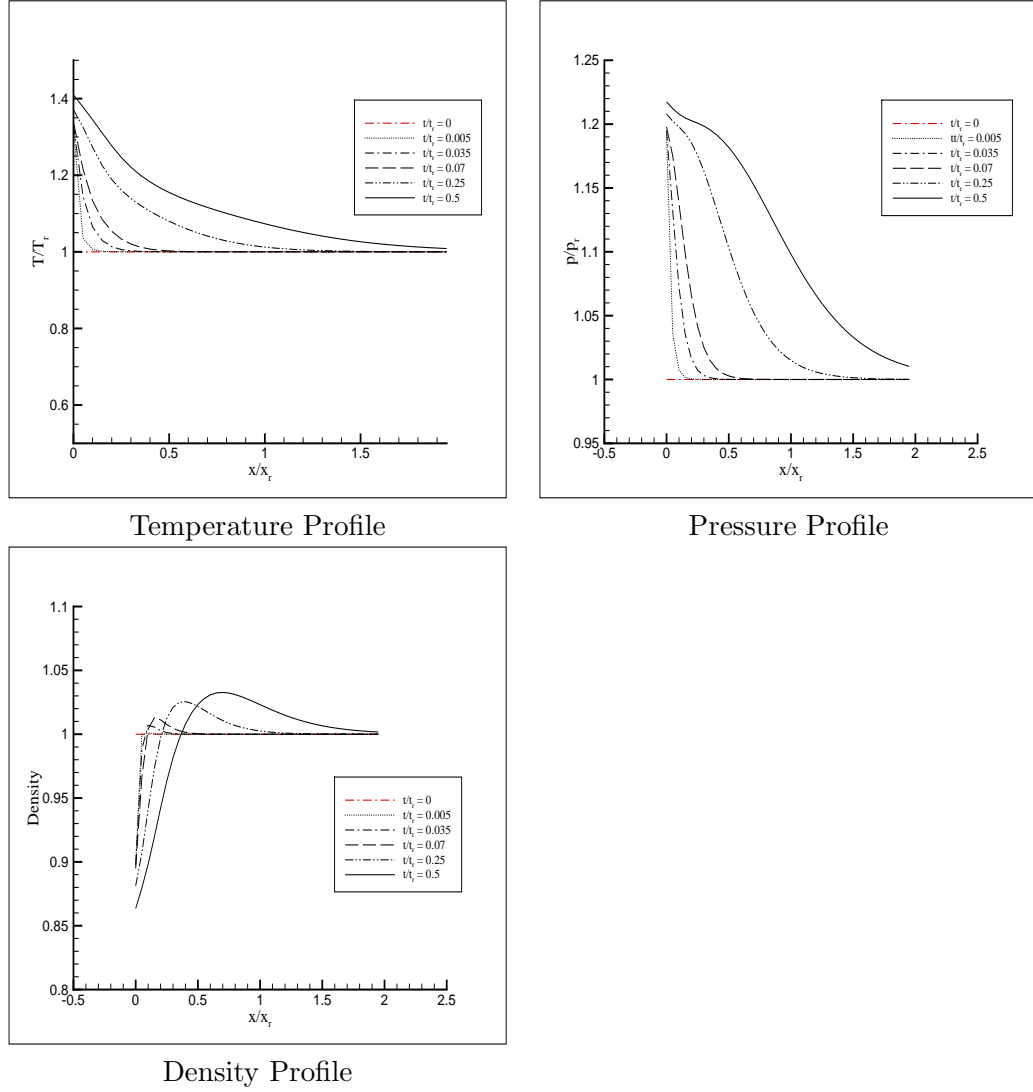


Figure 5.16: Formation of a shock wave by an initial sudden change of wall temperature from T_0 to $2T_0$.

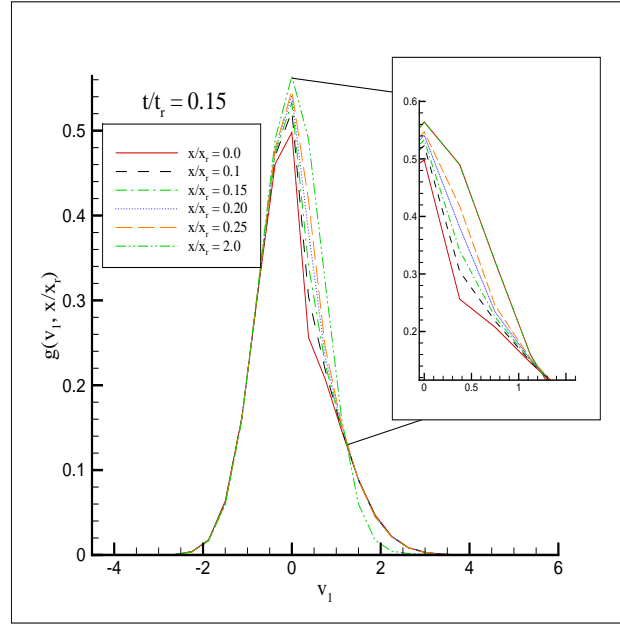
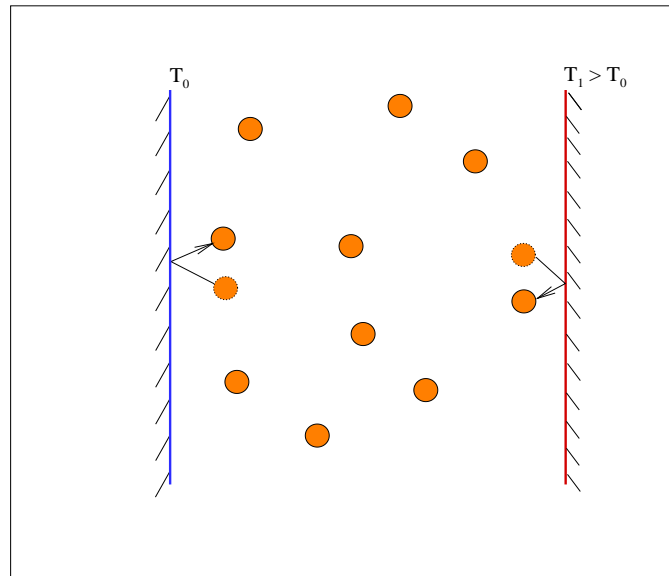


Figure 5.17: Marginal Distribution at $t = 0.5t_r$ for $N = 16$.



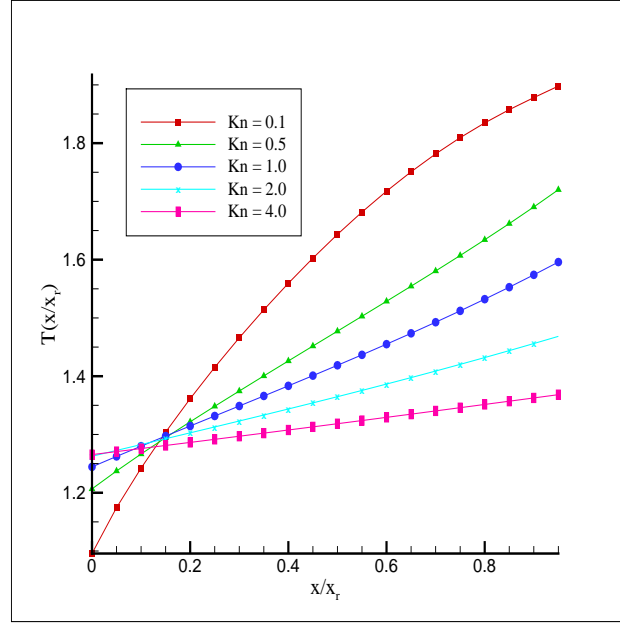


Figure 5.18: Stationary Temperature Profile for increasing Knudsen number values.

such a flow becomes uniform even in the x_1 direction i.e. the state of the gas is independent of x_1 . We consider here the stationary flows for range of Kn between 0.1 to 4. The stationary temperature profiles for $Kn = 0.1, 0.5, 1, 2, 4$ have been plotted in figure 5.5.3. With larger values of Kn , we find that the temperature profiles get flatter and flatter. An increase in the Knudsen number value implies that the gas is becoming more and more rarefied and that the only interactions the gas molecules have are with the walls where they exchange their temperatures. The corresponding stationary density profiles have been plotted in figure 5.5.3.

5.5.4 Classic Shock in an Infinite Tube: Supersonic \rightarrow Subsonic Flow

Consider a time-independent unidirectional flow in x_1 direction in an infinite expanse of a gas, where the states at infinity are both uniform and their velocity distributions are Maxwellians with corresponding parameters as explained in the preamble for this

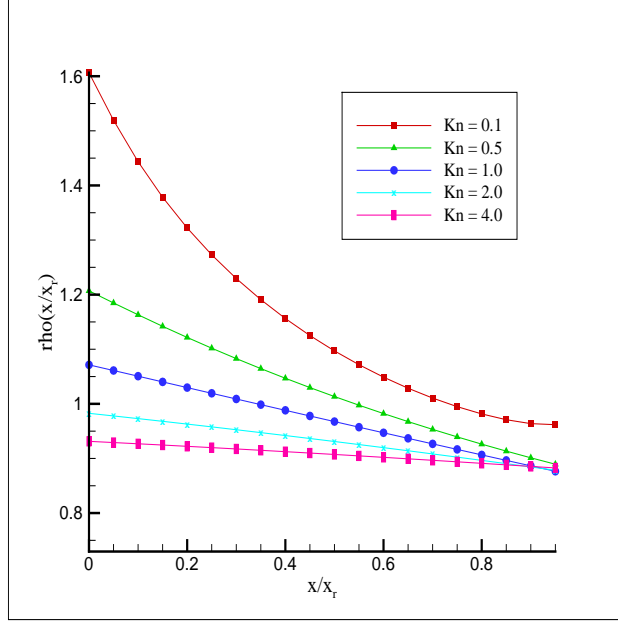


Figure 5.19: Stationary Density Profile for increasing Knudsen number values.

section. That is,

$$f \rightarrow \frac{\rho_l}{\sqrt{2\pi RT_l}} \exp\left(-\frac{|\mathbf{v} - \delta_1 \mathbf{V}_l|^2}{2RT_l}\right), \quad \text{as } x_1 \rightarrow -\infty,$$

$$f \rightarrow \frac{\rho_r}{\sqrt{2\pi RT_r}} \exp\left(-\frac{|\mathbf{v} - \delta_1 \mathbf{V}_r|^2}{2RT_r}\right), \quad \text{as } x_1 \rightarrow \infty.$$

The Maxwellian parameters satisfy the *Rankine-Hugoniot* relations. We take ρ_l, T_l , and l_0 as the reference density, temperature and lengths respectively. The shock profile is best considered in the frame of reference moving with the shock in steady state. The relevant parameter for the shock is the inflow Mach number M , defined as the ratio of the inflow velocity relative to the shock and the speed of sound,

$$M = \frac{V_l}{c} = \frac{V_l}{\sqrt{\gamma T_l}} = \frac{V_l}{\sqrt{\gamma}},$$

where c is the speed of sound and $\gamma = \frac{5}{3}$ for monatomic gases. For simple notation, the “hats” in the nondimensional notation are dropped.

For the purpose of numerical computations, the inflow temperature T_l is chosen as the free parameter and $\rho_l = 0.5$. Then the rest of the parameters take the following values in terms of T_l :

$$\begin{aligned} V_l &= \sqrt{\frac{5T_l}{3}}M, \\ \rho_r &= \frac{4M^2}{M^2 + 3}\rho_l, \\ T_r &= \frac{(M^3 + 3)(5M^2 - 1)}{16M^2}T_l, \\ V_r &= \frac{M^2 + 3}{4M}\sqrt{\frac{5T_l}{3}}. \end{aligned}$$

These are derived from the *Rankine-Hugoniot* relations, which give the boundary conditions under which the steady shock wave can be observed.

When discussing shock structure, one often looks at the entropy production in the shock. Such an analysis shows that the entropy must grow across the shock. This requirement combined with *Rankine-Hugoniot* relations (5.5.1) produces a requirement on the inflow Mach number:

$$\left(\frac{5M^2 - 1}{4}\right)^3 \left(\frac{M^2 + 3}{4M^2}\right)^5 \geq 1 \Rightarrow M \geq 1.$$

Thus, a shock can only be observed for Mach numbers $M \geq 1$, i.e., when the inflow velocity is supersonic. The Mach number behind the shock has to satisfy

$$M_r = \frac{V_r}{c} = \frac{V_r}{\sqrt{5T_r/3}} = \sqrt{\frac{M^2 + 3}{5M^2 - 1}} \leq 1.$$

These conditions imply that the flow velocity changes from being supersonic to subsonic in a shock, while density and temperature grow. In Figure 5.5.4, we plot

the density, temperature and pressure profiles for $M = 1.5$, and $Kn = 1$ for Maxwell type interactions.

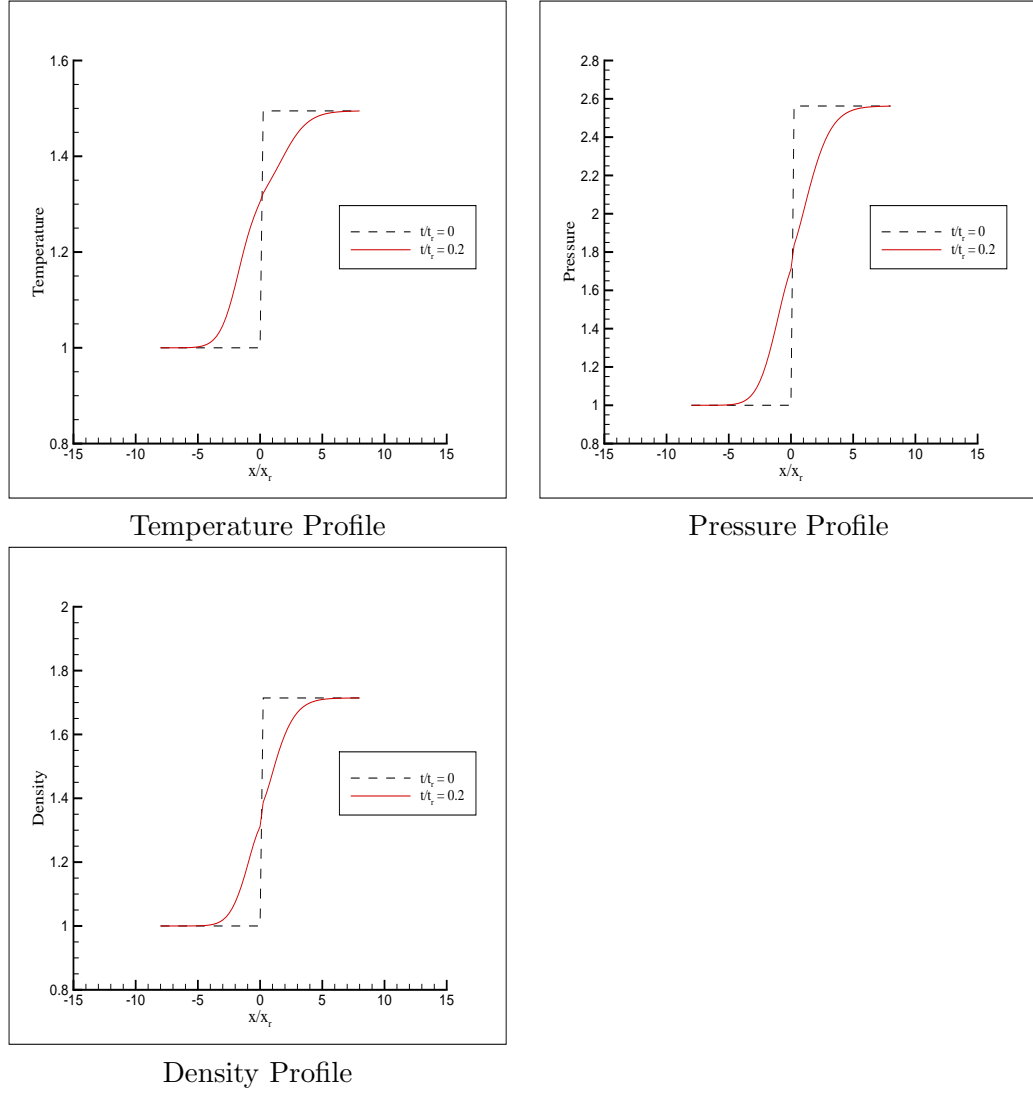


Figure 5.20: Stationary Shock: Mach number 1.5, and $Kn = 1$, Maxwell interactions.

Chapter 6

Conclusions and Future Work

In this dissertation, an accurate deterministic spectral method is presented which conserves all relevant moments of the Boltzmann collision integral. The proposed method works for both the conservative (locally elastic collisions) and non-conservative (linear Boltzmann, inelastic collisions) regimes. In the existing literature on spectral deterministic methods, the proposed method for the numerical approximation of the space inhomogeneous, time dependent Boltzmann equation is the first scheme that is conservative. Typical to any spectral method, the spectral accuracy is indeed controlled by the number of Fourier modes N , and a new Fourier approximation estimate is proven. The traditional proof for periodic functions has been extended for compactly supported functions. The conservation of moments is enforced by using the moment equations as constraints in an *isomoment* (continuous in time) or a *Lagrange optimization* (discrete in time) problem. The conservation correction that ensues is proven to be bounded by the spectral accuracy of the unconserved scheme. This guarantees overall spectral accuracy of the proposed isomoment spectral method. Such an estimate does not exist in the literature for spectral deterministic methods.

We studied the correction estimate of the Lagrange optimization problem for both elastic and inelastic collisions for the space homogeneous Boltzmann equation based on the method proposed in [52]. As expected, the correction estimate was directly proportional to the spectral accuracy of the unconserved method. Using a stan-

dard Fourier approximation error estimate as the starting point, we proved a new result in the $L_k^2(\Omega_v)$ norm for a finite domain $\Omega_v = [-L, L]^3$. We then extended the bounded estimate of the asymmetric collision integral in [48] to a finite domain for variable hard potentials for both elastic and inelastic collisions. Combining all of the above results, we proved the overall error estimate $\|Q(f, f) - Q_C^\Pi(f^\Pi, f^\Pi)\|_{L^2(\Omega_v)}$ in (3.3.33). As expected apriori, (3.3.33) reveals that, if the number of Fourier modes N is increased then, all the terms in (3.3.33) become small for $|\alpha|, |\gamma| \geq 1$.

This is the first method of its kind that requires no modification to compute both elastic and inelastic collisions. In comparison with the known analytical results (moment equations for elastic BTE, BKW self-similar solution, and attracting Bobylev-Cercignani-Gamba self-similar solutions for elastic collisions in a slow down process), the computed ones are found to be very close. The method employs a Fast Fourier Transform for faster evaluation of the collision integral. Even though the method is implemented for a uniform grid in velocity space, it can be implemented for a non-uniform velocity grid. The only challenge in this case is computing the Fast Fourier Transform on such a non-uniform grid. There are available packages for this purpose, but such a non-uniform FFT can also be implemented using certain high degree polynomial interpolation, and this possibility is currently being explored. The integration over the unit sphere is avoided completely and only a simple integration over a regular velocity grid is needed. Even though a trapezoidal rule is used as an integration rule, other integration rules like a Gaussian quadrature can be used to get better accuracy. For time discretization, a simple Euler scheme is used. The proposed method has a big advantage over other non-deterministic methods, as the exact distribution function can actually be computed instead of just the averages.

The numerical results for space inhomogeneous problems show the effectiveness of

the present method in solving a wide class of problems. Especially, *shock structure* analysis is performed for the classic stationary shock and Riemann problems. The supersonic to subsonic flow is shown for the stationary shock problem wherein the initial conditions and the states at infinities satisfy the *Rankine-Hugoniot* relations. Other shock structure properties are also analyzed. For the Riemann problem, it is observed that for smaller Knudsen numbers, the computed macroscopic profiles approach the ones expected for a fluid type flow. In addition, the effect of sudden change of wall temperature, that reflects gas diffusively as done in [85], is also analysed. The results in this case are found to be in complete agreement with the results obtained with a BGK method.

We are currently analyzing the importance of N , the velocity discretizations for space inhomogeneous Boltzmann calculations. In the case of a space inhomogeneous spherical Boltzmann shock analysis calculation [51], we see that we require $N_D > N_S$, where N_D is the number of Fourier modes near discontinuity in \mathbf{v} and N_S is the number of Fourier modes near a smooth region in \mathbf{v} . The reason is not only to make sure that we have a good spectral accuracy and convergence but also to eliminate the effect of Gibbs phenomenon [51]. Granular flows can be analysed deterministically using the present method, and such inelastic problems are currently being explored. In addition, Rayleigh-Benard convective flows and Taylor-Couette flows are also being numerically studied.

Bibliography

- [1] R. J. Alonso and I. M. Gamba. Propagation of l^1 and l^∞ Maxwellian weighted bounds for derivatives of solutions to the homogeneous elastic Boltzmann equation. *Submitted to publication*, 2007.
- [2] Ricardo Alonso and I.M. Gamba. $l^1 - l^{infy}$ maxwellian bounds for the derivatives of the solution of the homogeneous boltzmann equation. *Journal de Mathematiques Pures et Appliquees (to appear)*, 2008.
- [3] G. A. Bird. *Molecular Gas Dynamics*. Clarendon Press, Oxford, 1994.
- [4] A. V. Bobylev. Exact solutions of the Boltzmann equation. (*Russian*) *Dokl. Akad. Nauk SSSR*, 225:1296–1299, 1975.
- [5] A. V. Bobylev. Exact solutions of the nonlinear Boltzmann equation and the theory of relaxation of a Maxwellian gas. *Translated from Teoreticheskaya i Matematicheskaya Fizika*, 60:280 – 310, 1984.
- [6] A. V. Bobylev. The theory of the nonlinear spatially uniform Boltzmann equation for maxwell molecules. *Mathematical physics reviews; Soviet Sci. Rev. Sect. C Math. Phys. Rev.*, 7:111–233, 1988.
- [7] A. V. Bobylev. Moment inequalities for the Boltzmann equation and applications to spatially homogeneous problems. *J. Statist. Phys.*, 88(5-6):1183–1214, 1997.
- [8] A. V. Bobylev, J. A. Carrillo, and I. M. Gamba. On some properties of kinetic and hydrodynamic equations for inelastic interactions. *Journal of Statistical Physics*, 98:743–773, 2000.
- [9] A. V. Bobylev, J. A. Carrillo, and I. M. Gamba. On some properties of kinetic and hydrodynamic equations for inelastic interactions. *J. Statist. Phys.*, 98(3-4):743–773, 2000.
- [10] A. V. Bobylev and C. Cercignani. Discrete velocity models without nonphysical invariants. *Journal of Statistical Physics*, 97:677–686, 1999.

- [11] A. V. Bobylev and C. Cercignani. Exact eternal solutions of the Boltzmann equation. *Journal of Statistical Physics*, 106:1019–1038, 2002.
- [12] A. V. Bobylev and C. Cercignani. The inverse laplace transform of some analytic functions with an application to the eternal solutions of the Boltzmann equation. *Applied Mathematics Letters*, 15:807–813(7), 2002.
- [13] A. V. Bobylev and C. Cercignani. Moment equations for a granular material in a thermal bath. *Journal of Statistical Physics*, 106:547–567(21), 2002.
- [14] A. V. Bobylev and C. Cercignani. Self-similar asymptotics for the Boltzmann equation with inelastic and elastic interactions. *Journal of Statistical Physics*, 110:333–375, 2003.
- [15] A. V. Bobylev, C. Cercignani, and I. M. Gamba. On the self-similar asymptotics for generalized non-linear kinetic Maxwell models. *to appear in Communication in Mathematical Physics*, 2006.
- [16] A. V. Bobylev, C. Cercignani, and G. Toscani. Proof of an asymptotic property of self-similar solutions of the Boltzmann equation for granular materials. *Journal of Statistical Physics*, 111:403–417, 2003.
- [17] A. V. Bobylev and I. M. Gamba. Boltzmann equations for mixtures of maxwell gases: Exact solutions and power like tails. *Journal of Statistical Physics*, 124:497–516, 2006.
- [18] A. V. Bobylev, I. M. Gamba, and V. Panferov. Moment inequalities and high-energy tails for Boltzmann equations with inelastic interactions. *Journal of Statistical Physics*, 116:1651–1682, 2004.
- [19] A. V. Bobylev, I. M. Gamba, and V. A. Panferov. Moment inequalities and high-energy tails for Boltzmann equations with inelastic interactions. *J. Statist. Phys.*, 116(5-6):1651–1682, 2004.
- [20] A. V. Bobylev, M. Groppi, and G. Spiga. Approximate solutions to the problem of stationary shear flow of smooth granular materials. *Eur. J. Mech. B Fluids*, 21:91–103, 2002.

- [21] A. V. Bobylev and S. Rjasanow. Difference scheme for the Boltzmann equation based on the Fast Fourier Transform. *European journal of mechanics. B, Fluids*, 16:22:293–306, 1997.
- [22] A. V. Bobylev and S. Rjasanow. Fast deterministic method of solving the Boltzmann equation for hard spheres. *European journal of mechanics. B, Fluids*, 18:55:869–887, 1999.
- [23] A. V. Bobylev and S. Rjasanow. Fast deterministic method of solving the Boltzmann equation for hard spheres. *Eur. J. Mech. B Fluids*, 18(5):869–887, 1999.
- [24] A. V. Bobylev and S. Rjasanow. Numerical solution of the Boltzmann equation using a fully conservative difference scheme based on the fast Fourier transform. In *Proceedings of the Fifth International Workshop on Mathematical Aspects of Fluid and Plasma Dynamics (Maui, HI, 1998)*, volume 29, pages 289–310, 2000.
- [25] A. V. Bobylev and S. Rjasanow. Numerical solution of the Boltzmann equation using fully conservative difference scheme based on the Fast Fourier Transform. *Transport Theory Statist. Phys.*, 29:289–310, 2000.
- [26] A.V. Bobylev, C. Cercignani, and I. M. Gamba. Generalized maxwell models and self-similar asymptotics. *to appear in Comm. Mathematical Physics*.
- [27] J. E. Broadwell. Study of rarefied shear flow by the discrete velocity method. *J. Fluid Mech.*, 19:401–414, 1964.
- [28] H. Cabannes. Global solution of the initial value problem for the discrete Boltzmann equation. *Arch. Mech. (Arch. Mech. Stos.)*, 30:359–366, 1978.
- [29] Russel E. Caflisch. The half-space problem for the Boltzmann equation at zero temperature. *Comm. Pure Appl. Math.*, 38(5):529–547, 1985.
- [30] Russel E. Caflisch and Basil Nicolaenko. Shock profile solutions of the Boltzmann equation. *Comm. Math. Phys.*, 86(2):161–194, 1982.
- [31] C. Cercignani. Recent developments in the mechanics of granular materials. *Fisica matematica e ingegneria delle strutture, Bologna: Pitagora Editrice*, pages 119–132, 1995.

- [32] C. Cercignani. Shear flow of a granular material. *Journal of Statistical Physics*, 102:1407–1415, 2001.
- [33] C. Cercignani and H. Cornille. Shock waves for a discrete velocity gas mixture. *Journal of Statistical Physics*, 99:115–140, 2000.
- [34] Carlo Cercignani, Aldo Frezzotti, and Patrick Grosfils. The structure of an infinitely strong shock wave. *Phys. Fluids*, 11(9):2757–2764, 1999.
- [35] Carlo Cercignani, Reinhard Illner, and Mario Pulvirenti. *The mathematical theory of dilute gases*, volume 106 of *Applied Mathematical Sciences*. Springer-Verlag, New York, 1994.
- [36] Carlo Cercignani, Reinhard Illner, and Mario Pulvirenti. *The mathematical theory of dilute gases*, volume 106 of *Applied Mathematical Sciences*. Springer-Verlag, New York, 1994.
- [37] Roland Duduchava, Ralf Kirsch, and Sergej Rjasanow. On estimates of the Boltzmann collision operator with cut-off. *Journal of Mathematical Fluid Mechanics*, 8:242–266(25), April 2006.
- [38] M. H. Ernst and R. Brito. Driven inelastic Maxwell models with high energy tails. *Phys. Rev. E*, 65(4):040301, Mar 2002.
- [39] M. H. Ernst and R. Brito. Scaling solutions of inelastic Boltzmann equations with over-populated high energy tails. *Journal of Statistical Physics*, 109:407–432, 2002.
- [40] F. Filbet, C. Mouhot, and L. Pareschi. Solving the Boltzmann equation in $n \log n$. *SIAM J. Sci. Comput.*, 28:1029–1053, 2006.
- [41] F. Filbet and G. Russo. High order numerical methods for the space non homogeneous Boltzmann equation. *Journal of Computational Physics*, 186:457–480, 2003.
- [42] F. Filbet and G. Russo. High order numerical methods for the space non homogeneous Boltzmann equation. *Journal of Computational Physics*, 186:457–480, 2003.

- [43] N. Fournier and S. Mischler. A Boltzmann equation for elastic, inelastic and coalescing collisions. *Journal de mathématiques pures et appliquées*, 84:1173–1234, 2005.
- [44] Matteo Frigo and Steven G. Johnson. Fast Fourier Transform of the west.
- [45] E. Gabetta, L. Pareschi, and G. Toscani. Relaxation schemes for nonlinear kinetic equations. *SIAM J. Numer. Anal.*, 34:2168–2194, 1997.
- [46] I. M. Gamba, V. Panferov, and C. Villani. Upper Maxwellian bounds for the spatially homogeneous Boltzmann equation. *submitted for publication*.
- [47] I. M. Gamba, V. Panferov, and C. Villani. On the Boltzmann equation for diffusively excited granular media. *Communications in Mathematical Physics*, 246:503–541(39), 2004.
- [48] I. M. Gamba, V. Panferov, and C. Villani. On the Boltzmann equation for diffusively excited granular media. *Comm. Math. Phys.*, 246(3):503–541, 2004.
- [49] I. M. Gamba, S. Rjasanow, and W. Wagner. Direct simulation of the uniformly heated granular Boltzmann equation. *Mathematical and Computer Modelling*, 42:683–700, 2005.
- [50] I.M. Gamba, V. Panferov, and C. Villani. Upper maxwellians bounds for the spatially homogeneous boltzmann equation. *Arch.Rat.Mech.Anal. (to appear)*, 2008.
- [51] Irene M. Gamba and Sri Harsha Tharkabhushanam. Shock formation and propagation using a spectral lagrangian space inhomogenous boltzmann method. *In preparation*.
- [52] Irene M. Gamba and Sri Harsha Tharkabhushanam. Spectral - lagrangian methods for collisional models of non - equilibrium statistical states. *Accepted in Journal of Computational Physics*, 2007.
- [53] Harold Grad. Singular and nonuniform limits of solutions of the Boltzmann equation. In *Transport Theory (Proc. Sympos. Appl. Math., New York, 1967)*, *SIAM-AMS Proc., Vol. I*, pages 269–308. Amer. Math. Soc., Providence, R.I., 1969.

- [54] R. L. Greenblatt and J. L. Lebowitz. Product measure steady states of generalized zero range processes. *J. Phys. A*, 39:1565–1573, 2006.
- [55] Leslie Greengard and Patrick Lin. Spectral approximation of the free-space heat kernel. *Appl. Comput. Harmon. Anal.*, 9(1):83–97, 2000.
- [56] Tommy Gustafsson. L^p -estimates for the nonlinear spatially homogeneous Boltzmann equation. *Arch. Rational Mech. Anal.*, 92(1):23–57, 1986.
- [57] Tommy Gustafsson. Global L^p -properties for the spatially homogeneous Boltzmann equation. *Arch. Rational Mech. Anal.*, 103(1):1–38, 1988.
- [58] M. Herty, L. Pareschi, and M. Seaid. Discrete-velocity models and relaxation schemes for traffic flows. *SIAM J. Sci. Comput.*, 28:1582–1596, 2006.
- [59] Lowell H. Holway, Jr. Kinetic theory of shock structure using an ellipsoidal distribution function. In *Rarefied Gas Dynamics, Vol. I (Proc. Fourth Internat. Sympos., Univ. Toronto, 1964)*, pages 193–215. Academic Press, New York, 1966.
- [60] I. Ibragimov and S. Rjasanow. Numerical solution of the Boltzmann equation on the uniform grid. *Computing*, 69:163–186, 2002.
- [61] R. Illner. On the derivation of the time-dependent equations of motion for an ideal gas with discrete velocity distribution. *J. de Mecanique*, 17:781–796, 1978.
- [62] S. Kawashima. Global solution of the initial value problem for a discrete velocity model of the Boltzmann equation. *Proc. Japan Acad. Ser. A Math. Sci.*, 57:19–24, 1981.
- [63] R. Kirsch and S. Rjasanow. A weak formulation of the Boltzmann equation based on the Fourier transform. *J. Stat. Phys.*, 129(3):483–492, 2007.
- [64] H. W. Liepmann, R. Narasimha, and M. T. Chahine. Structure of a plane shock layer. *The Physics of Fluids*, 5, 1962.
- [65] P.-L. Lions. Compactness in Boltzmann’s equation via Fourier integral operators and applications. I - III. *J. Math. Kyoto Univ.*, 34(3):539–584, 1994.

- [66] Tai-Ping Liu and Shih-Hsien Yu. Boltzmann equation: micro-macro decompositions and positivity of shock profiles. *Comm. Math. Phys.*, 246(1):133–179, 2004.
- [67] Krook Max and Wu Tai Tsun. Formation of Maxwellian tails. *Physical Review Letters*, 36:1107–1109, 1976.
- [68] L. Mieussens. Discrete-velocity models and numerical schemes for the Boltzmann-bgk equation in plane and axisymmetric geometries. *Journal of Computational Physics*, 162:429–466, 2000.
- [69] S. Mischler and C. Mouhot. Cooling process for inelastic Boltzmann equations for hard spheres. II. Self-similar solutions and tail behavior. *J. Stat. Phys.*, 124(2-4):703–746, 2006.
- [70] S. Mischler, C. Mouhot, and M. Rodriguez Ricard. Cooling process for inelastic Boltzmann equations for hard spheres. I. The Cauchy problem. *J. Stat. Phys.*, 124(2-4):655–702, 2006.
- [71] J. M. Montanero and A. Santos. Computer simulation of uniformly heated granular fluids. *Gran. Matt.*, 2:53–64, 2000.
- [72] Sung Joon Moon, M. D. Shattuck, and J.B. Swift. Velocity distributions and correlations in homogeneously heated granular media. *Physical Review E*, 64:031303, 2001.
- [73] H. M. Mott-Smith. The solution of the Boltzmann equation for a shock wave. *Physical Rev. (2)*, 82:885–892, 1951.
- [74] C. Mouhot and L. Pareschi. Fast algorithms for computing the Boltzmann collision operator. *Math. Comp.*, 75:1833–1852, 2006.
- [75] Clément Mouhot and Cédric Villani. Regularity theory for the spatially homogeneous Boltzmann equation with cut-off. *Arch. Ration. Mech. Anal.*, 173(2):169–212, 2004.
- [76] K. Nanbu. Direct simulation scheme derived from the Boltzmann equation i.monocomponent gases. *J. Phys. Soc. Japan*, 52:2042 – 2049, 1983.

- [77] T. Van Noije and M. Ernst. Velocity distributions in homogeneously cooling and heated granular fluids. *Gran. Matt.*, 1:57(1998).
- [78] Taku Ohwada. Structure of normal shock waves: direct numerical analysis of the Boltzmann equation for hard-sphere molecules. *Phys. Fluids A*, 5(1):217–234, 1993.
- [79] V. Panferov and S. Rjasanow. Deterministic approximation of the inelastic Boltzmann equation. *Unpublished manuscript*, 2004.
- [80] L. Pareschi and B. Perthame. A Fourier spectral method for homogenous Boltzmann equations. *Transport Theory Statist. Phys.*, 25:369–382, 2002.
- [81] L. Pareschi and G. Russo. Numerical solution of the Boltzmann equation. i. spectrally accurate approximation of the collision operator. *SIAM J. Numerical Anal. (Online)*, 37:1217–1245, 2000.
- [82] S. Rjasanow and W. Wagner. A stochastic weighted particle method for the Boltzmann equation. *Journal of Computational Physics*, pages 243–253, 1996.
- [83] S. Rjasanow and W. Wagner. *Stochastic Numerics for the Boltzmann Equation*. Springer, Berlin, 2005.
- [84] Harold Salwen, Chester E. Grosch, and Sigi Ziering. Extension of the Mott-Smith Method for a one-dimensional shock wave. *Phys. Fluids*, 7:180–189, 1964.
- [85] Yoshio Sone. *Molecular gas dynamics*. Modeling and Simulation in Science, Engineering and Technology. Birkhäuser Boston Inc., Boston, MA, 2007. Theory, techniques, and applications.
- [86] Shigeru Takata, Kazuo Aoki, and Carlo Cercignani. The velocity distribution function in an infinitely strong shock wave. *Phys. Fluids*, 12(8):2116–2127, 2000.
- [87] C. Villani. *Handbook of Fluid dynamics*, chapter A Review of Mathematical Topics in Collisional Kinetic Theory, pages 71–306. Elsevier, 2003.
- [88] W. Wagner. A convergence proof for Bird’s direct simulation monte carlo method for the Boltzmann equation. *Journal of Statistical Physics*, pages 1011–1044, 1992.

- [89] D. R. M. Williams and F.C. MacKintosh. Driven granular media in one dimension: Correlations and equation of state. *Phys. Rev. E*, 54:9–12, 1996.
- [90] Shih-Hsien Yu. Hydrodynamic limits with shock waves of the Boltzmann equation. *Comm. Pure Appl. Math.*, 58(3):409–443, 2005.
- [91] Y. Zheng and H. Struchtrup. A linearization of Mieussens’s discrete velocity model for kinetic equations. *Eur. J. Mech. B Fluids*, 26:182–192, 2007.

Index

Abstract, vi

Acknowledgments, v

Bibliography, 135

Dedication, iv

Vita

Tharkabhushanam Sri Harsha was born in Balanagar, Andhra Pradesh, India on 11 May 1979, the son of T. L. N. Sundara Raja and T. Vijaya Lakshmi. He received the Bachelor of Technology degree in Electronics and Communication Engineering from Jawaharlal Nehru Technological University, Hyderabad, India. He then attended University of Massachusetts at Amherst from Fall 2000 to Spring 2004 where he received his Masters degrees in Electrical Engineering and Applied Mathematics in May 2003 and May 2004 respectively with exceptional grades. He joined the Computational and Applied Mathematics doctoral program at University of Texas at Austin in Fall 2004. Since then, he has been working under the supervision of Professor Gamba in the area of kinetic equations. In specific, he has developed a new numerical method for solving the fully nonlinear Boltzmann equation.

Permanent address: House No. 339, Arora Colony - II,
Road No. 3, Banjara Hills,
Hyderabad, India, 500034

This dissertation was typeset with \LaTeX^\dagger by the author.

[†] \LaTeX is a document preparation system developed by Leslie Lamport as a special version of Donald Knuth's \TeX Program.